Analysis of the decay $\omega \to \pi^+\pi^-\pi^0$ with an extended Veneziano model

Andrea Celentano[1]
INFN, Sezione di Genova

January 18, 2016

[1]andrea.celentano@ge.infn.it

Abstract

In this note I describe the analysis of the decay $\omega \to \pi^+\pi^-\pi^0$ performed using an extended Veneziano model. The main goal of the analysis is to verify that the model is able to correctly describe the data, and to determine the corresponding free parameters (the Regge trajectory parameters) trough a maximum likelihood fit. From these, the ρ meson pole parameters are obtained and compared to the corresponding PDG values. Data were collected during the `g11a` run, by measuring the photo-production reaction $\gamma p \to p\omega$ in the energy range $2.0 < W < 2.45$ GeV.

Contents

Chapter 1

Introduction

In this note I describe the analysis of the decay $\omega \to \pi^+\pi^-\pi^0$ performed using the extended Veneziano model developed by M. Pennington and A. Szczepaniak [1], described in Section 1.2. The amplitude employed to fit the data is constructed starting from a set of covariant Veneziano terms, resulting to a finite sum of partial waves that receive contributions from selected Regge trajectories, including the daughters, while still keeping the proper asymptotic limit. Given the phase-space available to the $\omega \to \pi^+\pi^-\pi^0$ decay process, data sensitivity is limited to the first $\pi\pi$ Regge trajectory, containing the $\rho(770)$ pole. For this reason, the simple, linear parametrization of the real part of the Regge trajectory was employed. The imaginary part, instead, was "ad-hoc" tuned to reproduce the finite ρ width.

The data were collected at Jefferson Lab, using the CLAS detector, as part of the `g11a` run period in 2004. This data has been already analyzed by Mike Williams to extract the differential ω photo-production cross-section $\frac{d\sigma}{dt}$ and the ω spin density matrix elements ρ_{00}, ρ_{1-1}, $Re(\rho_{10})$, in the $\sqrt{s}$ range from threshold up to 2.84 GeV [2]. Unfortunately, the already-processed data, and the corresponding analysis tools, were lost few years ago when one of the raid disks at CMU crashed and was unable to be recovered [3].

The data employed in this analysis comes from Brian Vernansky PhD thesis. As a "preliminary" part of his work, Brian re-processed the original `g11a` data-set, starting from "cooked" data, to extract the above observables, in order to tune the analysis tools and procedures that he later employed in the analysis of the g1c and g8b data. He strictly followed the original analysis procedure from Mike Williams, described in [4], i.e. he applied to the cooked data the same set of selection cuts and corrections.

The input for this analysis are the fully reconstructed 4-vectors for the particles in the reaction $\gamma p \to p\omega \to p\pi^+\pi^-\pi^0$, associated, event-by-event, to a weight ("Q-value"), that gives the probability for each event to originate from the signal distribution [5]. Brian also provided me a large set of MonteCarlo events, generated according to a pure phase-space distribution, projected on the CLAS detector and then reconstructed using the "standard" CLAS procedures.

1.1 $\omega \to \pi^+\pi^-\pi^0$ decay distribution: general features

In this section, first I describe the general features of the $\omega \to \pi^+\pi^-\pi^0$ decay distribution, with the ω produced in the reaction $\gamma p \to p\omega$. Then, I present the specific Extended Veneziano Model used to analyze data. I work in the "Adair" reference frame, defined as the ω rest frame, with the z axis oriented along the photon momentum in the overall CM frame, and the scattered proton momentum lying in the $x - z$ plane.

Five independent kinematic variables are necessary to describe this process. The orientation of the normal to the decay plane, $\hat{n}_D$, is defined by the two angles θ_A and ϕ_A, while two more variables completely fix the kinematics of the pions on the decay plane. For these, one can use two of the three pion pairs invariant masses, related by:

$$M_W^2 - m_{\pi^+}^2 - m_{\pi^-}^2 - m_{\pi^0}^2 = s + t + u \quad , \tag{1.1}$$

where $s = m_{\pi^+\pi^0}^2$, $t = m_{\pi^0\pi^-}^2$, $u = m_{\pi^+\pi^-}^2$ are the pion pair invariant masses squared. Finally, the last kinematic variable corresponds to an overall rotation around the z axis: since neither the photon beam or the proton target are polarized, this rotation angle does not appear in the $\omega \to \pi^+\pi^-\pi^0$ decay distribution, and will be neglected.

The general decay amplitude for the process $\omega \to \pi^+\pi^-\pi^0$ follows directly from the 1^{--} nature of the ω meson:

$$A_\lambda = [(\vec{I}_{\pi^+} \times \vec{I}_{\pi^-}) \cdot \vec{I}_{\pi^0}] \cdot \varepsilon_{\mu\nu\alpha\beta}\, p_+^\nu p_-^\alpha p_0^\beta \varepsilon_\lambda^\mu\, F(s,t,u) \quad , \tag{1.2}$$

where:

- $p_{+,0,-}$ are the pions 4-momenta
- ε_λ is the omega polarization four-vector, for the polarization λ ($\lambda = -1, 0, 1$).
- The isospin factor $(\vec{I}_{\pi^+} \times \vec{I}_{\pi^-}) \cdot \vec{I}_{\pi^0}$ contributes with a constant phase i to the amplitude, and, therefore, can be neglected.
- $\varepsilon_{\mu\nu\alpha\beta}$ is the Levi-Civita tensor
- $F(s,t,u)$ is a general scalar function of Lorentz-invariant Dalitz variables (i.e. the pion pairs invariant masses squared).

I explicitely evaluate this in the Adair frame, where $p_+ + p_- + p_0 = (M_W; \vec{0})$. This gives:

$$A_\lambda = \varepsilon_{\mu\nu\alpha 0} M_\omega p_+^\nu p_-^\alpha \varepsilon_\lambda^\mu \cdot F(s,t,u) = M_\omega \cdot F(s,t,u) \cdot (\vec{p}_+ \times \vec{p}_-) \cdot \vec{\varepsilon}_\lambda \tag{1.3}$$

The corresponding decay intensity is obtained by squaring the amplitude and inserting the ω polarization matrix $\rho_{\lambda,\lambda'}^\omega$ (see [6], Eq. 6):

$$I = \sum_{\lambda,\lambda'} A_\lambda^* \rho_{\lambda,\lambda'}^\omega A_{\lambda'} \tag{1.4}$$

$$I = M_\omega^2 \cdot |F(s,t,u)|^2 \cdot \sum_{\lambda,\lambda'} (\vec{p}_+ \times \vec{p}_-) \cdot \vec{\varepsilon}_\lambda^* \rho_{\lambda,\lambda'}^\omega (\vec{p}_+ \times \vec{p}_-) \cdot \vec{\varepsilon}_{\lambda'} \tag{1.5}$$

The vector product $\vec{p}_+ \times \vec{p}_-$ is, by definition, orthogonal to the decay plane, and, therefore, can be written as $\hat{n}_D \cdot q$, with $q \equiv |\vec{p}_+ \times \vec{p}_-|$. Furthermore, which of the 3 pions 3-momenta are used in the calculation, and in which order, is irrelevant, since $\vec{p}_+ + \vec{p}_- + \vec{p}_0 = \vec{0}$ in Adair frame.

The intensity, therefore, reads:

$$I = q^2 M_\omega^2 \cdot |F(s,t,u)|^2 \cdot \sum_{\lambda,\lambda'} \hat{n}_D \cdot \vec{\varepsilon}_\lambda^*\, \rho_{\lambda,\lambda'}^\omega\, \hat{n}_D \cdot \vec{\varepsilon}_{\lambda'} \tag{1.6}$$

By elaborating this expression with the explicit form of ε_λ and $\hat{n}_D$ one gets:

$$I = q^2 M_\omega^2 \cdot |F(s,t,u)|^2 \cdot W(\theta_A, \phi_A, \rho^\omega) \quad , \tag{1.7}$$

where $W(\theta_A, \phi_A, \rho^\omega)$ is given in [6], Eq. 10. $W(\theta_A, \phi_A, \rho^\omega)$ gives the angular distribution of the ω decay plane. Since the ω meson is produced in the $\gamma p \to p\omega$ process, there is a direct relation between the ω polarization matrix and the incident photon polarization matrix in terms of the corresponding production amplitude T ([6], Eq. 2 and 3):

$$\rho^\omega = T\,\rho^\gamma\,T^\dagger \tag{1.8}$$

In case of unpolarized photon beam, this permits to simplify W to:

$$W(\theta_A, \phi_A) = (\frac{1}{2}(1-\rho_{00}) + \frac{1}{2}(3\rho_{00}-1)\cos^2\theta_A - \sqrt{2}Re(\rho_{10})\sin 2\theta_A \cos\phi_A - \rho^0_{1-1}\sin^2\theta_A\cos 2\phi_A) \tag{1.9}$$

Here, ρ_{00}, $Re(\rho_{10})$ and ρ^0_{1-1} are the ω spin-density matrix elements relevant for the unpolarized beam, unpolarized target case. They do explicitely depend on the production kinematic variables (W and $\cos\theta_{CM}$), as shown excplicitely by Eq. 1.8. For the kinematic range covered in this analysis, these spin-density matrix elements, together with the differential production cross-section, have been already measured [2].

The ω decay intensity, reported in Eq. 1.7, shows a complete factorization between the angular variables θ_A, ϕ_A and the Dalitz variables s, t, u: this permits to simplify the maximum likelihood fit procedure, focusing only on the Dalitz part, as explained later in Sec. 2.

1.2 Extended Veneziano Model

In the original Veneziano model [7] for the reaction $\omega \to \pi^+\pi^-\pi^0$, the scalar part of the amplitude is written as:

$$F(s,t,u) = (A_{n,m}(s,t) + A_{n,m}(t,u) + A_{n,m}(s,u)) \tag{1.10}$$

with the $A_{n,m}$ function given by:

$$A_{n,m}(s,t) = \frac{\Gamma(n-\alpha(s))\Gamma(n-\alpha(t))}{\Gamma(n+m-\alpha(s)-\alpha(t))} \tag{1.11}$$

with n, m positive integers, and $1 \le m \le n$. The lower limit on m guarantees that $F(s,t,u)$ has the expected high-energy behavior and the upper limit eliminates double poles in overlapping channnels. $\alpha(s) = \alpha_0 + s\alpha'$ is the leading linear Regge trajectory, denoted as α_s in the following. The nominal values of the Regge coefficients α_0 and α' are, respectively, 0.5 GeV and 0.9 GeV^{-2}.

The main properties of the original Veneziano amplitude are:

- Analyticity: F is an analytic function of the Dalitz variables, with singularities given by **poles** for negative integer arguments of Gamma function (double-poles are canceled by the denominator) and singularities of the Regge trajectory, typically cuts from $\mathcal{I}(\alpha)$.
- Crossing symmetry
- Proper Regge asymptotic behaviour: $A_{n,m}(s,t) \to \frac{1}{s}\Gamma(n-\alpha_s)(-s)^{-\alpha_t^m}$.

Specifically, the amplitude spectrum is characterized, for fixed n, by an infinite number of simple poles, labeled by a non-negative integer k, that are located at $s = s_{n+k}$, satisfying:

$$\alpha(s_{n+k}) = n + k \tag{1.12}$$

In the proximity of each pole, the amplitude reads:

$$A_{n,m}(s,t) \simeq \frac{\beta_{n,m,k}(t)}{s - s_{n+k}} \tag{1.13}$$

with the residue

$$\beta_{n,m,k}(t) = \frac{(-1)^k}{\alpha' k!} \frac{\Gamma(n-\alpha_t)}{\Gamma(m-k-\alpha_t)} \tag{1.14}$$

being a polynomial in t of order $L_{max} = k + n - m$.

It follows, therefore, that the original Veneziano amplitude $F(s,t,u)$ describes, in each channel, an infinite number of zero-width overlapping resonances: for fixed k, the resonance spin l is the range $1 \leq l \leq L_{max} + 1$ (the additional unit of angular momentum comes from the factor $\varepsilon_{\mu\nu\alpha\beta}\, p_+^\nu p_-^\alpha p_0^\beta \varepsilon_\lambda^\mu$ in the full decay amplitude).

The two integers n, m determine which resonances effectively contribute to the amplitude, while their location is uniquely determined by the form of the Regge trajectory trough Eq. 1.12.

The full reaction amplitude is, generally, a linear superposition of different terms, corresponding to different values of n and m:

$$A_{n,m}(s,t) \to A(s,t) = \sum_{n,m} c_{n,m} A_{n,m}(s,t) \quad , \tag{1.15}$$

where the (complex) coefficients $c_{n,m}$ need to be determined from the data.

In the past, different authors employed the Veneziano model, for example for the analysis of the at-rest process $N\overline{N} \to 3\pi$ [8, 9, 10]. However, these analysis were performed by truncating the sum of Eq. 1.15, therefore selecting *a-priori* the number of terms to include in the amplitude.

The approach of Pennington and Szczepaniak is, instead, more systematic. The amplitude is constructed starting from the non-truncated sum of Eq. 1.15: instead of directly fitting the coefficients $c_{n,m}$ to the data, these are selected a-priori, in order to get an amplitude with a defined and known number of resonances.

I discuss excplitely the case of an amplitude containing only the pole s_1 at $\alpha_s = 1$. This pole is present only in the term $A_{1,1}$, since all the others, with $n \geq 2$, have poles at $\alpha_s \geq 2$ (cfr. Eq 1.12). The single coefficient $c_{1,1}$ determines the corresponding residue. However, the $A_{1,1}$ term also contains poles at higher s values ($\alpha_s = 2, 3, \ldots$), with residues that are polynomial in t of order $1, 2, \ldots$. These higher mass poles must be canceled by the same poles in amplitudes $A_{n,m}$ with $n \geq 2$. It can be shown that this is achieved by selecting:

$$c_{n,1} = \frac{c_{1,1}}{\Gamma(n)} \quad , \; c_{n,2} = -\frac{c_{1,1}}{\Gamma(n-1)} \quad , \; c_{n,m} = 0 \text{ for } m \geq 3 \tag{1.16}$$

The resulting amplitude is:

$$A_1(s,t) = c_{1,1} \frac{2 - \alpha_s - \alpha_t}{(1-\alpha_s)(1-\alpha_t)} \tag{1.17}$$

This can be generalized to construct the amplitude A_n having only the poles at $\alpha_s = n$:

$$A_n(s,t) = \frac{(2n - \alpha_s - \alpha_t)}{(n-\alpha_s)(n-\alpha_t)} \sum_{i=1}^{n} c_{n,i} (-\alpha_s - \alpha_t)^{i-1} \tag{1.18}$$

The large s behaviour of A_n is s^{n-1} and not the expected Regge one, $s^{\alpha_t - 1}$. Such a behavior, infact, can emerge only from an infinite number of $s-$channel poles, while, by construction, A_n contains only a **finite** number of resonances, all located at $\alpha_s = n$. Therefore, to restore the proper asymptotic behavior, other poles must be considered.

This can be done as follows. Suppose that the "typical" energy scale of the reaction under anaylsis is E_0. If one introduces in the amplitude poles located at $\alpha_s \geq N$, with $N = \alpha' E_0^2$, these will contribute as a smooth background in the kinematic region of interest, with a negligible

effect on the "true" resonances there present. However, their introduction permits to restore the Regge behavior. The A_n amplitude now reads:

$$A_n(s,t;N) = \frac{(2n-\alpha_s-\alpha_t)}{(n-\alpha_s)(n-\alpha_t)} \sum_{i=1}^{n} c_{n,i}(-\alpha_s-\alpha_t)^{i-1} \cdot \frac{\Gamma(N+1-\alpha_s)\Gamma(N+1-\alpha_t)}{\Gamma(N+1-n)\Gamma(N+n+1-\alpha_s-\alpha_t)} \tag{1.19}$$

1.2.1 Reaction Amplitude and Intensity

The full reaction amplitude and intensity are here reported for completeness:

$$F(s,t,u) = \sum_{n=1}^{n_{max}} (A_n(s,t;N) + A_n(t,u;N) + A_n(s,u;N)) \tag{1.20}$$

$$A_\lambda(s,t,u) = \varepsilon_{\mu\nu\alpha\beta}\, p_+^\nu p_-^\alpha p_0^\beta \varepsilon_\lambda^\mu\, F(s,t,u) \tag{1.21}$$

$$A_\lambda(s,t,u) = \varepsilon_{\mu\nu\alpha\beta}\, p_+^\nu p_-^\alpha p_0^\beta \varepsilon_\lambda^\mu \cdot \sum_{n=1} (A_n(s,t;N) + A_n(t,u;N) + A_n(s,u;N)) \tag{1.22}$$

$$I \propto \sum_{\lambda,\lambda'} A_\lambda \rho_{\lambda,\lambda'} A_{\lambda'}^* \tag{1.23}$$

1.2.2 The $\omega \to \pi^+\pi^-\pi^0$ decay

The application of the Pennington-Szczepaniak extended Veneziano model to the $\omega \to \pi^+\pi^-\pi^0$ decay is here discussed.

- The physical content of the decay amplitude scalar part follows from the nature of each A_n factor. Specifically, $A_n(s,t)$ contains poles at $\alpha_s = n$, with the residue

  $$\beta_n = \sum_{i=1}^{n} c_{n,i}(-n-\alpha_t)^{i-1}$$

  being a polynomial in t of order $n-1$. Considering the further unit of angular momentum carried by the factor $\varepsilon_{\mu\nu\alpha\beta}\, p_+^\nu p_-^\alpha p_0^\beta \varepsilon_\lambda^\mu$, it follows that A_n describes the decay of the ω via the coupling to indermediate, degenerates, isospin-1 $\pi-\pi$ resonances (i.e. ρ resonances), with angular momenta $1 \ldots (n+1)$, i.e. $\omega \to \pi\rho \to \pi\pi\pi$

- Bose statistics and isospin conservation require the full reaction amplitude to be symmetric for the exchange of any two pions. Since the kinematic factor $\varepsilon_{\mu\nu\alpha\beta}\, p_+^\nu p_-^\alpha p_0^\beta \varepsilon_\lambda^\mu$ is manifestly anti-symmetric, the scalar part $F(s,t,u)$ must be anti-symmetric too. This forbids the presence of spin-even $\pi\pi$ resonances.

  This constraint must be applied at the level of the single factors A_n that apper in the full reaction amplitude (cfr. Eq. 1.20). As said before, each A_n contains poles at $\alpha_s = n$, with the residue being a polynomial in t of order $n-1$. Decoupling of the spin-even resonances implies that $Res\, A_n$ should be an even function of t. This is obtained by fixing some of the coefficients $c_{n,i}$.

  For example, for $n=2$, $Res\, A_2 = c_{2,1} - c_{2,2}(2+\alpha_t)$. The decoupling of the spin-2 resonance requires fixing $c_{2,2} = 0$. This amplitude, therefore, describes **only** the coupling of the ω to the $\rho'\pi$ system, being ρ' the spin-1 $\pi\pi$ resonance at $\alpha_s = 2$, i.e. the ρ_{1450}.

- The nominal Regge trajectory parametrization, $\alpha_s = \alpha_0 + s \cdot \alpha'$ is purely real. Therefore, from Eq. 1.12 it follows that the poles contained in the extended Veneziano Model correspond to zero-width resonances. In order to re-introduce the finite ρ resonances width, the trajectory is modified as follows:

$$\alpha_s = \alpha_0 + s \cdot \alpha' + ig\sqrt{s - 4m_\pi^2} \tag{1.24}$$

  The parameter g determines the resonances width. The nominal value is $g = 0.12$, corresponding, for the $\rho(770)$ state, to $\Gamma = 0.124$ GeV.

1.3 Goals of the analysis

The goals of this analysis are the following:

- Qualitatively verify that the extended Veneziano Model is able to reproduce the data for this reaction, adopting the nominal Regge trajectory parametrization. In order to evaluate systematic effects, the check is performed independently in different bins of the center-of-mass energy W: being this a production variable, no dependence on it is expected.
- Estimate the sensitivity to higher ρ excited states, other than the $\rho(770)$, i.e. verify the effect of introducing in the amplitude the terms $A_2, A_3, \ldots$. This is performed using the nominal Regge trajectory parametrization.
- Leave the Regge trajectory parameters α', α^0, g as free parameters and fit them to the data, to determine the sensitivity to the $\rho(770)$ pole parameters. The fit is performed independently in bins of W to evaluate the systematic effects.

Chapter 2

$\omega \to \pi^+\pi^-\pi^0$: extended maximum likelihood fit procedure

In this section, I describe the procedure that I adopted to fit the extended Veneziano model to the $\omega \to \pi^+\pi^-\pi^0$ decay, via an extended maximum likelihood fit. In particular, I discuss what is the role of the production kinematic variables (W and $\cos\theta_{CM}$) and observables (differential cross section and spin-density matrix elements).

2.1 Extended maximum likelihood fits

The goal of an extended maximum likelihood procedure is to fit a parametrized intensity for a certain reaction to a set of unbinned data, in order to extract the value of the corresponding free parameters and obtain the acceptance-corrected event yield. The intensity normalization is always a free parameter in the fit.

The main quantity of interest is the *likelihood* $\mathcal{L}$, defined as the product of the occurrence probabilities of the measured events, according to the model used to derive the process intensity:

$$\mathcal{L} = \prod_i^n P_i(\tau_i, \vec{x}) \, , \tag{2.1}$$

where the product is extended over all the n measured events, each described by a set of kinematic variables τ_i, and $\vec{x}$ are the parameters to be extracted from the data. For each event, the probability is proportional to the intensity multiplied by the detector acceptance ε, which in turns is a function of the final state kinematic variables:

$$P_i(\tau_i, \vec{x}) \propto I(\tau_i, \vec{x}) \cdot \varepsilon(\tau_i) \tag{2.2}$$

The overall normalization is fixed requiring that the integral of the intensity multiplied by the detector acceptance, over the full final state phase space, is equal to the average number of expected events μ:

$$\mu(\vec{x}) = \int I(\tau, \vec{x}) \cdot \varepsilon(\tau) d\tau \tag{2.3}$$

$$P_i(\tau_i, \vec{x}) = \frac{I(\tau_i, \vec{x}) \cdot \varepsilon(\tau_i)}{\int I(\tau, \vec{x}) \cdot \varepsilon(\tau) d\tau} \tag{2.4}$$

The total number of measured events n itself is a statistical variable, distributed according to the Poisson statistics. A proper factor accounting for the probability to measure *exactly* n events has thus to be introduced into the likelihood expression, getting its final expression:

$$\mathcal{L} = \frac{\mu^n e^{-\mu}}{n!} \cdot \prod_i^n \frac{I(\tau_i, \vec{x}) \cdot \varepsilon(\tau_i)}{\int I(\tau, \vec{x}) \cdot \varepsilon(\tau) d\tau} \tag{2.5}$$

The expression for $\mathcal{L}$ in Eq. 2.5 can be simplified noting that, for the n events that have been actually measured in the experiment, the acceptance was one by definition. Also, Eq. 2.3 can be used to cancel the factor μ^n, thus leaving the following expression:

$$\mathcal{L} = \frac{e^{-\mu}}{n!} \cdot \prod_i^n I(\tau_i, \vec{x}) \tag{2.6}$$

The goal of an extended maximum likelihood fit is to maximize the likelihood to obtain the value of the free parameters $\vec{x}$. For computational reasons, it is preferable instead to *minimize* the inverse of its natural logarithm, that, a part from inessential constant factors, is given by the following expression:

$$-\ln \mathcal{L} \propto -\sum_i^n \ln I(\tau_i, \vec{x}) + \mu(\vec{x}) \tag{2.7}$$

If there are weights w_i associated with the measured events, such as the "Q-value", the above expressions has to be modified in:

$$-\ln \mathcal{L} \propto -\sum_i^n w_i \cdot \ln I(\tau_i, \vec{x}) + \mu(\vec{x}) \tag{2.8}$$

The first term in Eq. 2.7 and Eq. 2.8 involves a sum over all the measured events, and it is calculable exactly given the expression for the intensity, for each combination of the parameters $\vec{x}$. The second term, instead, requires the knowledge of the detector acceptance as a function of the final state phase space variables and has to be calculated by MonteCarlo, generating a large set of N_{gen} MonteCarlo events, projecting to the experimental detector, and finally reconstructing using the *same* algorithm employed for the data. This leaves N_{acc} reconstructed events, for which $\varepsilon(\tau_i) = 1$.

The mean value of total expected events is then given by:

$$\mu(\vec{x}) = \frac{\boldsymbol{\tau}}{N_{gen}} \sum_i^{N_{acc}} I(\tau_i, \vec{x}) \quad , \tag{2.9}$$

where the factor $\boldsymbol{\tau}$ represents the total volume of the final state phase space. Since the reaction dynamics is explicitly included in the definition of μ via the intensity I, MonteCarlo events have to be generated according to a flat phase space distribution.

Knowing the value of the free parameters in the intensity, the acceptance-corrected event yield is then computed as:

$$\mu^0(\vec{x}) = \frac{\boldsymbol{\tau}}{N_{gen}} \sum_i^{N_{gen}} I(\tau_i, \vec{x}) \tag{2.10}$$

Furthermore,

2.1.1 Example: constant intensity

It is instructive to consider the case of a maximum likelihood fit performed with a constant intensity, $I = I_0$, where only the normalization factor I_0 (and thus the acceptance-corrected event yield) has to be determined.

The log-likelihood reads:

$$-\ln \mathcal{L} = -\ln I_0 \cdot \sum_i^n \omega_i + \boldsymbol{\tau} I_0 \frac{N_{acc}}{N_{gen}} \tag{2.11}$$

and the corresponding minimum is for:

$$I_0 = \frac{N_{gen}}{N_{acc}} \cdot \frac{\sum_i^n \omega_i}{\boldsymbol{\tau}} \tag{2.12}$$

The acceptance-corrected event yield is:

$$\mu^0(\vec{x}) = \boldsymbol{\tau} \cdot I_0 = \sum_i^n \omega_i \,/\, \frac{N_{acc}}{N_{gen}} \tag{2.13}$$

This result is in agreement with the "classical" acceptance-corrected event yield calculation, given by the ratio between the number of measured events and the experimental detector acceptance.

2.1.2 AmpTools software

In this analysis, I employed the AmpTools software to perform maximum likelihood fits to the data. AmpTools, designed by H. Matevosyan, R. Mitchell, and M. Shepherd at Indiana University, is a collection of C++ libraries that are useful for performing unbinned maximum likelihood fits to data, using a set of interfering amplitudes [11]. It provides a set of routines that manage the technical aspects of performing fits to large sets of data, without imposing *any* constraints on the physics.

The AmpTools "core" is the `Amplitude` class. It contains the template of a physical amplitude involved in the process under study. On a general view, it is a mechanism to turn a set of four vectors describing an event into a complex number, representing the physics amplitude. The `Amplitude` class contains a pure-virtual method, `calcAmplitude(GDouble **pKin)`, that actually defines how the amplitude is calculated, given the particle four-vectors. The user has to write his own amplitudes, overriding this method. The user also needs to specify how amplitudes have to be summed, i.e. coherently or not, and the which are the free parameters to extract from the data.

2.2 Application to the $\omega \to \pi^+\pi^-\pi^0$ process

For the decay process $\omega \to \pi^+\pi^-\pi^0$, the intensity expression that I fit to the data is that of Eq. 1.7. Here, I want to discuss the following points:

- The $W(\theta_A, \phi_A)$ factor is completely known, and does not include any free parameter, the spin-density matrix elements being already measured for this kinematic regime. Is it possible to avoid the corresponding computation in each fit iteration, to speed-up the process?

- The intensity expression for the decay process only does not depend on the production cross-section. However, the CLAS detector acceptance does: for a fixed kinematic configuration τ_D of the decay process, the detector acceptance $\varepsilon(\tau)$ does **also** depend on the kinematic configuration of the production process τ_P. How it is possible to handle this?

The answer to the second question is simple: the full process $\gamma p \to p\omega \to p\pi^+\pi^-\pi^0$ has to be considered, with the intensity:

$$I = I_P \cdot I_D = \frac{d\sigma}{d\cos_{CM}} \cdot q^2 M_\omega^2 \cdot |F(s,t,u)|^2 \cdot W(\theta_A, \phi_A, \rho^\omega) \tag{2.14}$$

The answer to the first question, instead, comes from the following theorem (see Appendix A for the demonstration):

Theorem 1. *Assume a reaction R, with the final state phase-space τ being factorized as $\tau = \tau_\mathbf{1} \cdot \tau_\mathbf{2}$. Assume also that the intensity I for the reaction can written as $I = I_1(\tau_1) \cdot I_2(\tau_2, \vec{x})$, where the first factor does not include free parameters, while the second does. Then, the likelihood function obtained from the full intensity I is equivalent to the likelihood obtained by considering the I_2 factor only, provided that a weight k_i is assigned to each of the MonteCarlo events -generated and reconstructed -, with $k_i = I_1(\tau_1^i)$, and that the average number of measured events is computed as:*

$$\mu(\vec{x}) = \frac{\sum_{i=1}^{N_{acc}} k_i I_2(\tau_2, \vec{x})}{N_{gen}} \tag{2.15}$$

The application of the theorem to this analysis permits to perform a maximum likelihood fit using only the "reduced" decay intensity $I_D^R = q^2 \cdot |F(s,t,u)|^2$, provided that, before the fit, the "weight" $w = \frac{d\sigma}{d\cos_{CM}} \cdot M_\omega^2 \cdot W(\theta_A, \phi_A, \rho^\omega)$ is assigned to each of the generated and reconstructed MonteCarlo events.

To do so, I used the data reported in [2], by performing a linear interpolation.

Chapter 3

Data agreement with previous results

Before proceeding further in the analysis, I performed a check to verify the agreement with the previous results from M. Williams analysis. As said before, the original dataset for that analysis was lost. Therefore, I could olny compare the published results, namely the differential cross section $\frac{d\sigma}{d\cos_{CM}}$ and the spin-density matrix elements. The main goal of this check is to verify that the re-analysis procedure operated by B. Vernansky on the `g11a` dataset, following strictly the procedure adopted by M. Williams, gives compatible results for the above observables.

Preliminarly, I compared the number of signal events (i.e. the non-acceptance corrected event yield) as a function of W with the result reported, in form of a plot, in M. Williams thesis (Fig. 3.19). Being this quantity independent from the MC procedure, this comparison permits to identify any difference associated directly to the signal extraction from the measured data.

3.1 Procedure

I binned data in W and $\cos\theta_{CM}$ bins. For W, I selected 45 bins from 2.0 to 2.45 GeV, each bin with a 10 MeV width, while for $\cos\theta_{CM}$ I employed 16 bins, from -0.8 to +0.8, each bin with .1 width. This division is the same as the one used in the original Williams paper.

In each bin, I performed an extended maximum likelihood fit, with the *full* reaction intensity (Eq. 2.14). I set $F(s,t,u) = 1$, as was done in the original Williams paper. The effect of this choice will be discussed in the following. The corresponding free parameters are: the 3 spin density matrix elements and the overall normalization, evaluated at the kinematic point corresponding to the bin itself.

The spin-density matrix elements are obtained directly from the fit. The differential-cross section, instead, has to be computed from the acceptance-corrected event yield μ^0, via the formula:

$$\frac{d\sigma}{d\cos\theta_{CM}} = \frac{\mu^0}{\mathcal{L}_{target}} \cdot \frac{1}{\mathcal{F}'(W)} \cdot \frac{1}{BF(\omega \to \pi\pi\pi)} \cdot \frac{1}{\Delta\cos\theta} \quad , \tag{3.1}$$

where:

- $\mathcal{L}_{target}$ is the number of scatter centers per unit of area in the target. This is computed as $N_{Avo} \cdot \rho_{target} \cdot L_{target}/A_{target}$. For the `g11a` run, $\mathcal{L}_{target} = (1.715 \pm 0.003) \cdot 10^{24}$ cm^{-2}. All the details about the calculation of this quantity, as well as its indetermination, are reported in Williams thesis, Sec. 7.2.1.

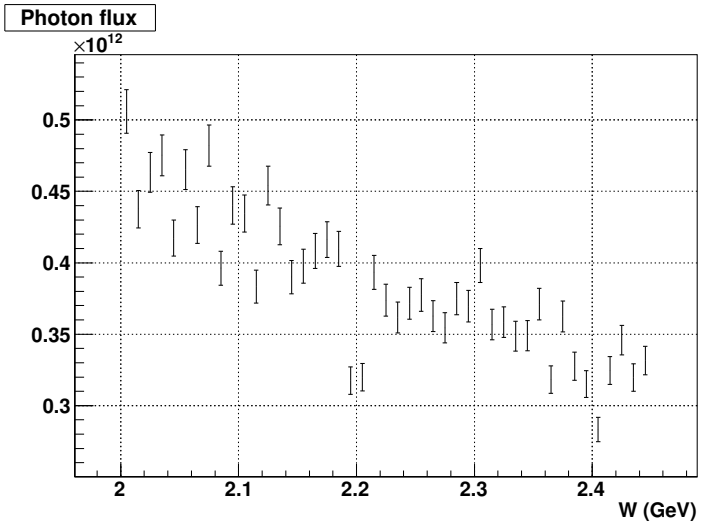

Figure 3.1: The **corrected** photon flux incident on the target, as a function of W, together with the systematic error (3.04 %).

- $\mathcal{F}'(W)$ is the *corrected* number of incident photons in the W bin. This is obtained from the un-corrected flux obtained from the *gflux* method [12], applying the corrections specific to the `g11a` run, namely the "Live-time correction" and the "Un-Triggered T-Counter Correction". These are described in Williams thesis, Sec. 4.5.2 and 4.5.3. The second correction has to be applied only to the flux data for $W < 1.95$ GeV and, therefore, is not relevant for this analysis.

  The systematic uncertainty associated to the corrected photon flux has two contributions: the photon transmission efficiency (0.5%) and the live-time correction (3%) (see [2], Sec VII). Adding these in quadrature, the overall systematic uncertainty is $\simeq 3.04\%$.

  The corrected flux is reported in Fig. 3.1.

- $\Delta \cos\theta = 0.1$ is the width of each $\cos\theta$ bin.

- $BF \simeq 0.891$ is the $\omega \to \pi^+\pi^-\pi^0$ decay branching fraction.

3.2 Results

3.2.1 Event yield (not acceptance corrected)

The two event yields (M. Williams analysis / this analysis) are reported in Fig.3.2, left panel. The right panel reports the event yields ratio, as a function of W.

I decided to **not** quote any statistical or systematic error, since the two observables are extracted from the same dataset, using the same analysis procedure. Instead, I decided to quote a 1% systematic error to the M. Williams results, due to the data digitization procedure (data were extracted from the plot on the PhD thesis).

The ratio R manifestly shows a systematic trend, depending on the center-of-mass energy W. It decreases from $R \simeq 1$ at $W = 2.00$ GeV to $R \simeq 0.92$ for $W > 2.10$ GeV, and then stabilizes.

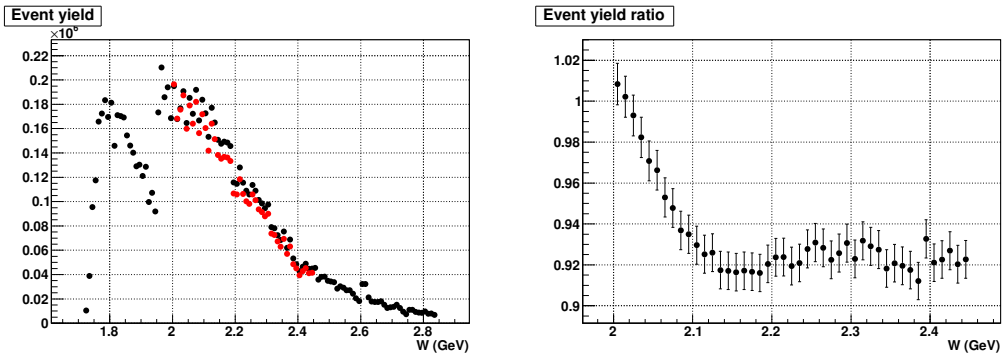

Figure 3.2: Left: event yield as a function of W. Black: M. Williams analysis (datapoints extracted from the PhD thesis). Red: this analysis. Right: ratio of the two event yield, as a function of W. See text for the description of the error bars.

3.2.2 Cross section and spin-density matrix elements

The result of the cross-section and spin-density matrix comparison is reported, for all W bins, in Appendix B. In each page, the top-left plot reports the cross-section, while the central-row plots report the spin-density matrix elements, as a function of $\cos\theta_{CM}$.

The ratio between the two cross-sections is reported in the top-central plot. Results from M. Williams analysis are reported in black, while results from this analysis are reported in red. The blue data points will be described later in the next section.

3.3 Conclusions

The agreement between the spin-density matrix elements determined in this analysis and those reported by M. Williams is very good, for all W and $\cos\theta_{CM}$ bins.

The ratio between the differential reaction cross-section reported determined in this analysis and that from M. Williams, instead, shows a systematic positive offset from the expected unitary value, for all W bins, i.e. the differential cross-section here determined is **larger** than the one reported in Williams paper. Since the not-acceptance corrected yield ratio is $\simeq 0.92$, this suggests the presence of some systematic effect in the acceptance calculation (i.e. on the MC events projection on CLAS and reconstruction), and/or in the photon flux determination.

Furthermore, for a given W bin, the cross-sections ratio is not constant, but fluctuates as a function of $\cos(\theta)_{CM}$. This fluctuation is of the order of $\simeq 10\%$ for all W bins.

As explained before (Sec. 2.2), the differential production cross-section and the spin-density matrix elements for the reaction $\gamma p \to p\omega$ are only used to assign a weight to the MonteCarlo events (generated and accepted). The weights are employed in the Maximum Likelihood Fit procedure to account in an "effective way" for the dependence of the CLAS acceptance on the production variables (W and $\cos(\theta)_{CM}$) and on the $\omega \to \pi^+\pi^-\pi^0$ decay plane orientation.

Therefore, for a given W bin, a constant shift in the differential cross-section is not an issue in this analysis, since the weights can be re-scaled arbitrarly without any effect in the Likelihood computation. However, the $\cos(\theta)_{CM}$-dependent fluctuation would introduce a systematic effect on the Likelihood normalization term. This effect is expected to be an higher-order one, since it affects only the CLAS acceptance dependence on the production variables.

I evaluated explicitly how this effect influences the outcome of this analysis: procedure and results are discussed in the next Chapter.

Chapter 4

Effect of cross-section and spin density matrix-elements systematic uncertainty

Before moving forward and discuss in detail the results obtained from the analysis of the $\omega \to \pi^+\pi^-\pi^0$ reaction with the Pennington-Szczepaniak extended Veneziano model, I want to discuss the effect of the systematic effects underlined in the previous Chapter, i.e. the fact that the $\gamma p \to p\omega$ reaction cross-section and the density matrix elements obtained from this analysis, using B. Vernansky dataset, do not completely agree with the origina `g11` analysis.

First, I'll show that the effect is **not** related to specific choice of $F(s,t,u)$ in the full reaction intensity, i.e. I'll demonstrate that results obtained from this dataset for the above observables are the same for the simplest choice $F = 1$ and for the Pennington-Szczepaniak model.

Then, I'll show that, even introducing a random shift in the MC event weights - the only quantities in this analysis that depend on the above observables - the obtained results are compatible, meaning that the actual effect of this systematic shift is not the dominant uncertainty in the analysis.

4.1 $F \neq 1$

In the previous Chapter, I evaluated the differential reaction cross-section and the spin-density matrix elements by setting $F(s,t,u) = 1$ in the full reaction intensity (Eq. 2.14), following what was done in the previous `g11` analysis. However, in this analysis I consider $F \neq 1$, by using the Pennington-Szczepaniak extended Veneziano model.

By following the argument introduced in the previous Chapters, one can conclude that, even if these two observables are only related to the $\gamma p \to p\omega$ production reaction, the CLAS acceptance does also depend on the $\omega \to \pi^+\pi^-\pi^0$ decay kinematics. Therefore, effect of $F(s,t,u)$ could in principle manifest in the acceptance evaluation and, thus, in the extraction of the cross-section and of the spin-density matrix elements, altough this should be an higher-order effect.

Here, I show that actually this does not introduce any significal effect in the measurement of these observables.

4.1.1 Procedure

I repeated the extraction of the differential reaction cross-section and the spin-density matrix elements as described in the previous Chapter. However, in the intensity parametrizetion I introduced:

$$F(s,t,u) = A_1(s,t,N) + A_1(s,u,N) + A_1(t,u,N) \quad , \tag{4.1}$$

i.e. I included the first term in the series of Eq. 1.20, corresponding to the presence of the $\rho(770)$ pole. As discussed in the next Chapter, this term is the dominat one in the series that defines F (Eq.1.20). I used the nominal expression of the $\pi\pi$ Regge Trajectory (Eq. 1.24).

4.1.2 Results and discussion

The differential cross-section and the spin-density matrix elements extracted from the fits with the F expression given above are reported, for all the W and $\cos(\theta)$ bins in the plots of Appendix B, blue points.

Results obtained in the two cases, $F = 1$ and $F \neq 1$ are compatible. This demonstrates that the effect of F in the extraction of the differential reaction cross-section and the spin-density matrix elements is negligible, as expected.

4.2 Systematic uncertainty in the differential cross-section and spin-density matrix elements

The differential production cross-section and the spin-density matrix elements for the reaction $\gamma p \to p\omega$ are employed in this analysis to assign a weight to the MonteCarlo events (generated and accepted): these are employed in the Maximum Likelihood Fit procedure to account for the dependence of the CLAS acceptance on the production variables (W and $\cos(\theta_{CM})$) and on the $\omega \to \pi^+\pi^-\pi^0$ decay plane orientation.

These observables were discussed in the previous Chapter, and compared with those from [2]. While a good agreement was found for the spin-density matrix elements, the differential reaction cross-section showed discrepancies, thus showing the presence of unknown systematic effects.

For a given W bin, a constant shift in the differential cross-section is not an issue in this analysis, since weights can be globally re-scaled without any effect in the Likelihood computation. However, a $\cos(\theta_{CM})$-dependent fluctuation would introduce a systematic effect on the Likelihood normalization term, since the $\omega \to \pi^+\pi^-\pi^0$ reaction analysis is performed by merging together, for the same W-bin, all the events in the $\cos(\theta_{CM})$ range.

In this Section, I discuss how this effect would affect the Maximum-Likelihood fit results.

4.2.1 Procedure

I used the simplest parametrization of the decay intensity presented before, that includes the $\rho(770)$ pole only:

$$F(s,t,u) = A_1(s,t,N) + A_1(s,u,N) + A_1(t,u,N) \quad , \tag{4.2}$$

I used the nominal expression of the $\pi\pi$ Regge Trajectory (Eq. 1.24).

For each W bins, I performed two Maximum-Likelihood fits. In the first, I calculated MonteCarlo weights starting with the cross-section and spin-density matrix elements obtained from [2]. In the second, instead, the weights were re-computed with the above observables randomly smeared by 10%. Smearing was applied independently in each W and $\cos(\theta_{CM})$ bin.

4.2.2 Results and discussion

The F parametrization here employed does not include any free parameter. Therefore, to compare the two cases, the one with nominal weights with the one with smeared weights, I decided to look at the pion-pairs invariant mass distributions, comparing data with the fit results. The choice of these observables derives from the fact that they enter directly in the parametrization of the $\omega \to \pi^+\pi^-\pi^0$ intensity that I employ in this analysis.

For each W bin, the obtained results are reported in Appendix C: blue points are data, red line is the fit result with nominal weights, green line is the fit result with smeared weights. Clearly, the two curves are almost equivalent in all W bins: this demonstrates that the effect of the systematic uncertainty on the cross-section and on the spin-density matrix elements on the event weights is negligible, and do not affect the fit results.

Furthermore, the good agreement between the fit results and data demonstrates the validity of the Pennington-Sczepaniak model in the description of the $\omega \to \pi^+\pi^-\pi^0$ reaction: this is discussed in detail in the next Chapter.

Chapter 5

Application of the Pennington-Szczepaniak model

Bibliography

[1] A. P. Szczepaniak and M. R. Pennington, Phys. Lett. B **737**, 283 (2014).

[2] M. Williams *et al.* [CLAS Collaboration], Phys. Rev. C **80**, 065208 (2009) [arXiv:0908.2910 [nucl-ex]].

[3] B. Vernansky, private communication.

[4] M. Williams. *"Measurement of Differential Cross Sections and Spin Density Matrix Elements along with a Partial Wave Analysis for $\gamma p \to p\omega$ using CLAS at Jefferson Lab."* Ph.D. thesis, Carnegie Mellon University, 2007.

[5] M. Williams, M. Bellis and C. A. Meyer, arXiv:0804.3382 [physics.data-an].

[6] K. Schilling, P. Seyboth and G. E. Wolf, Nucl. Phys. B **15**, 397 (1970) [Nucl. Phys. B **18**, 332 (1970)].

[7] G. Veneziano, Nuovo Cimento, 57 (1968)

[8] C. Lovelace, Phys. Lett. 25B (1968), 264

[9] G. Altarelli, Phys. Rev. 183 (1969), 1469

[10] G. P. Gopal, Phys. Rev. D 3 (1971), 2262

[11] H. Matevosyan, R. Mitchell and M. Shepherd, `http://amptools.sourceforge.net/index.php/Main_Page`

[12] J. Ball and E. Pasyuk. "Photon Flux Determination Through Sampling of "out-of-time" Hits with the Hall B Photon Tagger." CLAS Note 2005-002.

Appendix A

Theorem

Theorem 1. *Assume a reaction R, with the final state phase-space τ being factorized as $\tau = \tau_{\mathbf{1}} \cdot \tau_{\mathbf{2}}$. Assume also that the intensity I for the reaction can written as $I = I_1(\tau_1) \cdot I_2(\tau_2, \vec{x})$, where the first factor does not include free parameters, while the second does. Then, the likelihood function obtained from the full intensity I is equivalent to the likelihood obtained by considering the I_2 factor only, provided that a weight k_i is assigned to each of the MonteCarlo events -generated and reconstructed -, with $k_i = I_1(\tau_1^i)$, and that the average number of measured events is computed as:*

$$\mu(\vec{x}) = \frac{\sum_{i=1}^{N_{acc}} k_i I_2(\tau_2, \vec{x})}{N_{gen}} \tag{A.1}$$

Proof

Appendix B

Data agreement with previous results: plots

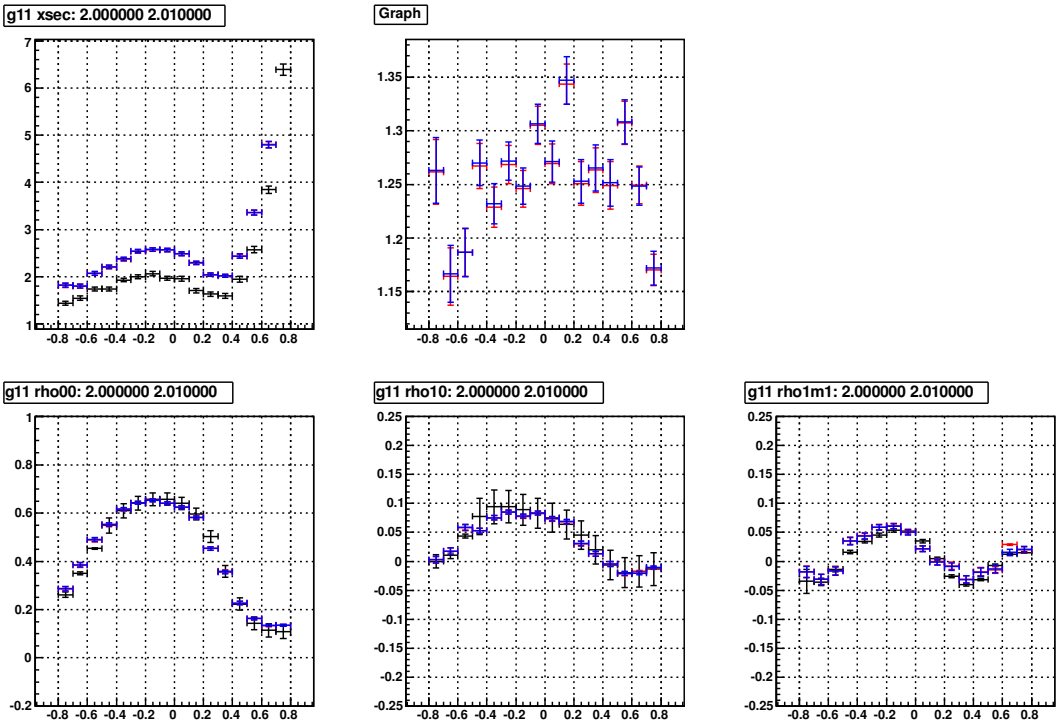

Bin 0 : W = 2.00 - 2.01 GeV

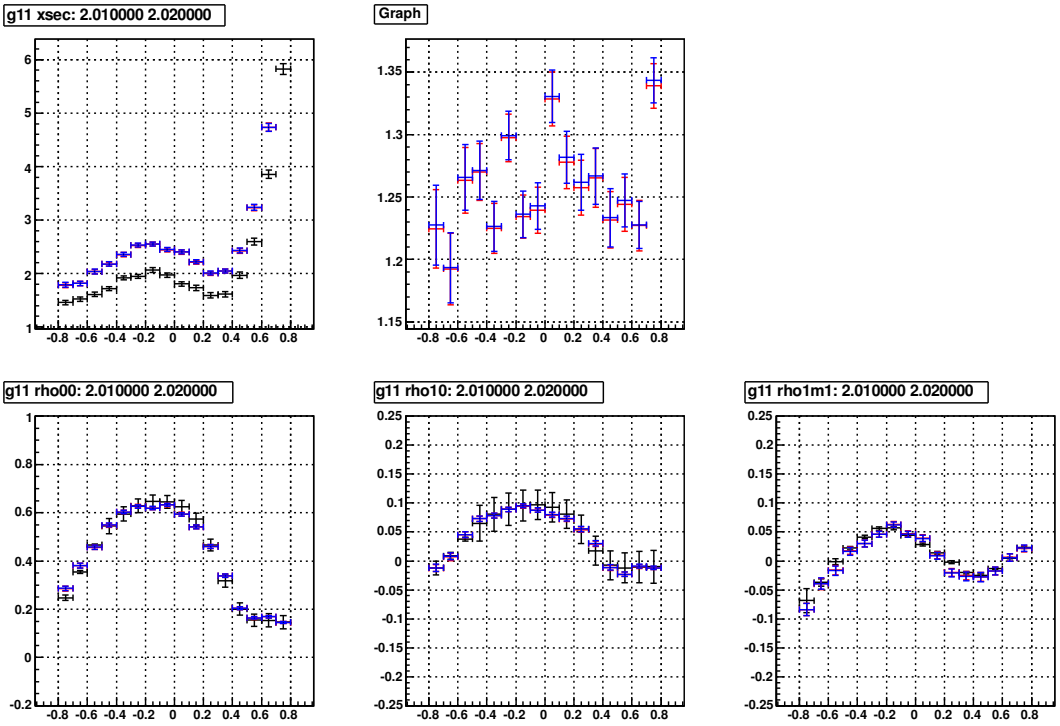

Bin 1 : $W = 2.01$ - 2.02 GeV

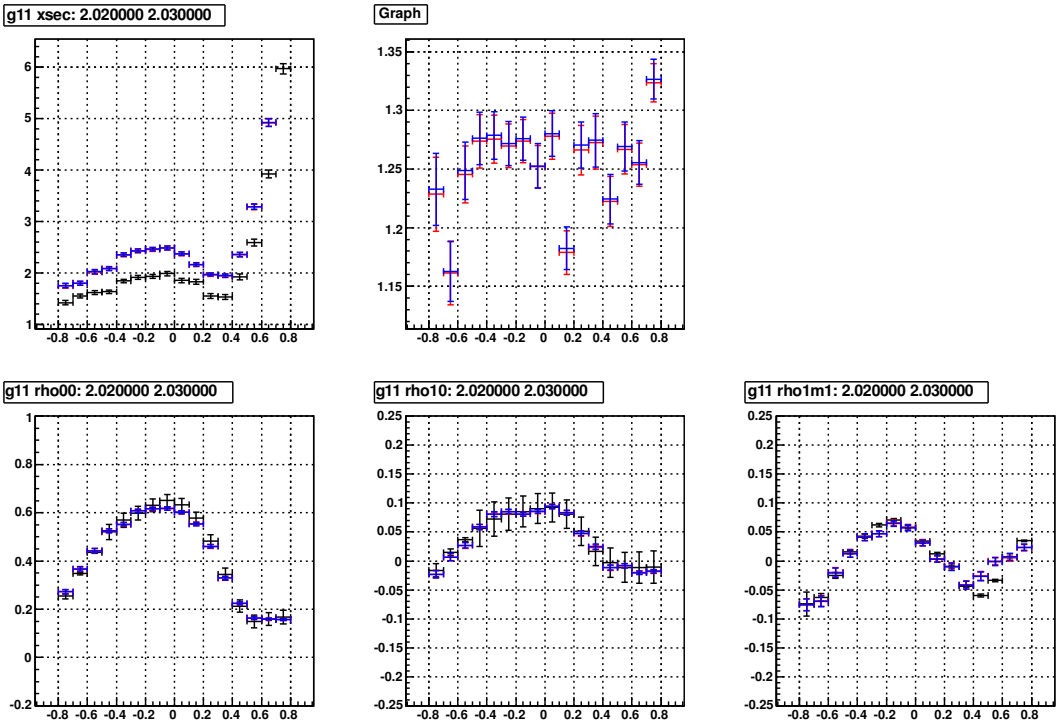

Bin 2 : $W = 2.02$ - 2.03 GeV

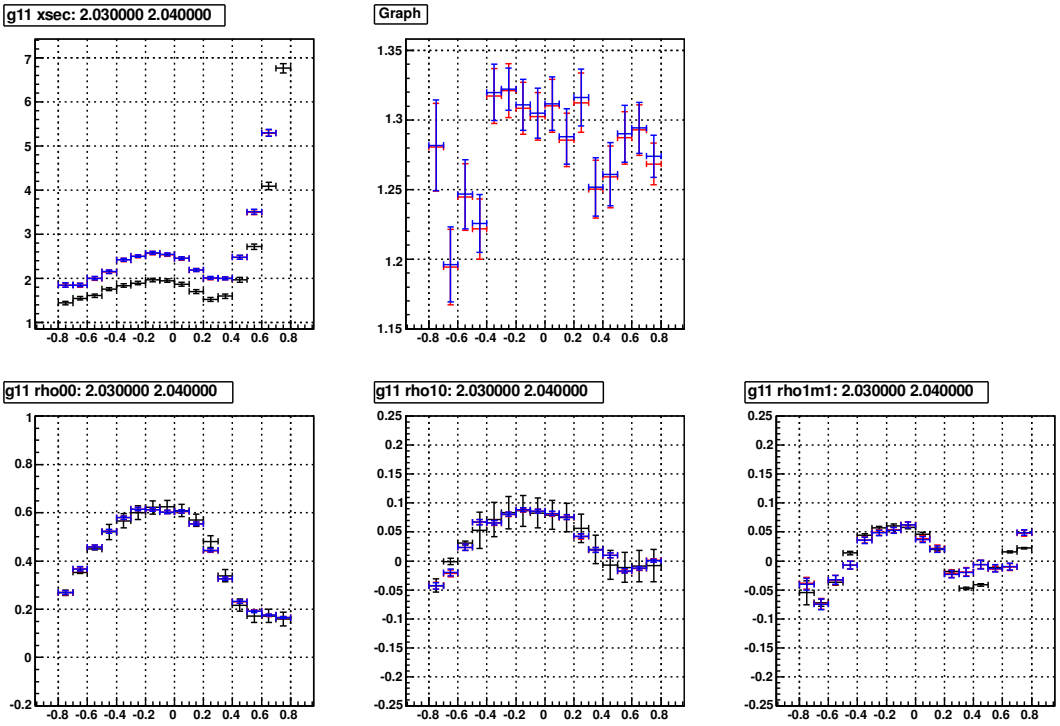

Bin 3 : $W = 2.03$ - 2.04 GeV

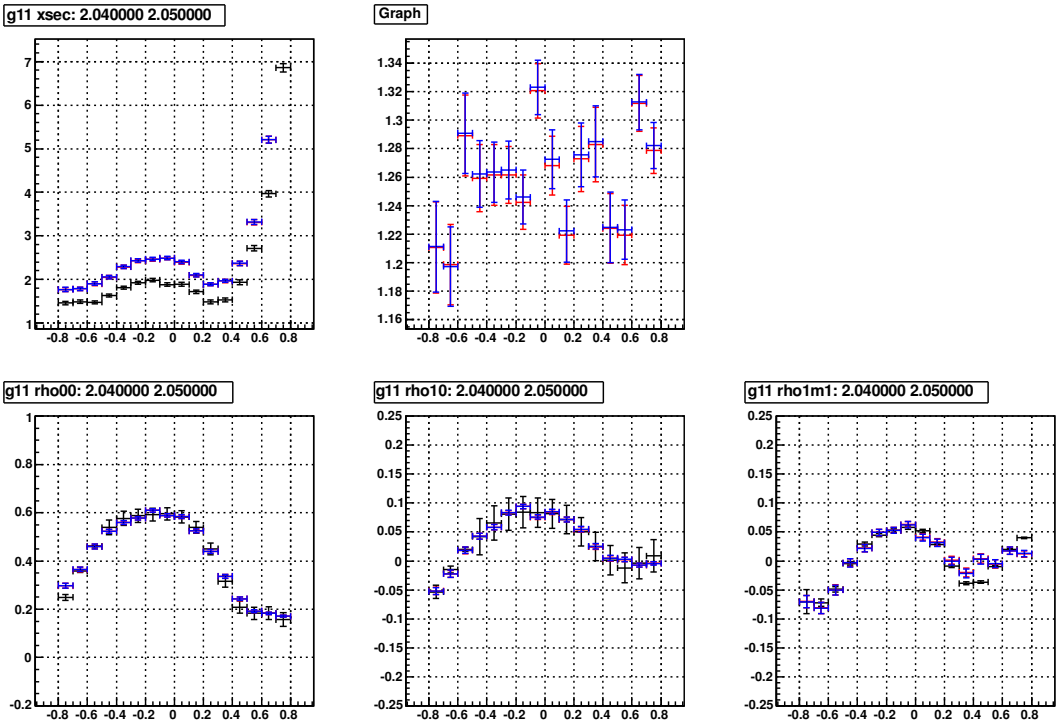

Bin 4 : $W = 2.04$ - 2.05 GeV

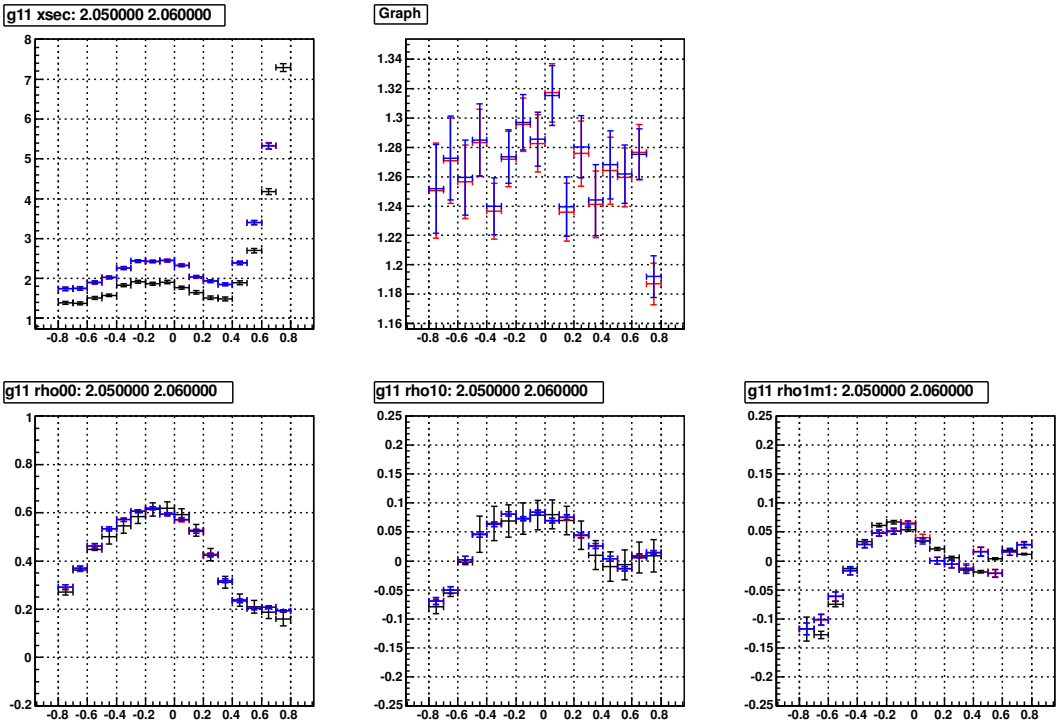

Bin 5 : $W = 2.05$ - 2.06 GeV

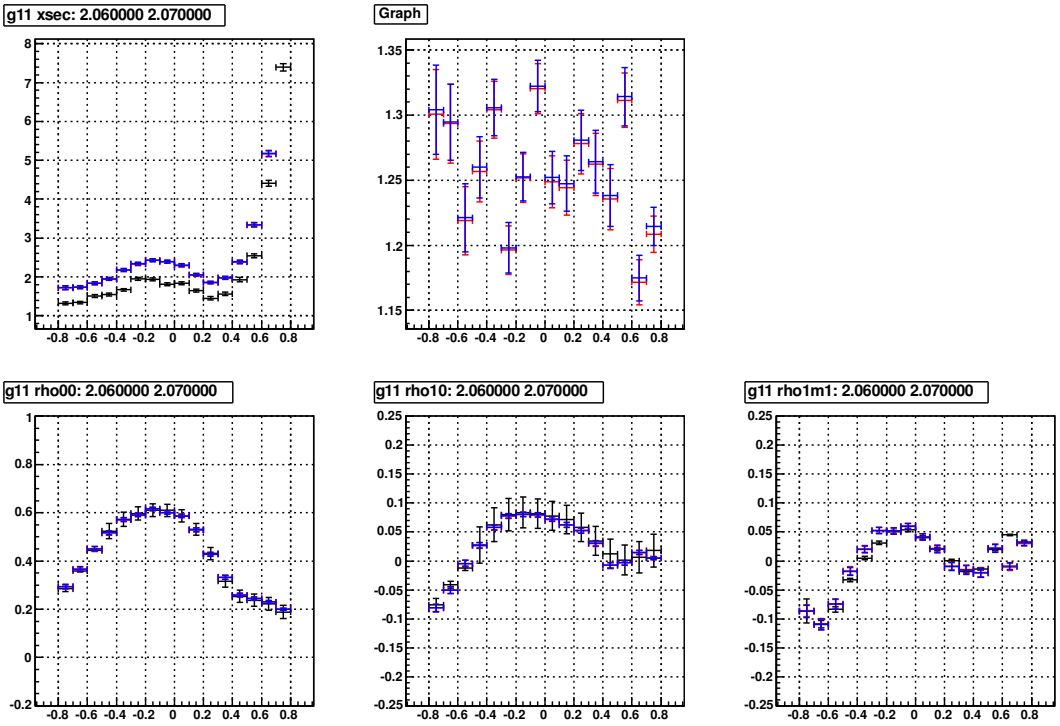

Bin 6 : $W = 2.06$ - 2.07 GeV

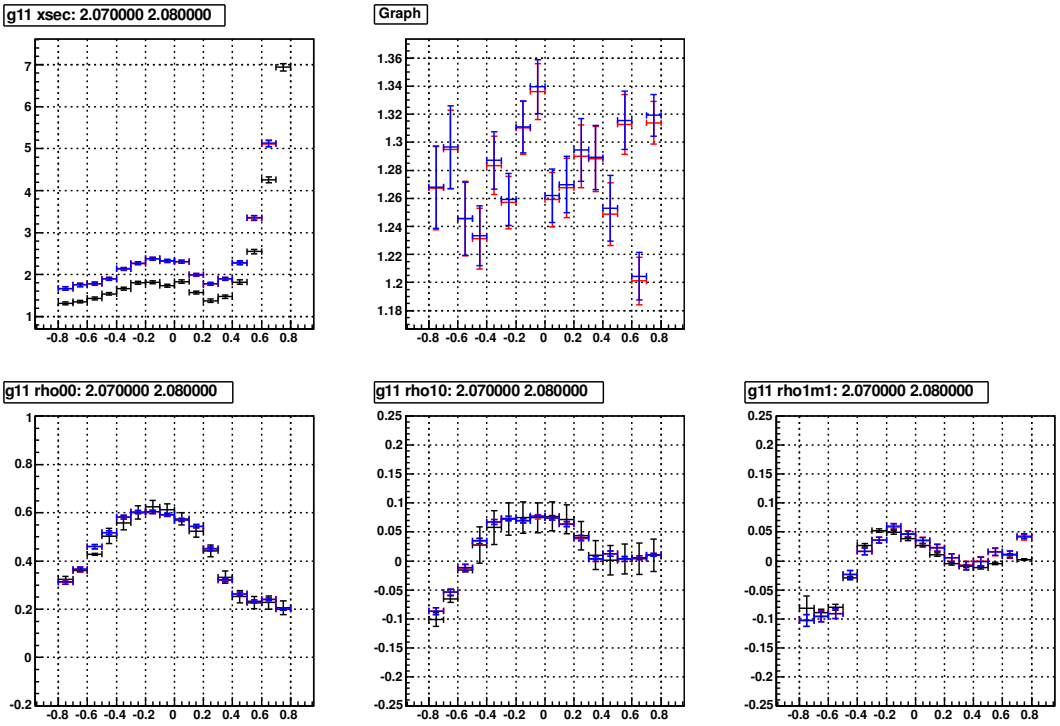

Bin 7 : $W = 2.07$ - 2.08 GeV

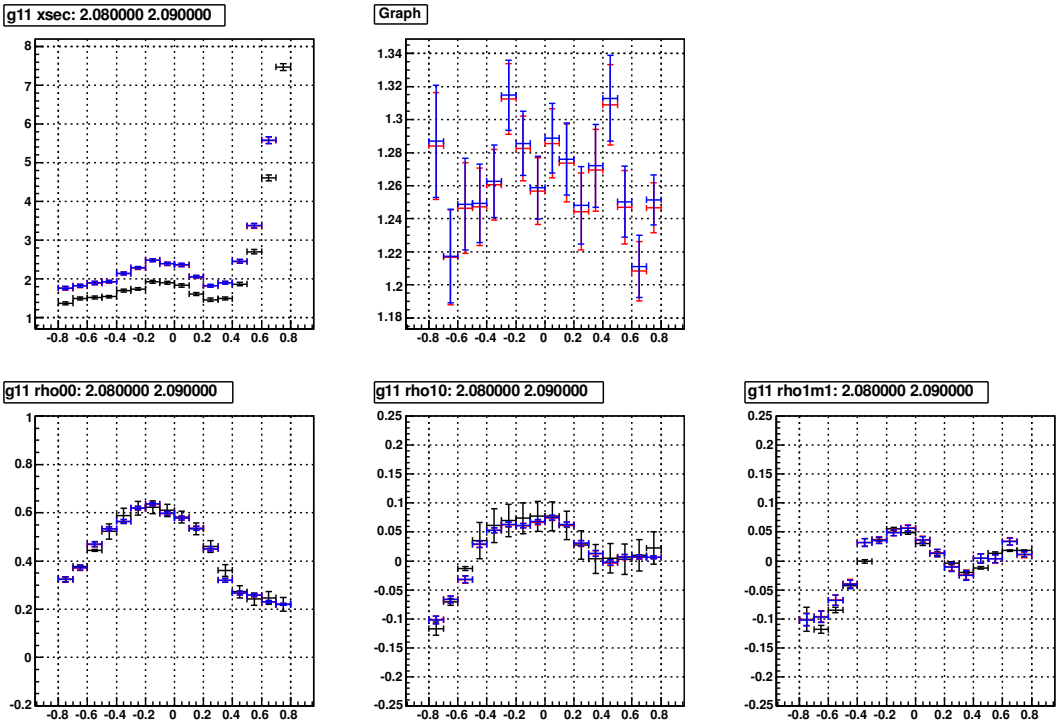

Bin 8 : $W = 2.08$ - 2.09 GeV

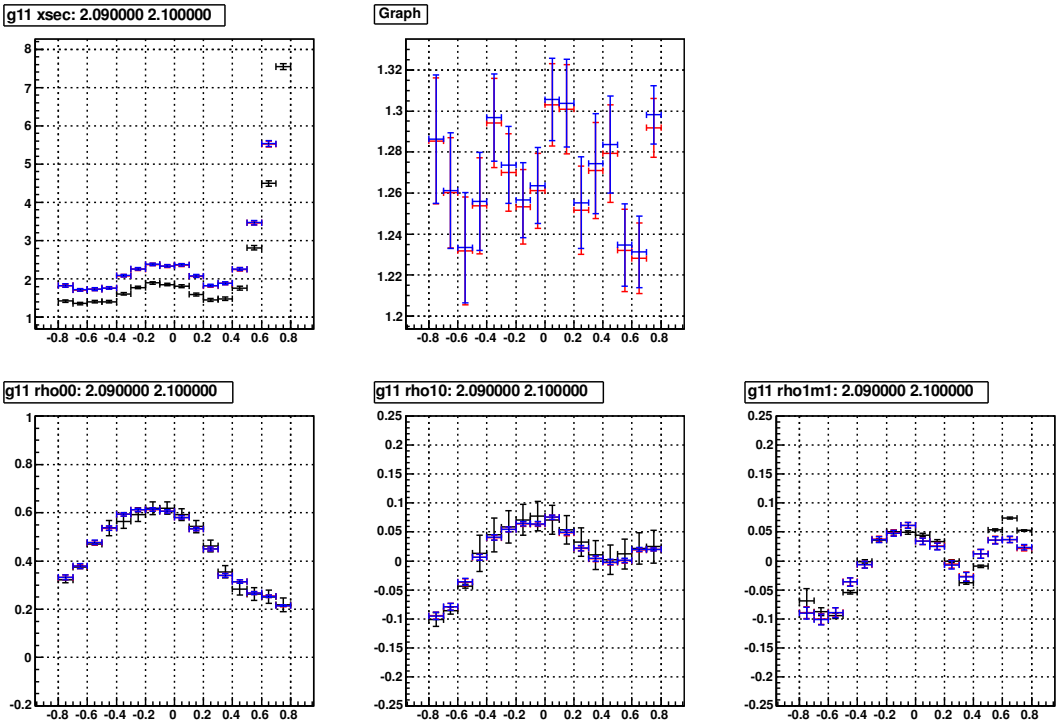

Bin 9 : $W = 2.09$ - 2.10 GeV

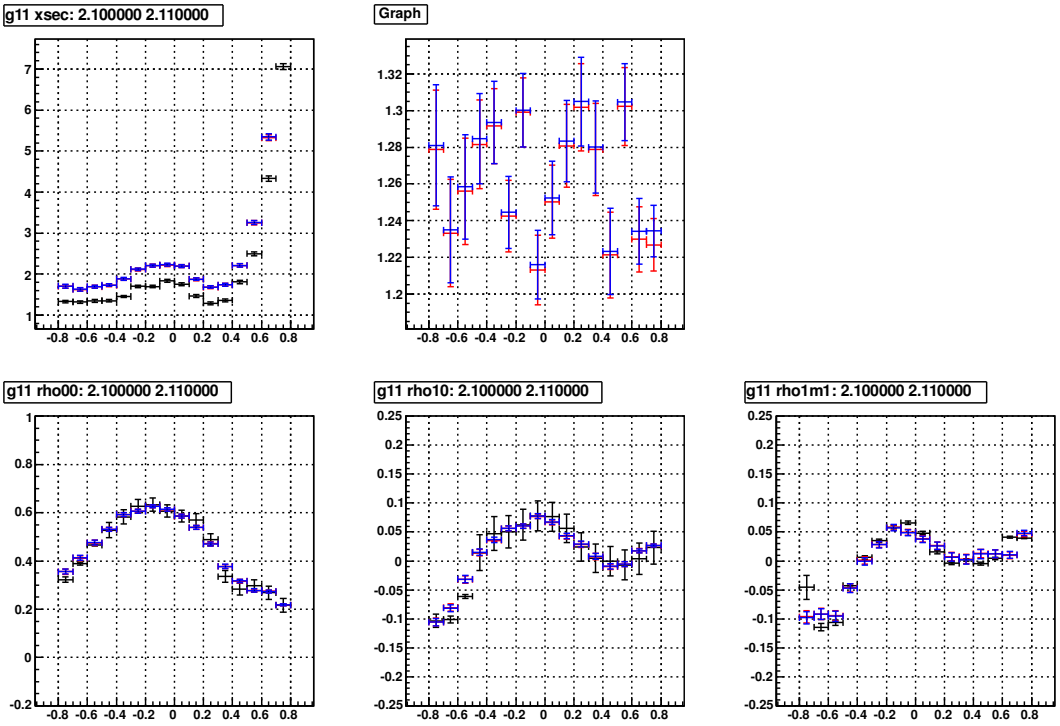

Bin 10 : $W = 2.10$ - 2.11 GeV

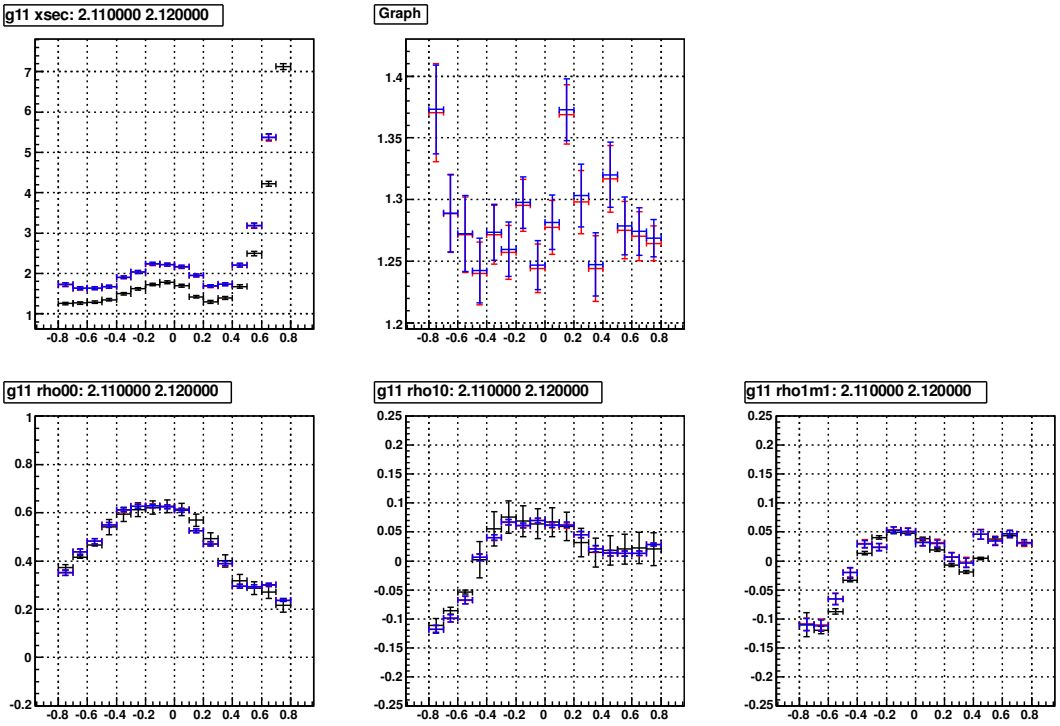

Bin 11 : $W = 2.11$ - 2.12 GeV

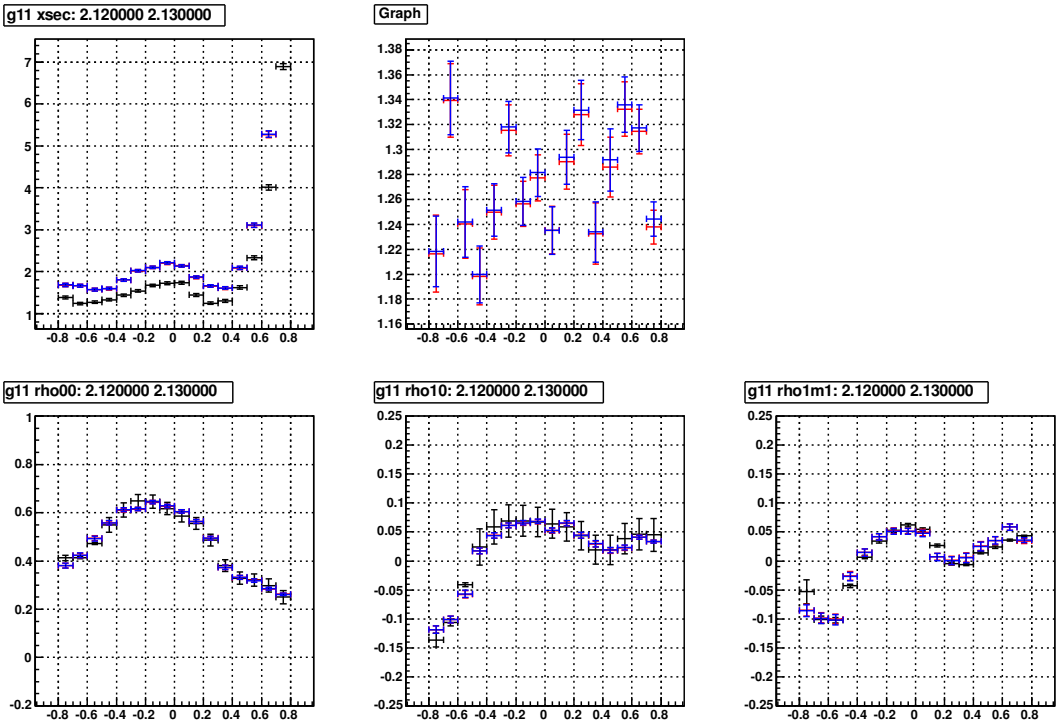

Bin 12 : $W = 2.12$ - 2.13 GeV

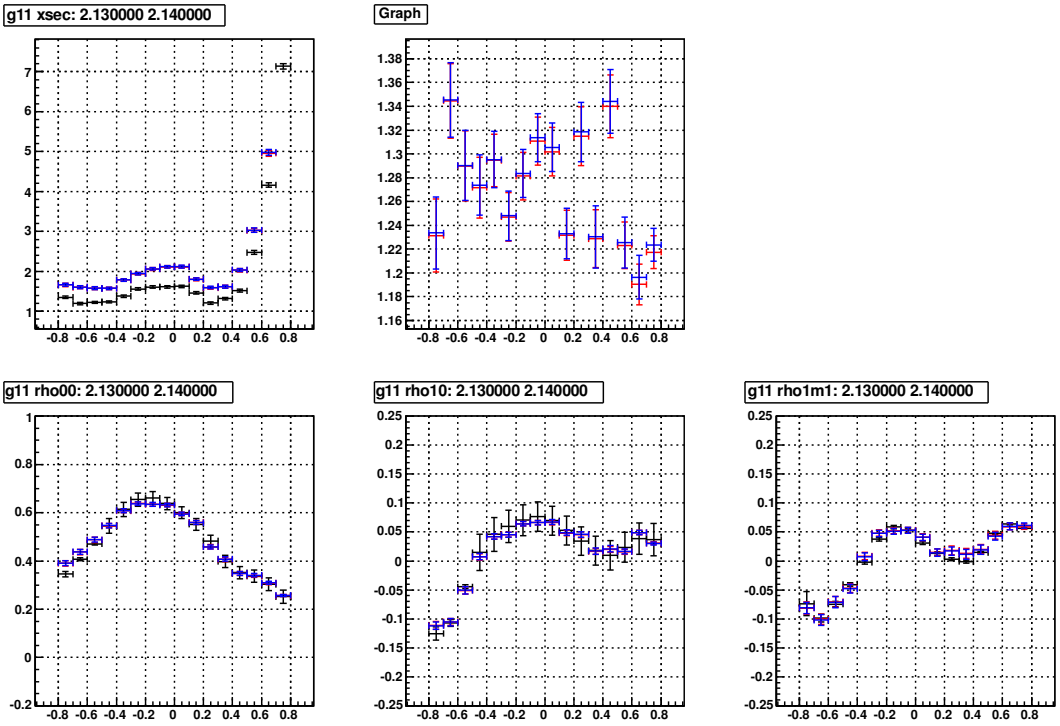

Bin 13 : $W = 2.13$ - 2.14 GeV

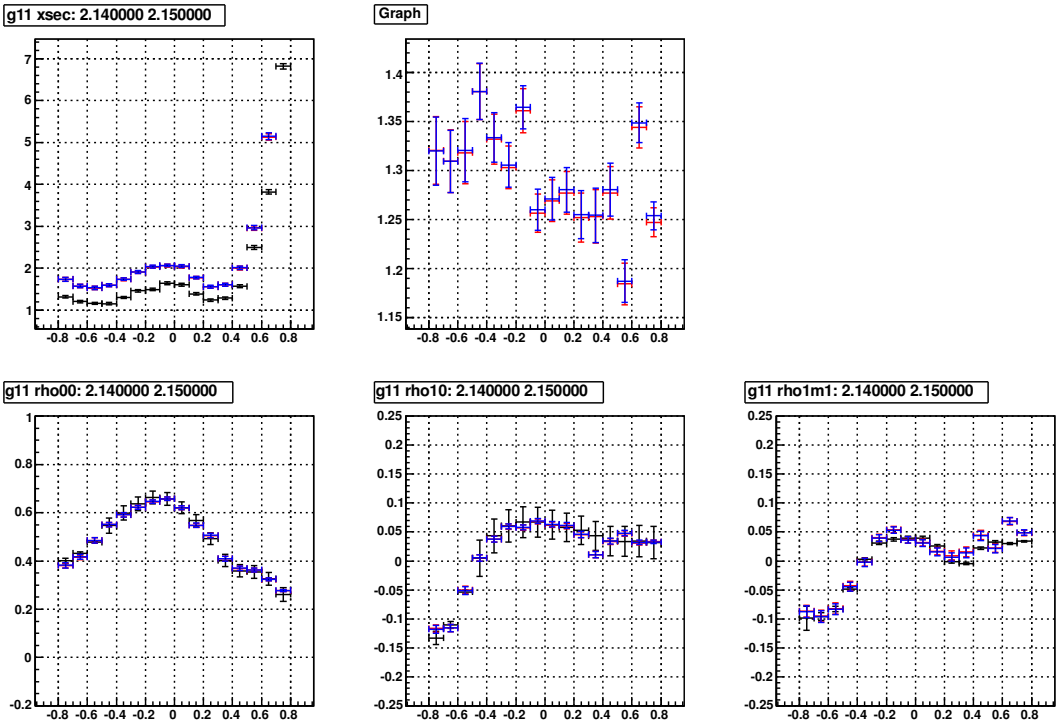

Bin 14 : $W = 2.14$ - 2.15 GeV

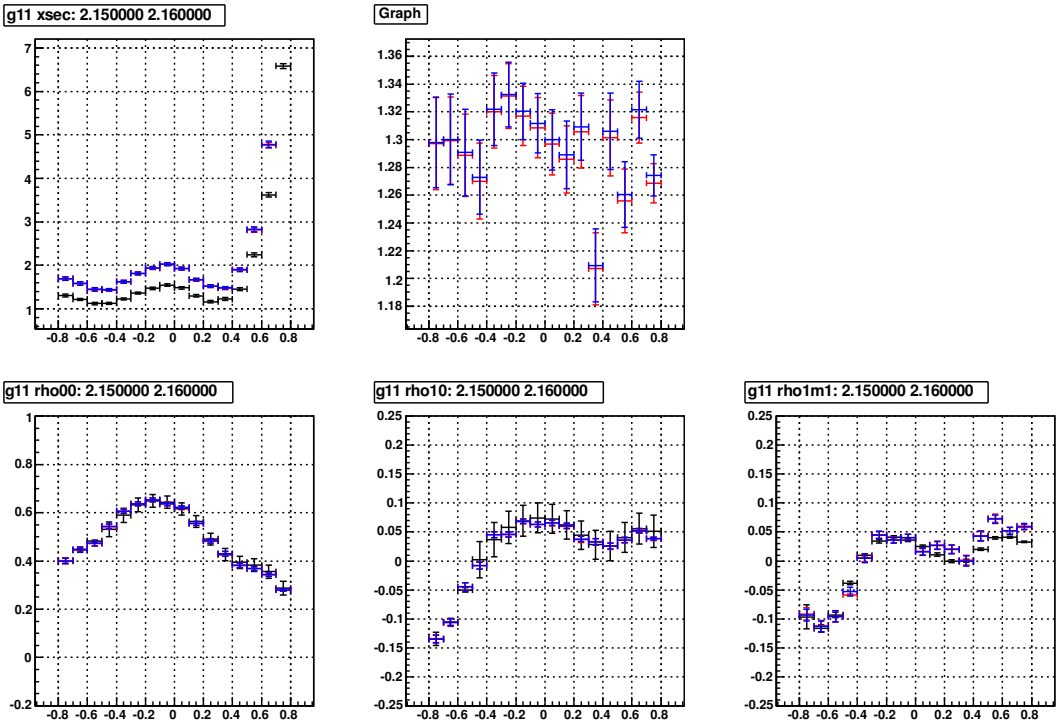

Bin 15 : $W = 2.15$ - 2.16 GeV

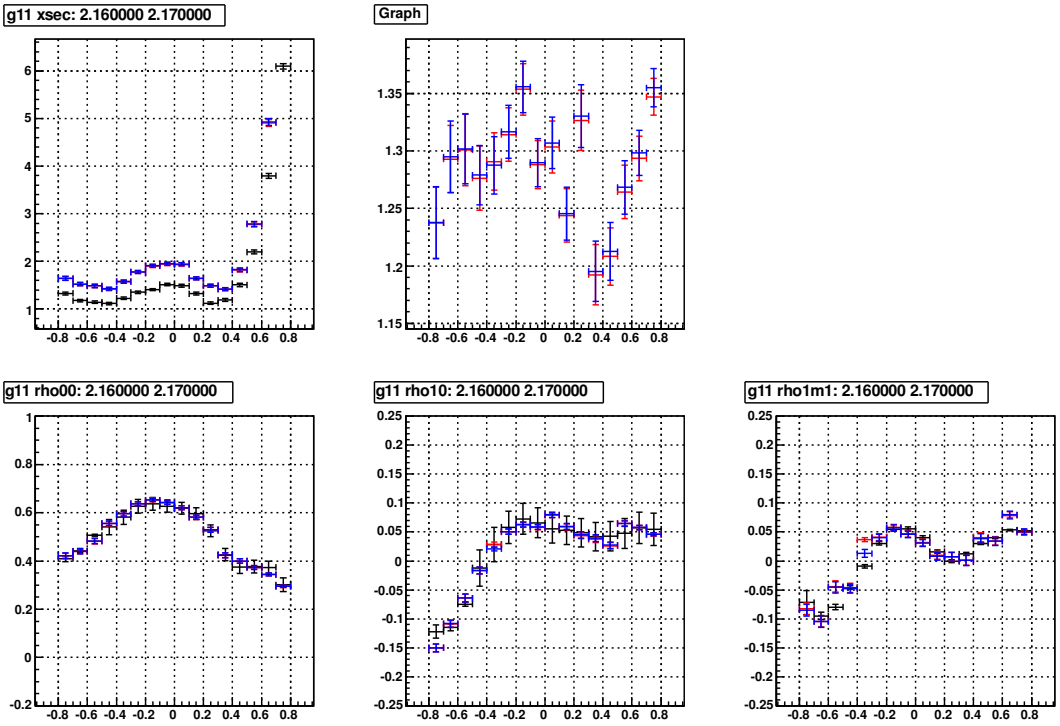

Bin 16 : $W = 2.16$ - 2.17 GeV

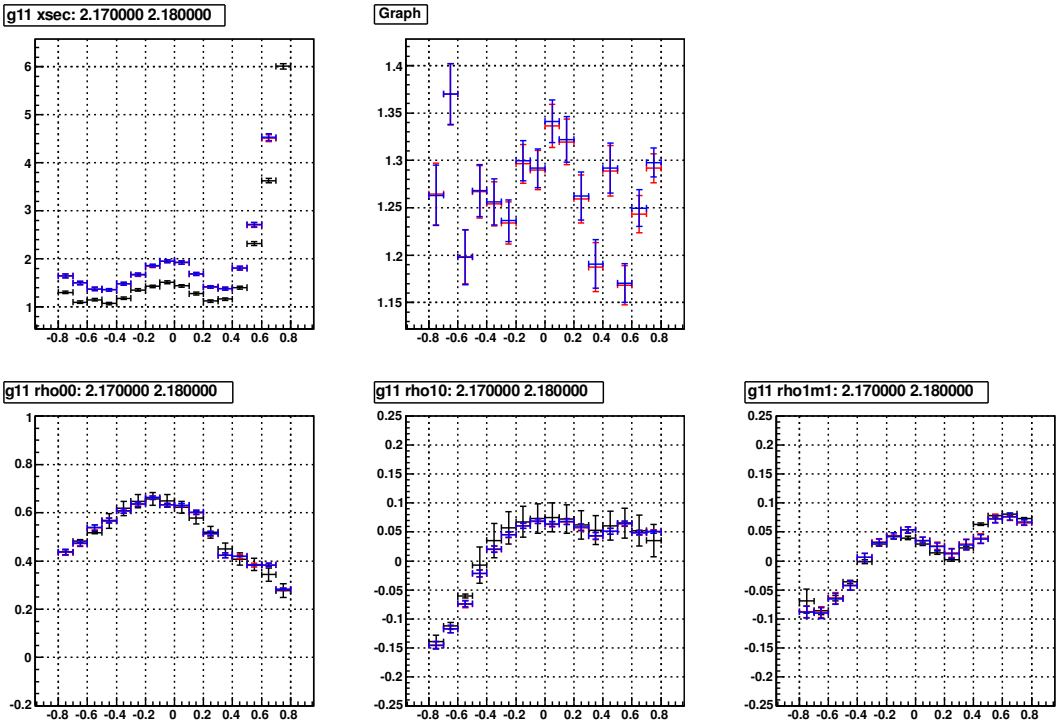

Bin 17 : $W = 2.17$ - 2.18 GeV

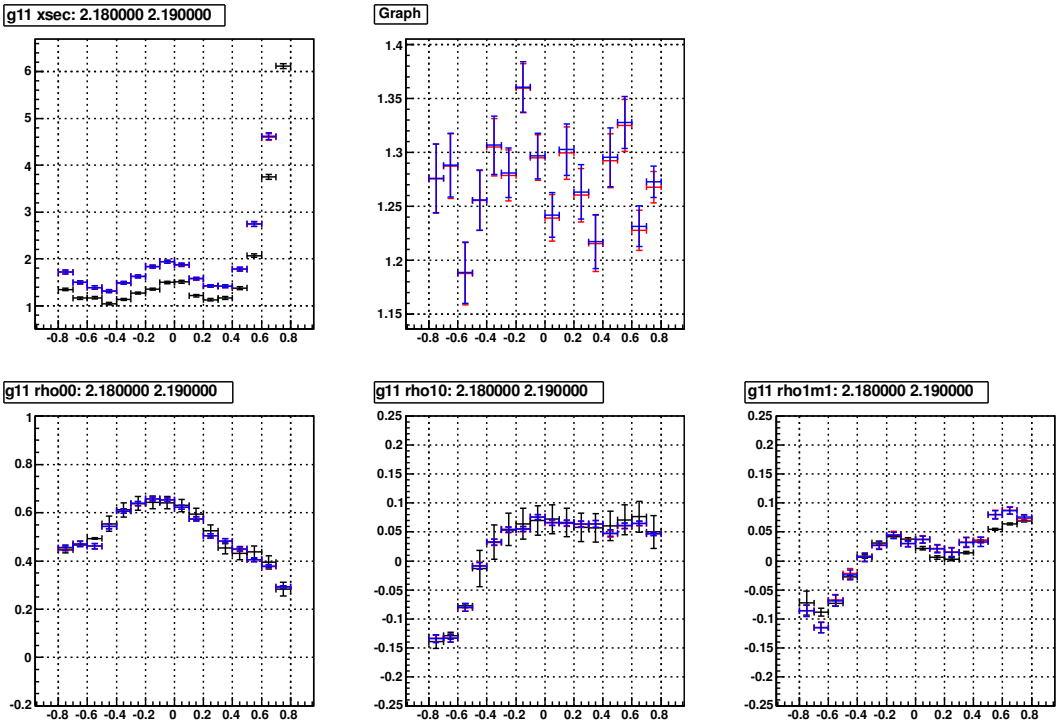

Bin 18 : $W = 2.18$ - 2.19 GeV

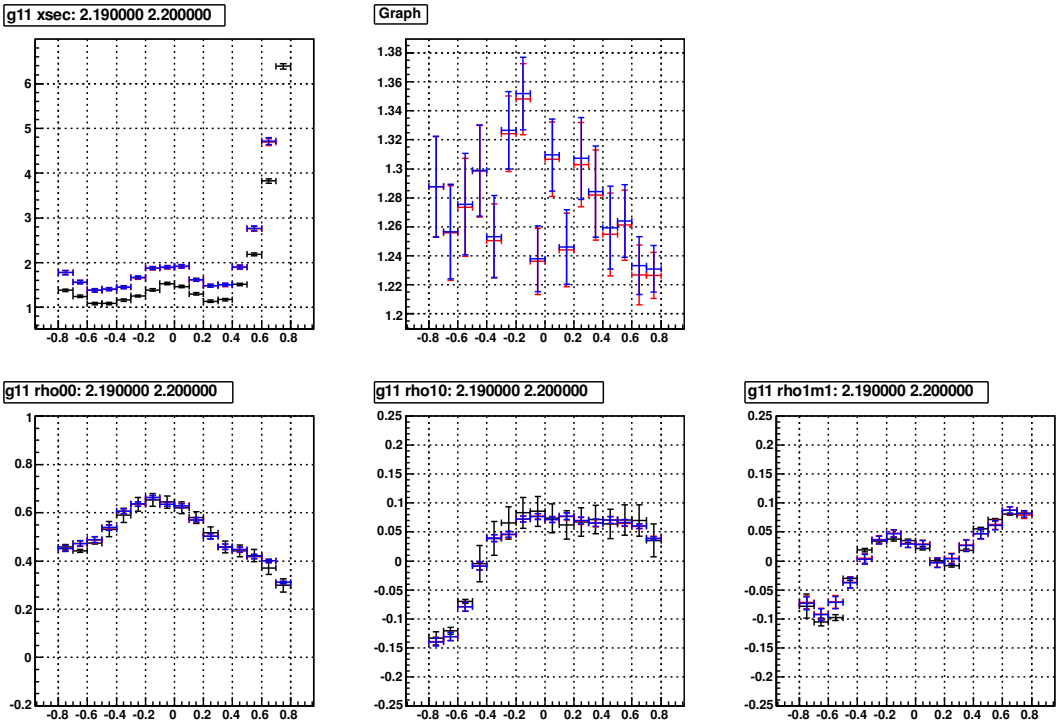

Bin 19 : $W = 2.19$ - 2.20 GeV

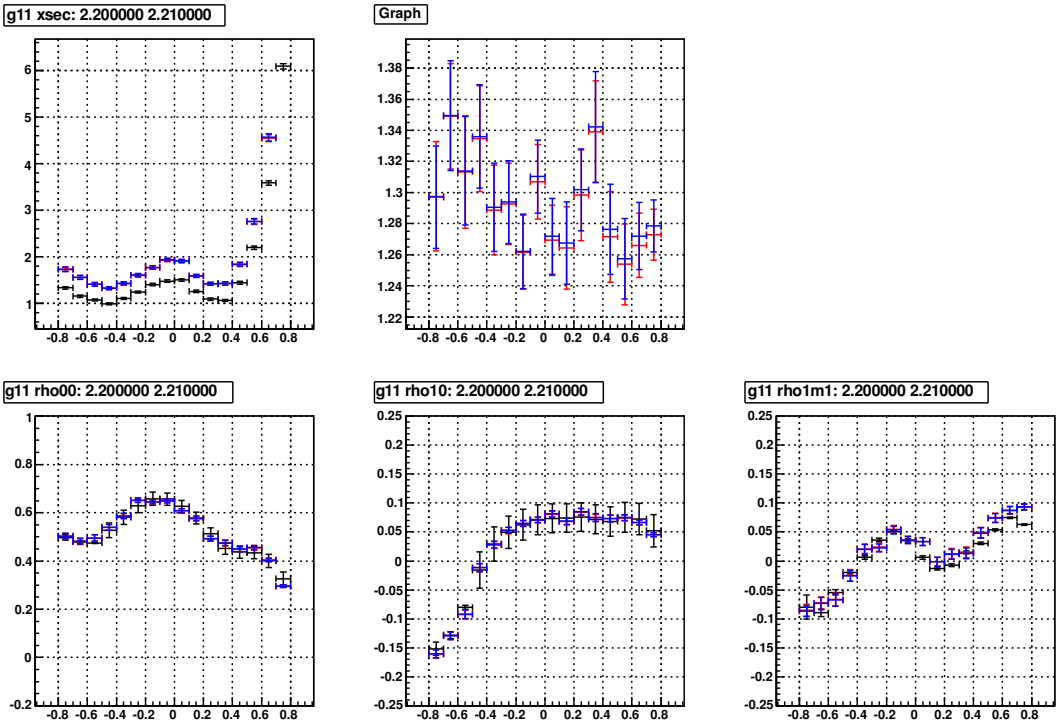

Bin 20 : $W = 2.20$ - 2.21 GeV

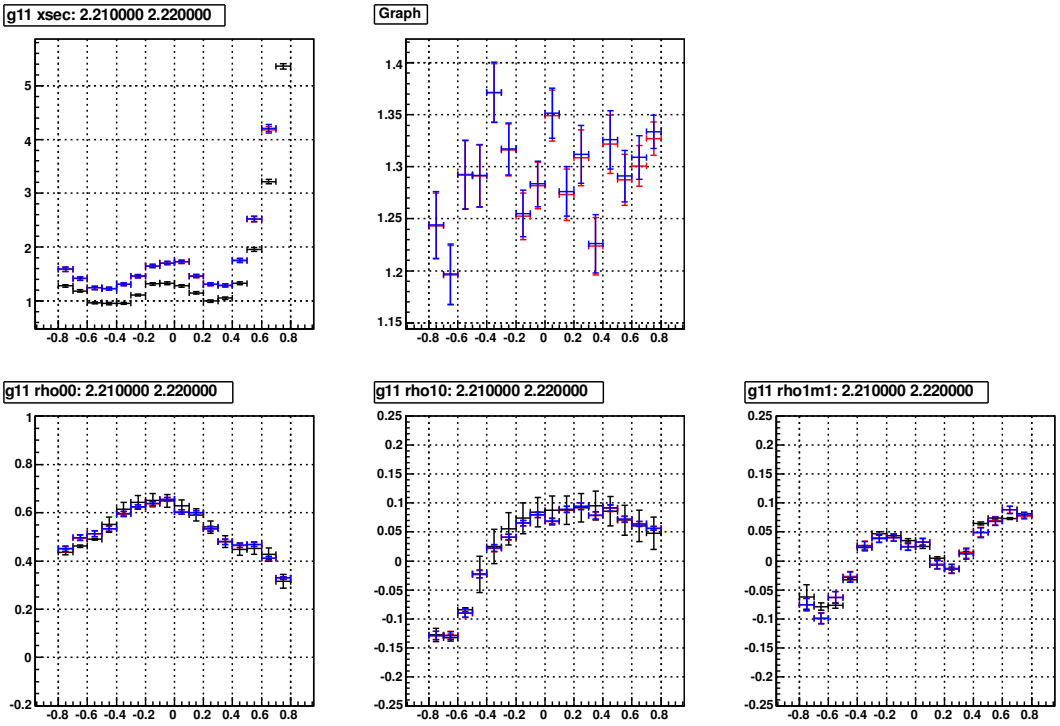

Bin 21 : $W = 2.21$ - 2.22 GeV

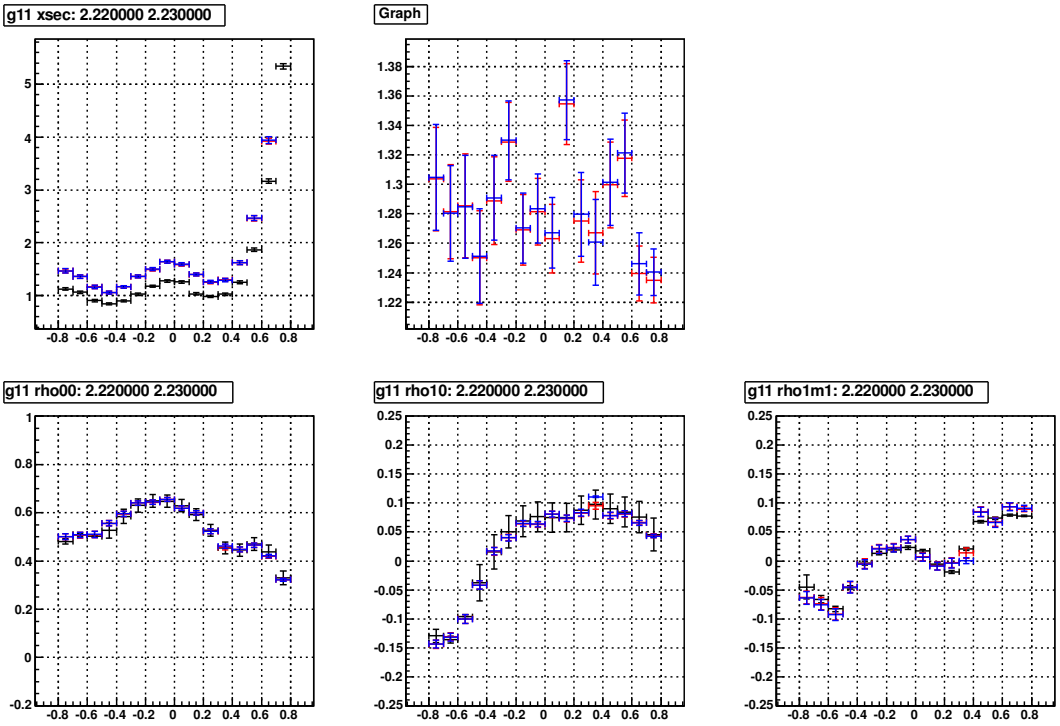

Bin 22 : $W = 2.22$ - 2.23 GeV

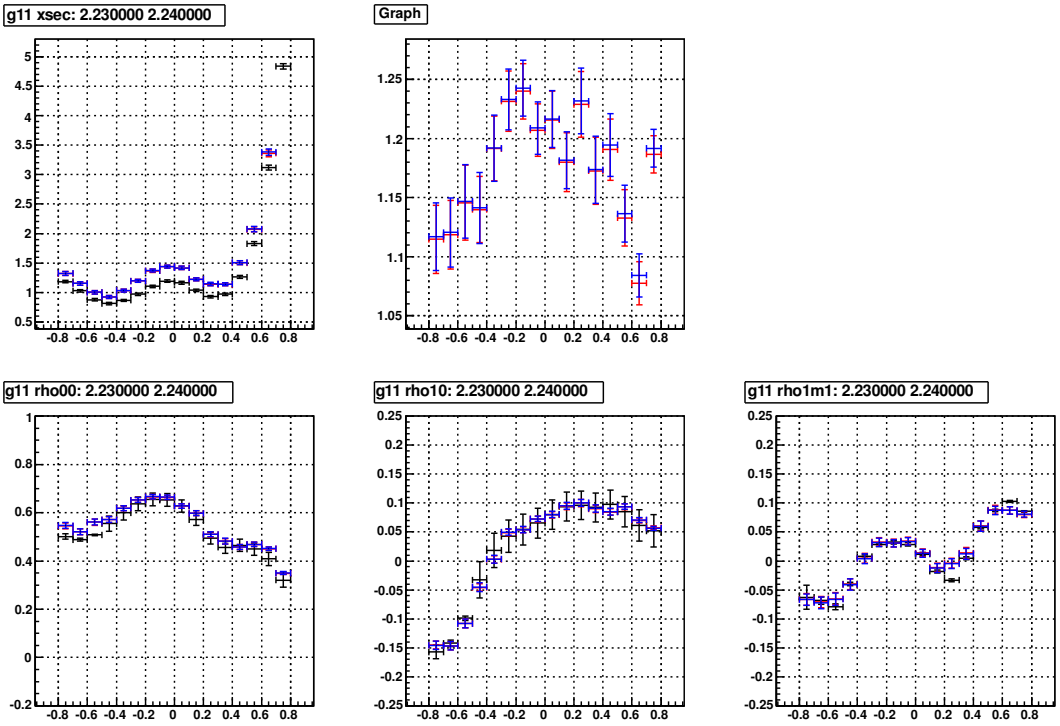

Bin 23 : $W = 2.23$ - 2.24 GeV

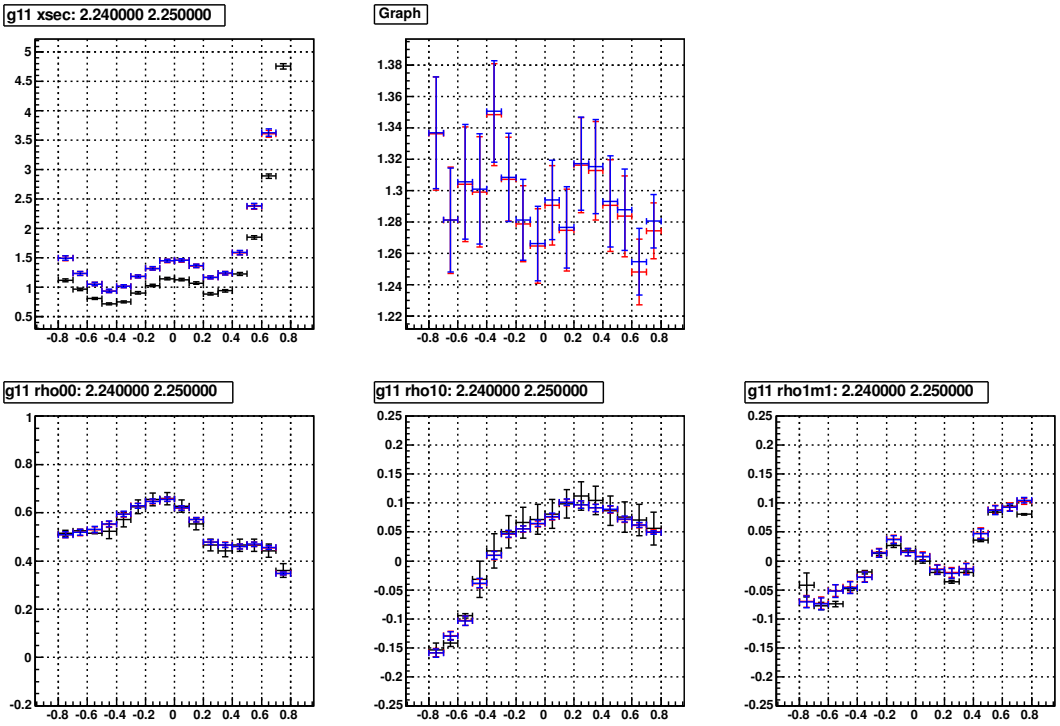

Bin 24 : $W = 2.24$ - 2.25 GeV

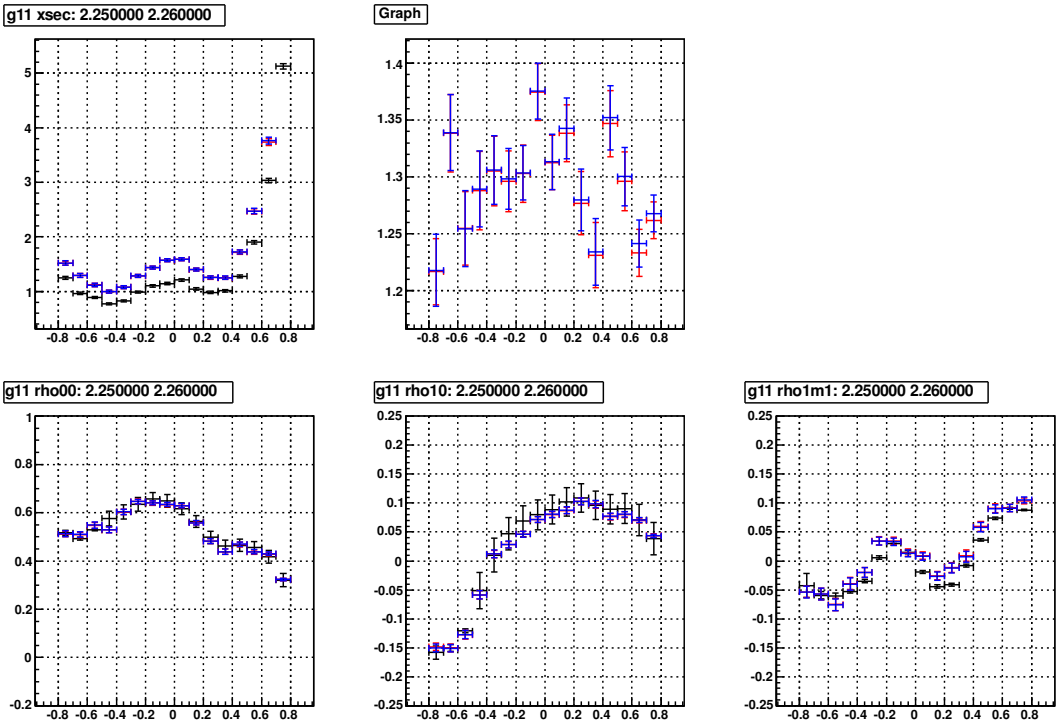

Bin 25 : $W = 2.25$ - 2.26 GeV

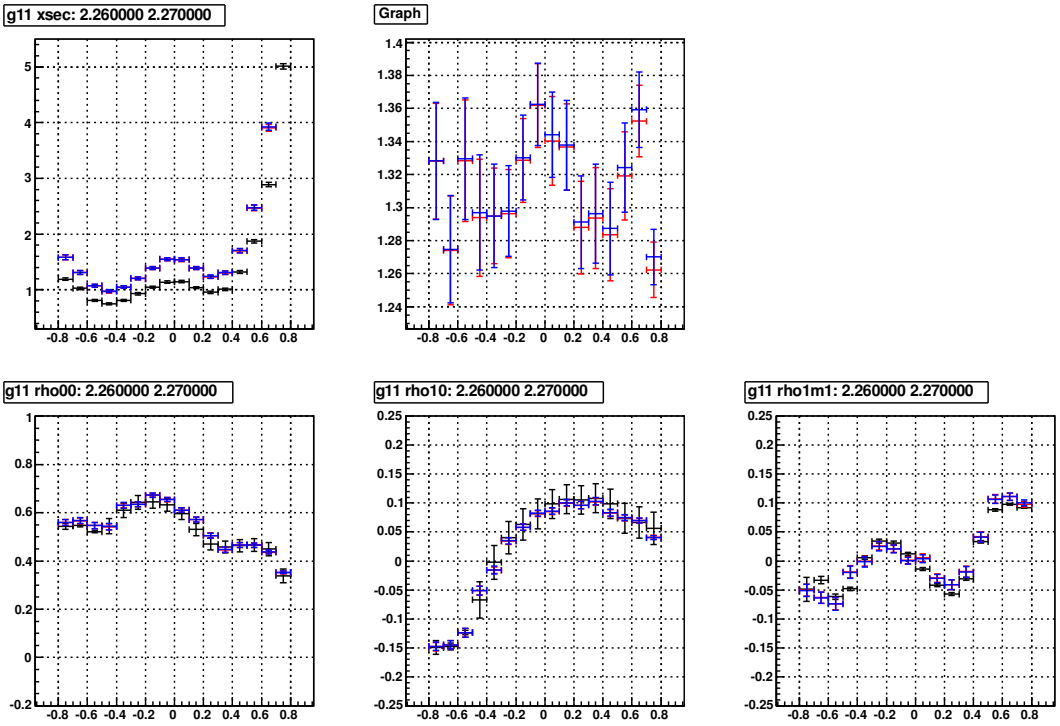

Bin 26 : $W = 2.26$ - 2.27 GeV

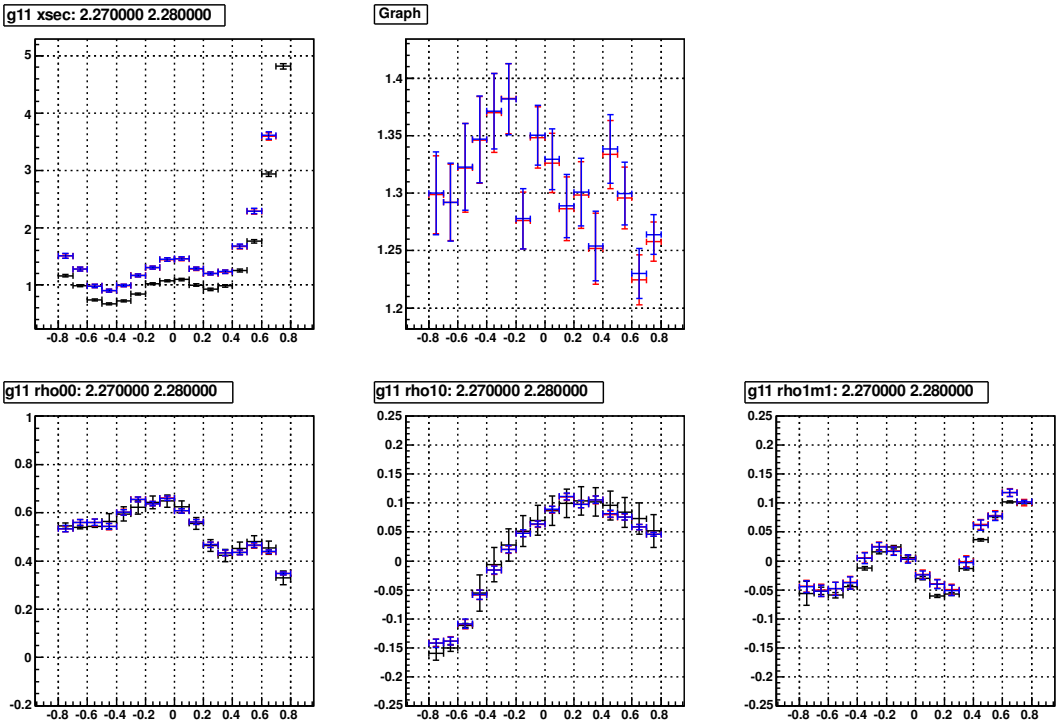

Bin 27 : $W = 2.27$ - 2.28 GeV

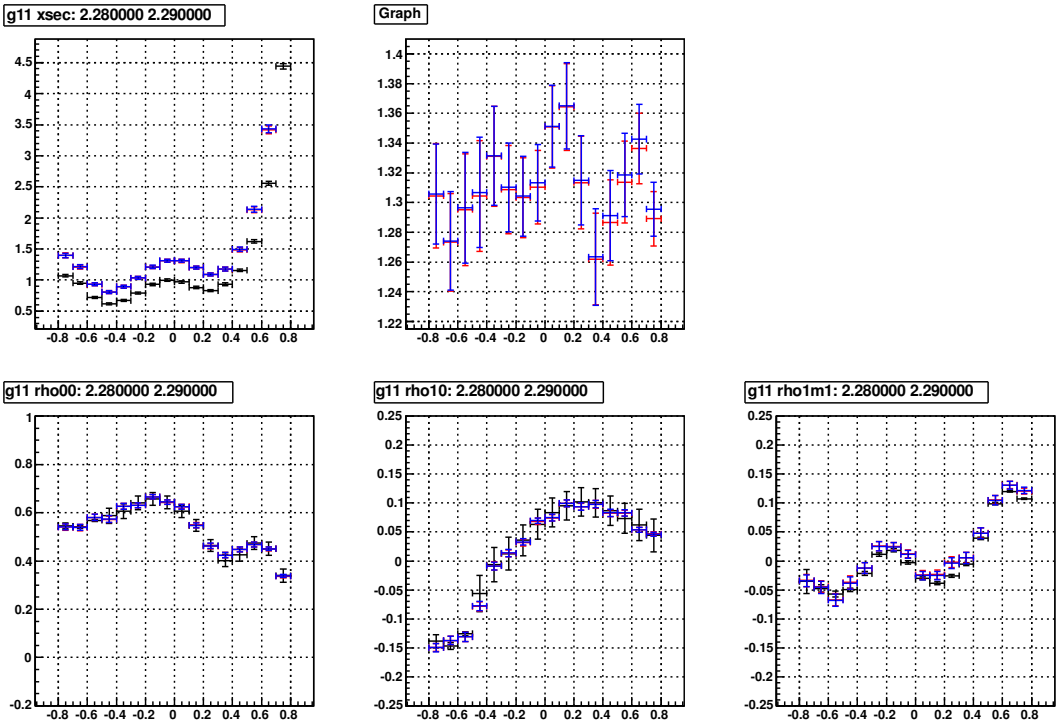

Bin 28 : $W = 2.28$ - 2.29 GeV

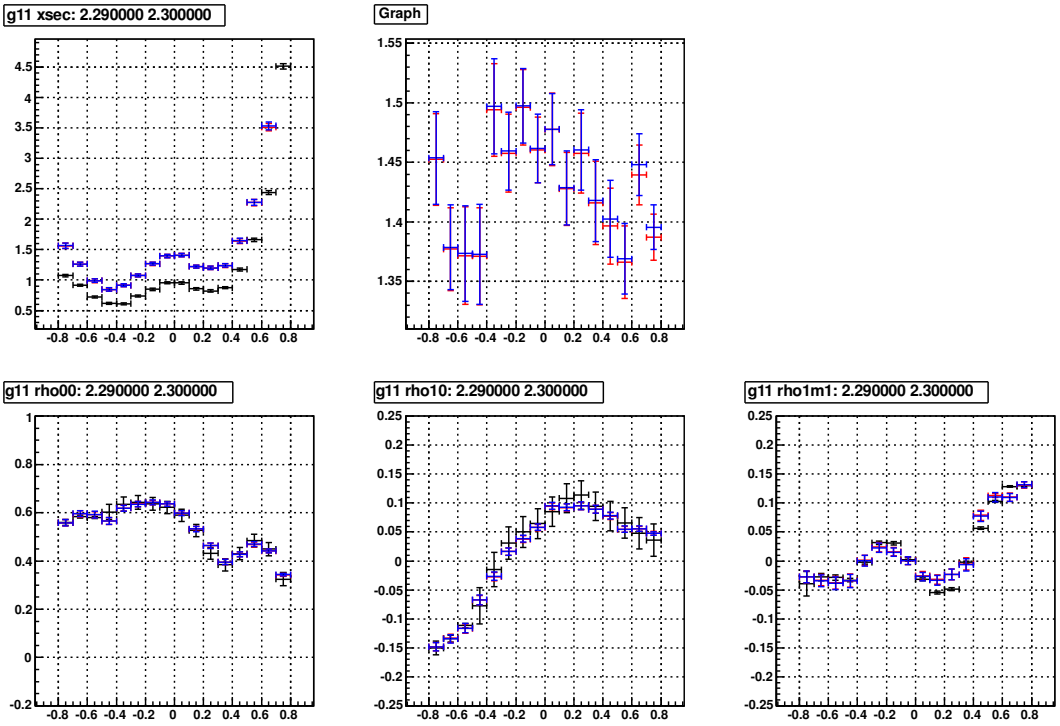

Bin 29 : $W = 2.29$ - 2.30 GeV

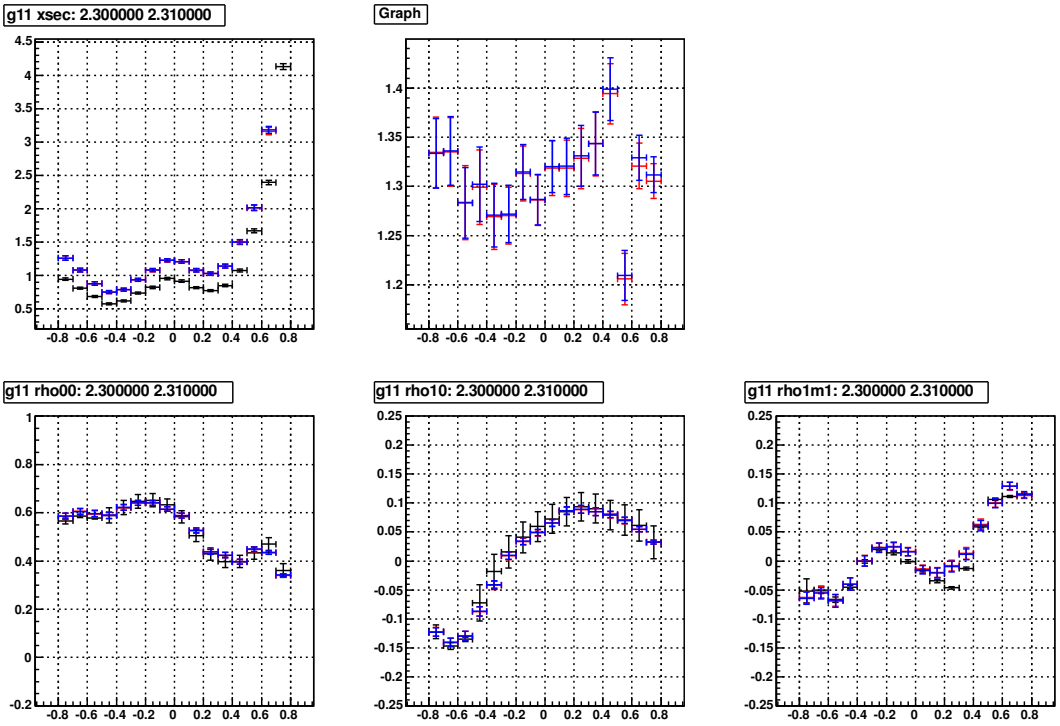

Bin 30 : $W = 2.30$ - 2.31 GeV

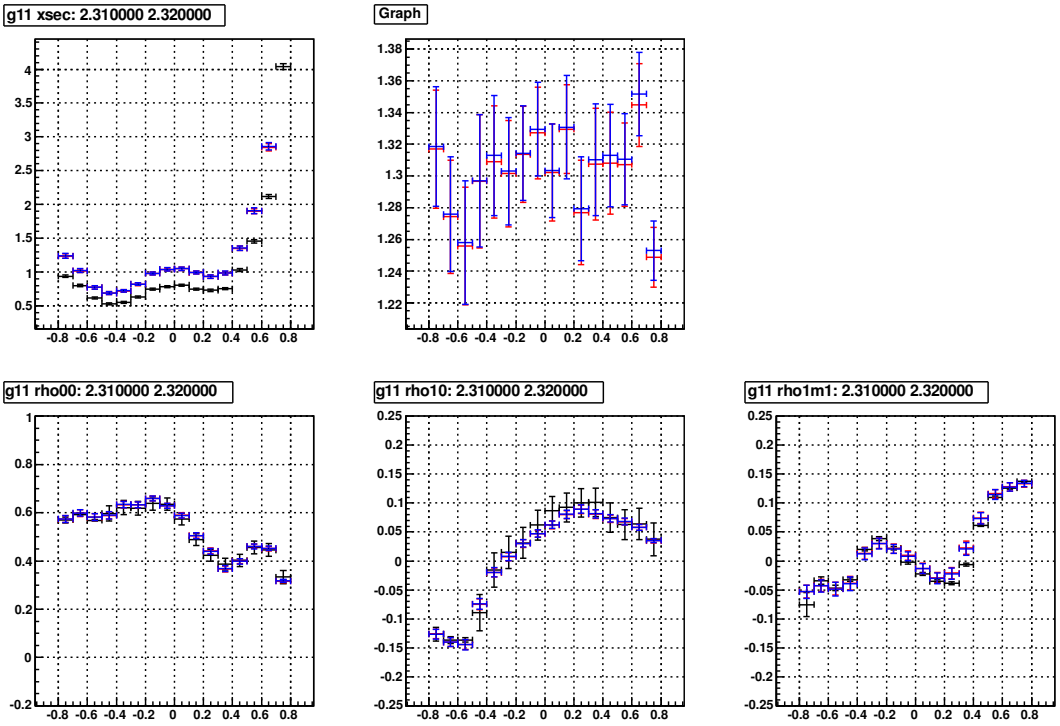

Bin 31 : $W = 2.31$ - 2.32 GeV

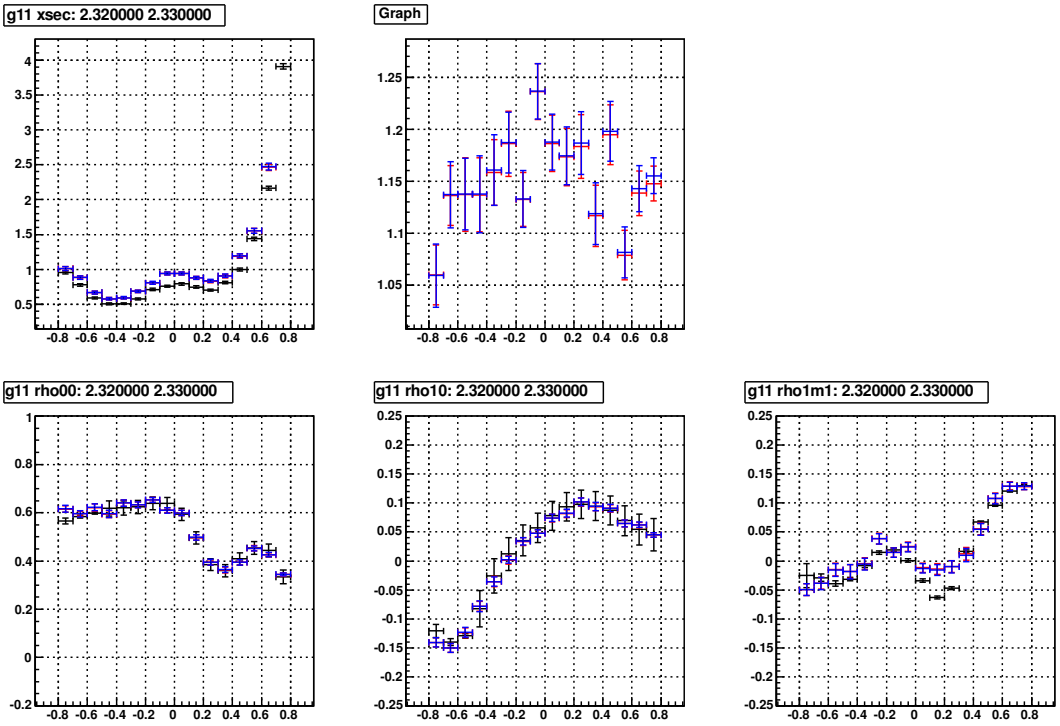

Bin 32 : $W = 2.32$ - 2.33 GeV

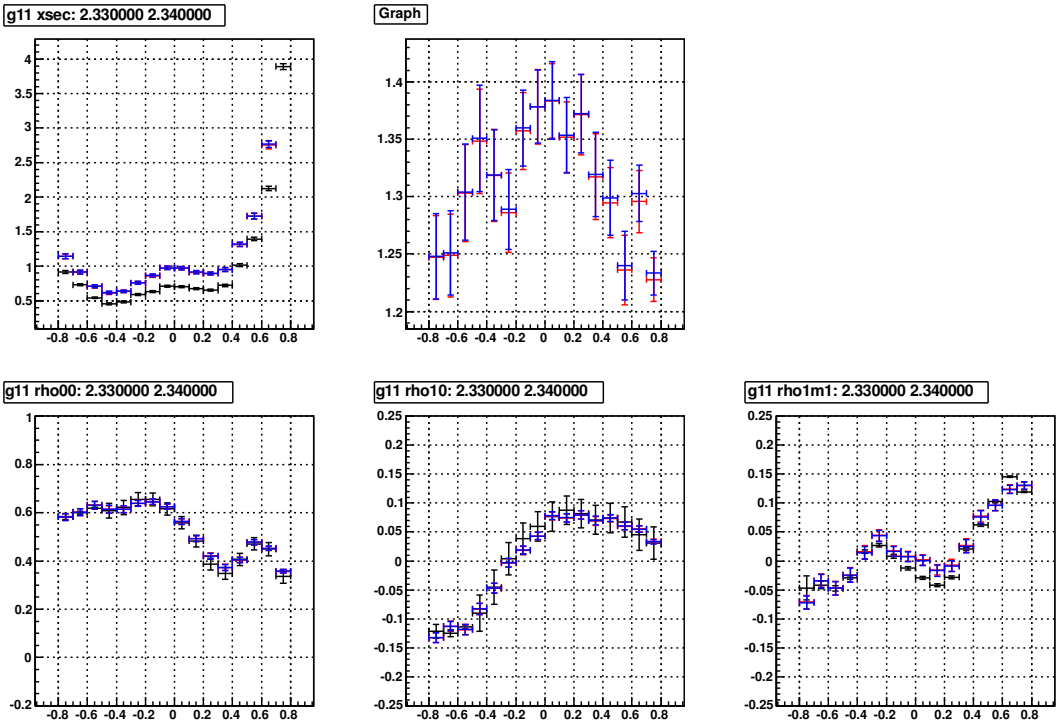

Bin 33 : $W = 2.33$ - 2.34 GeV

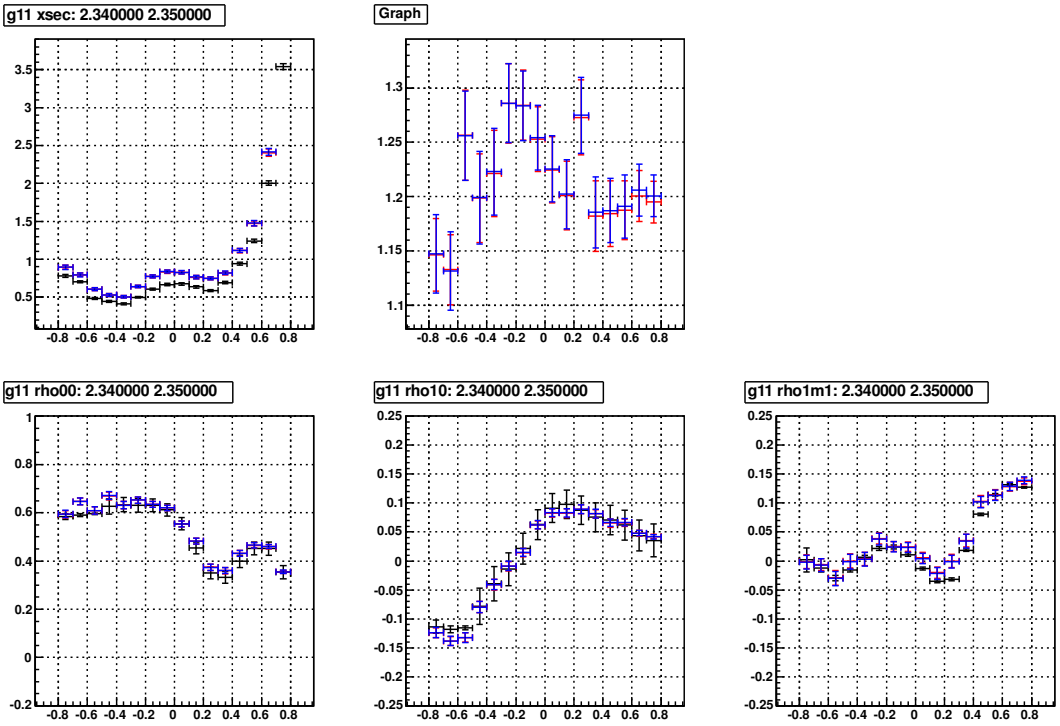

Bin 34 : $W = 2.34$ - 2.35 GeV

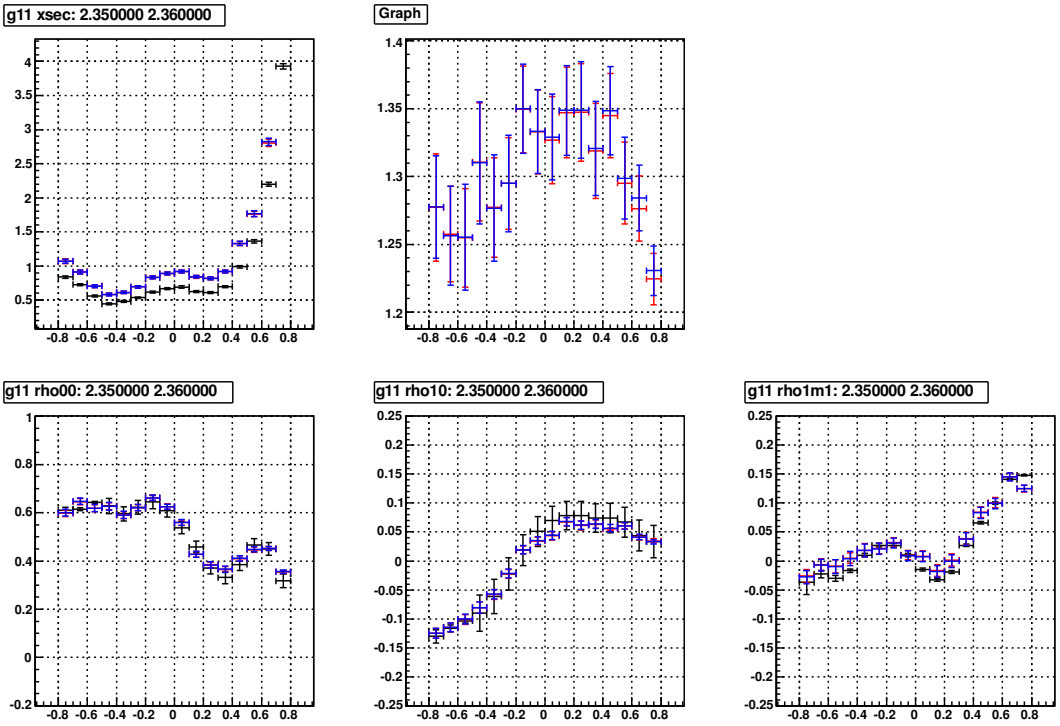

Bin 35 : $W = 2.35$ - 2.36 GeV

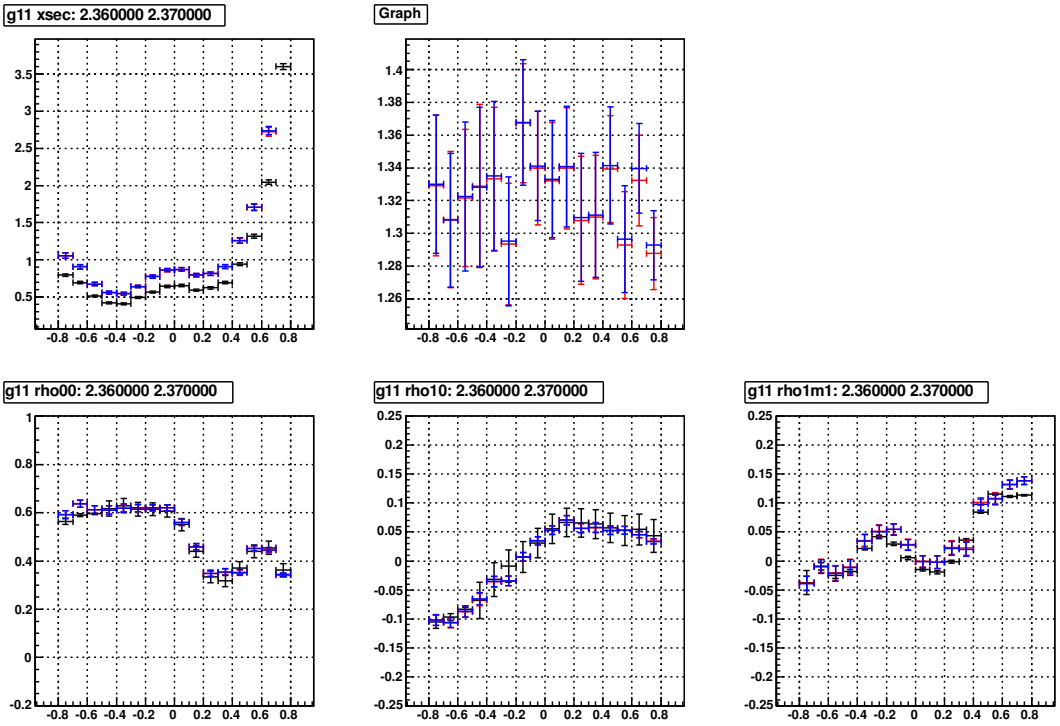

Bin 36 : $W = 2.36$ - 2.37 GeV

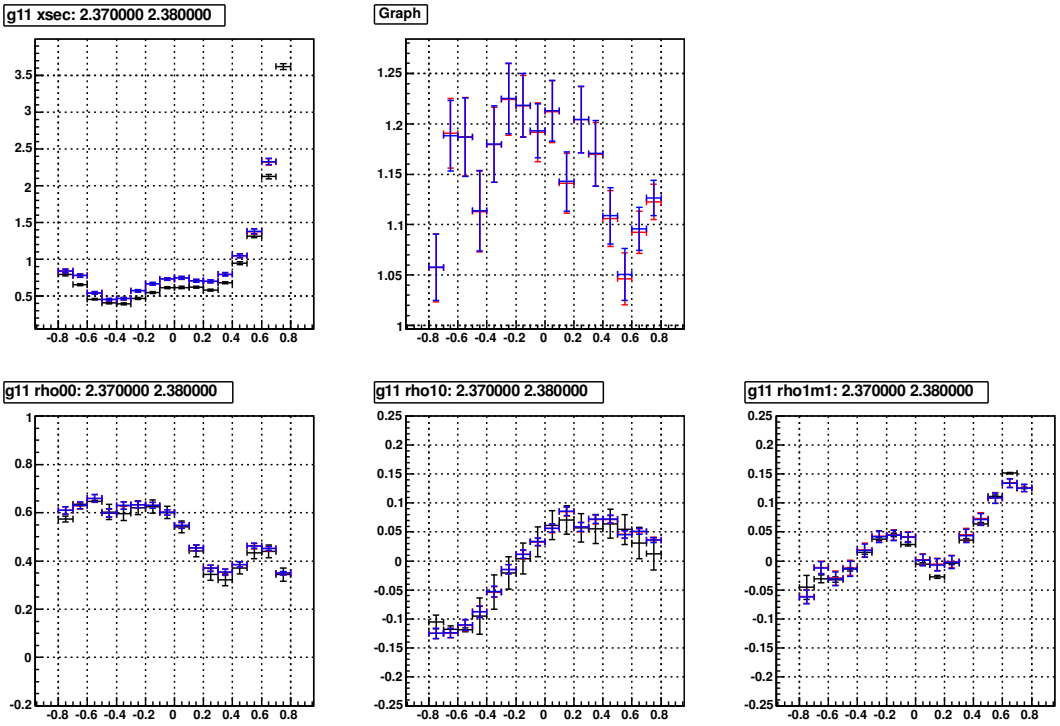

Bin 37 : $W = 2.37$ - 2.38 GeV

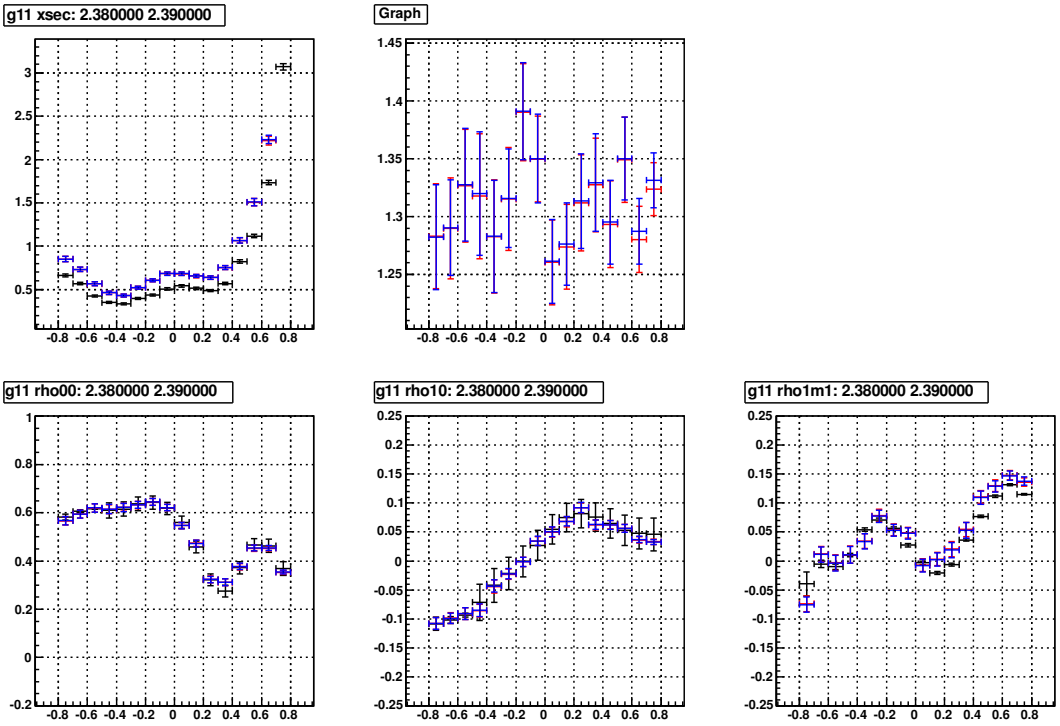

Bin 38 : $W = 2.38$ - 2.39 GeV

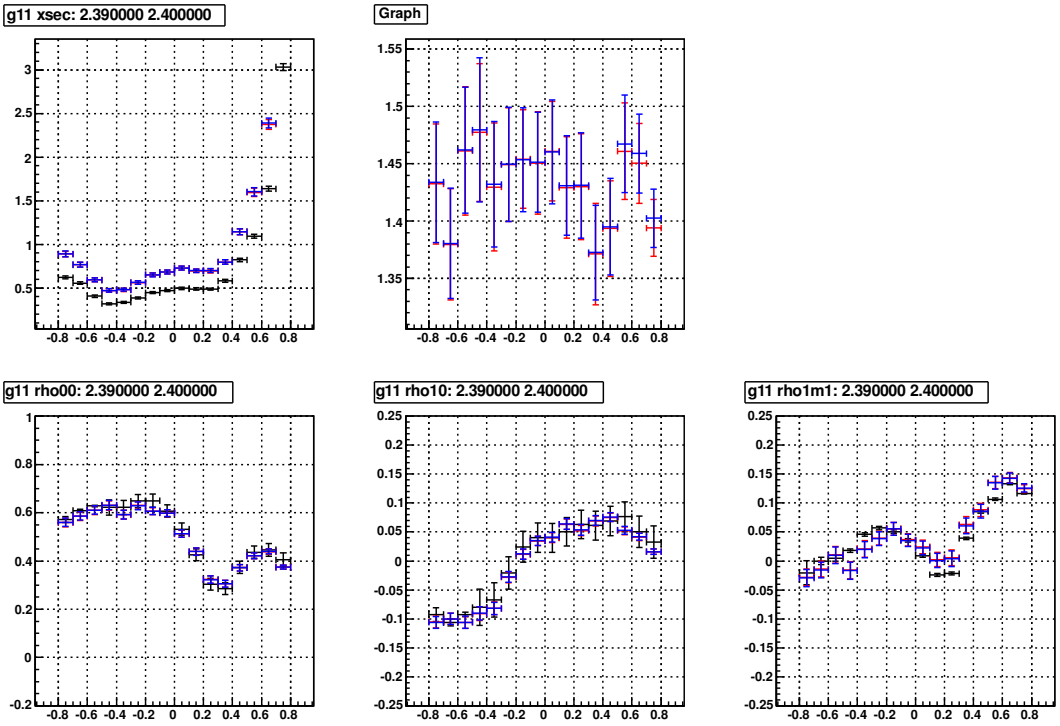

Bin 39 : $W = 2.39$ - 2.40 GeV

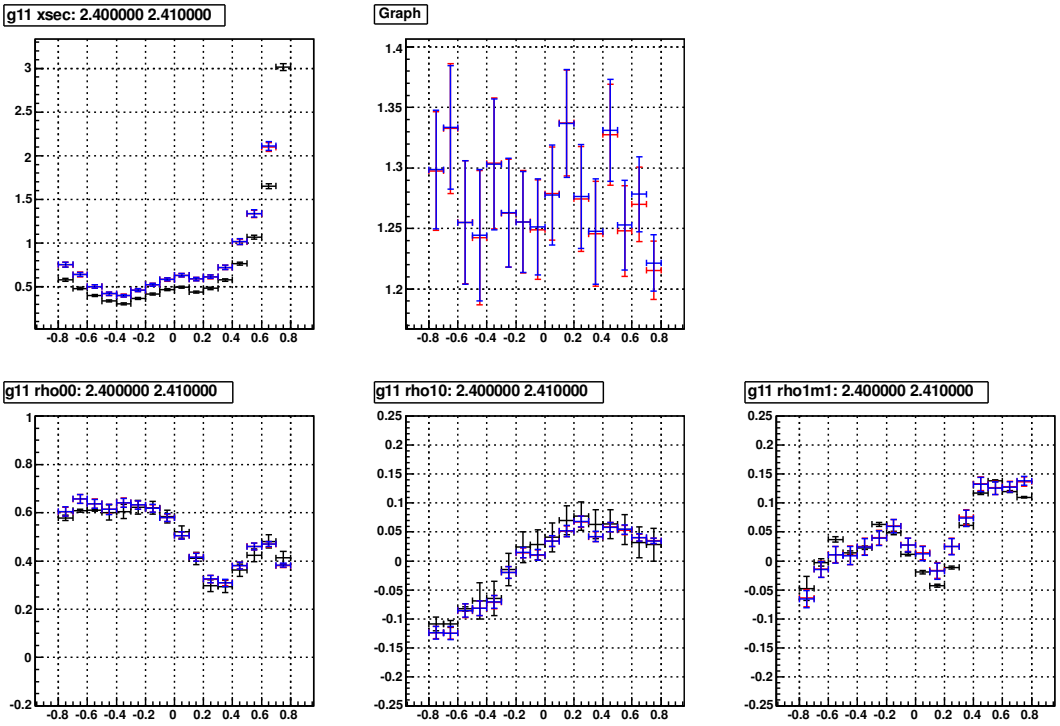

Bin 40 : $W = 2.40$ - 2.41 GeV

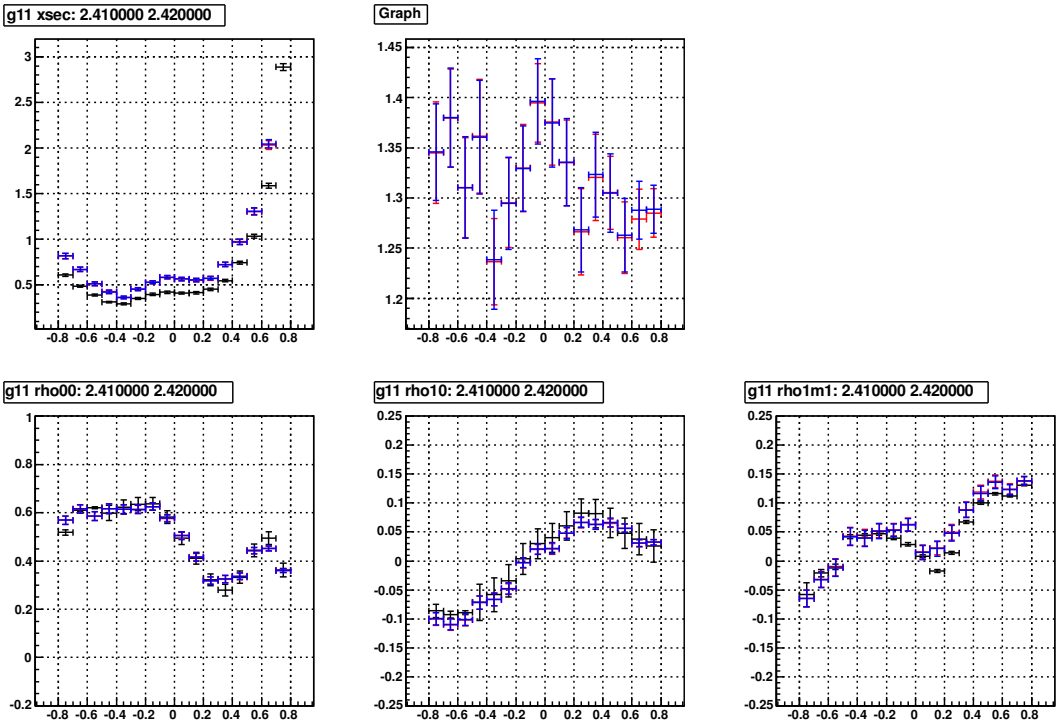

Bin 41 : $W = 2.41$ - 2.42 GeV

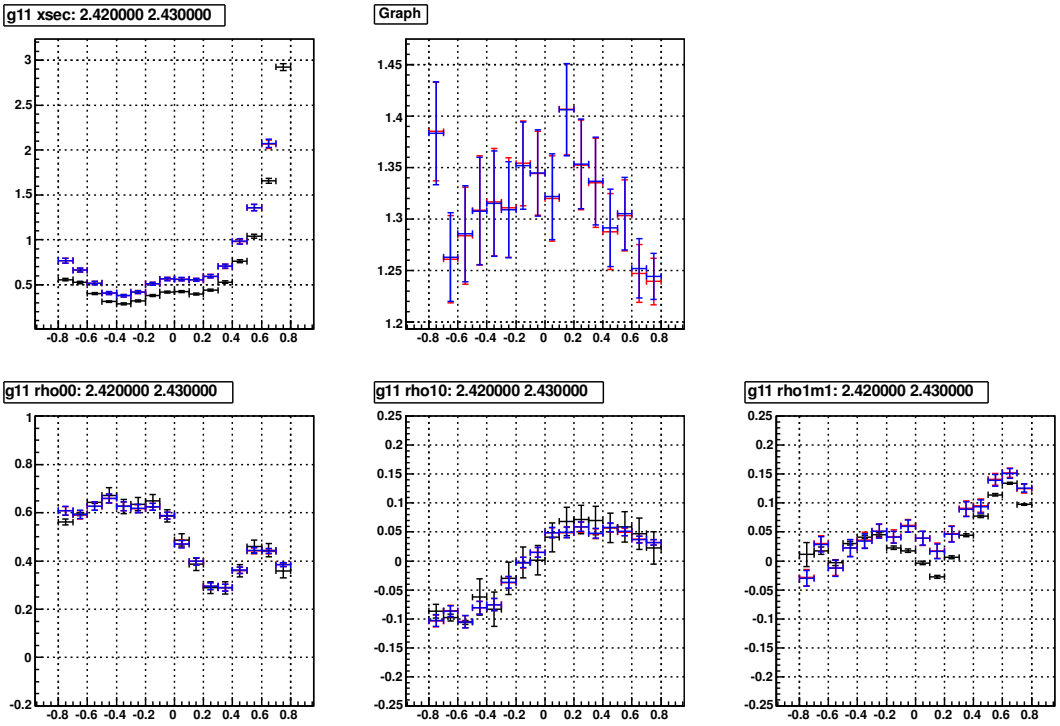

Bin 42 : $W = 2.42$ - 2.43 GeV

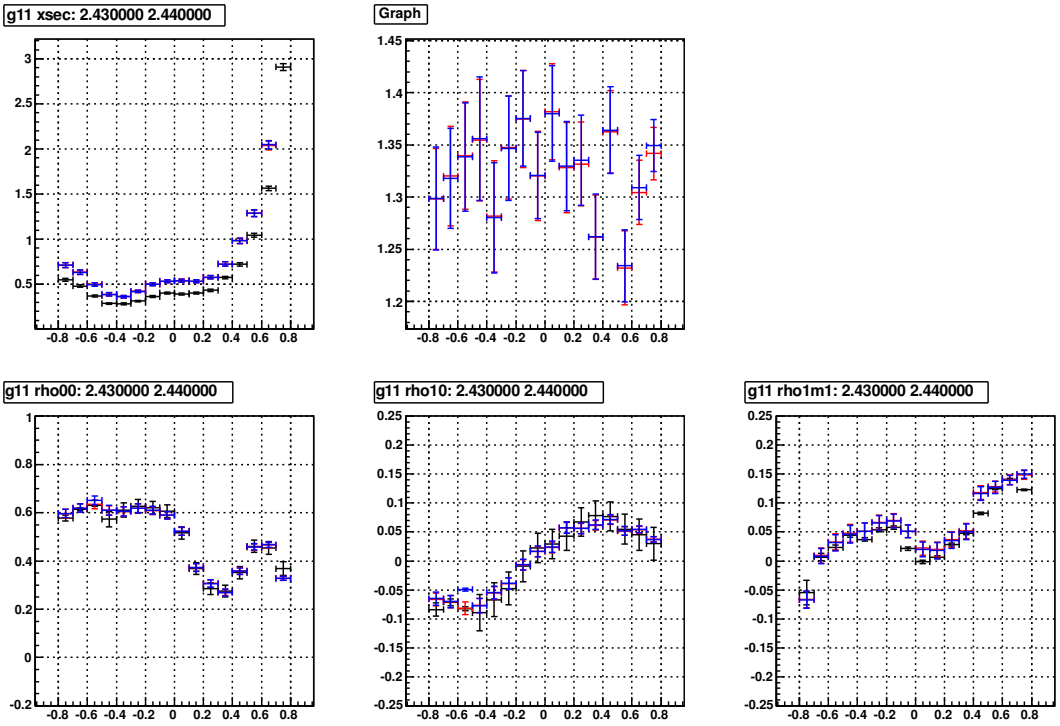

Bin 43 : $W = 2.43$ - 2.44 GeV

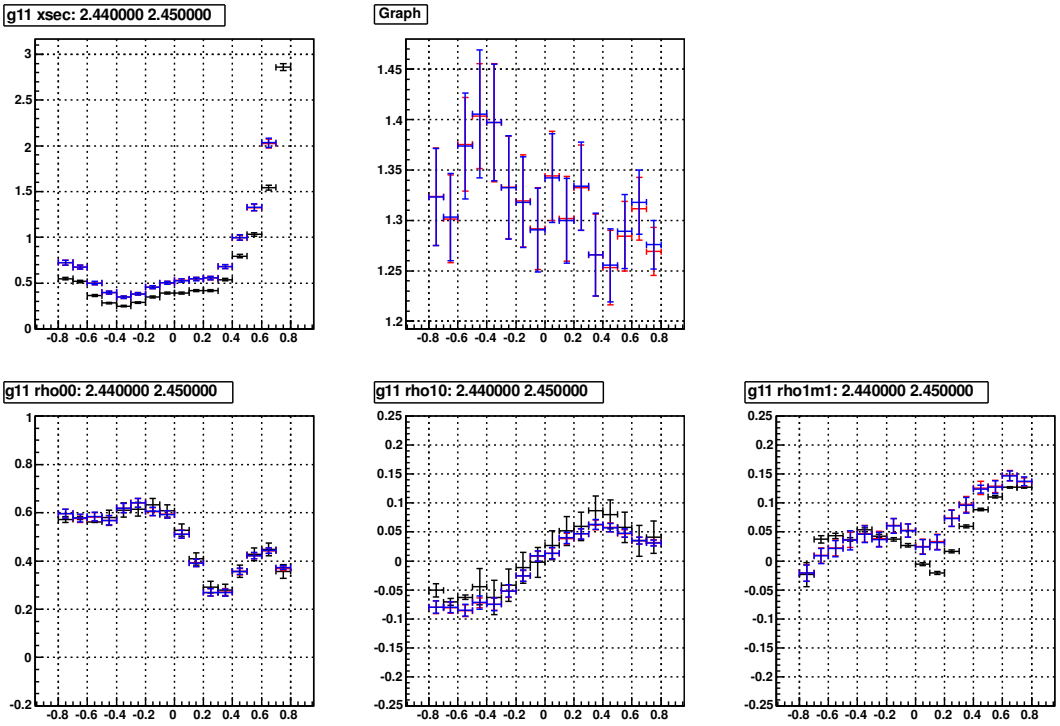

Bin 44 : $W = 2.44$ - 2.45 GeV

Appendix C

Cross-section systematic effects

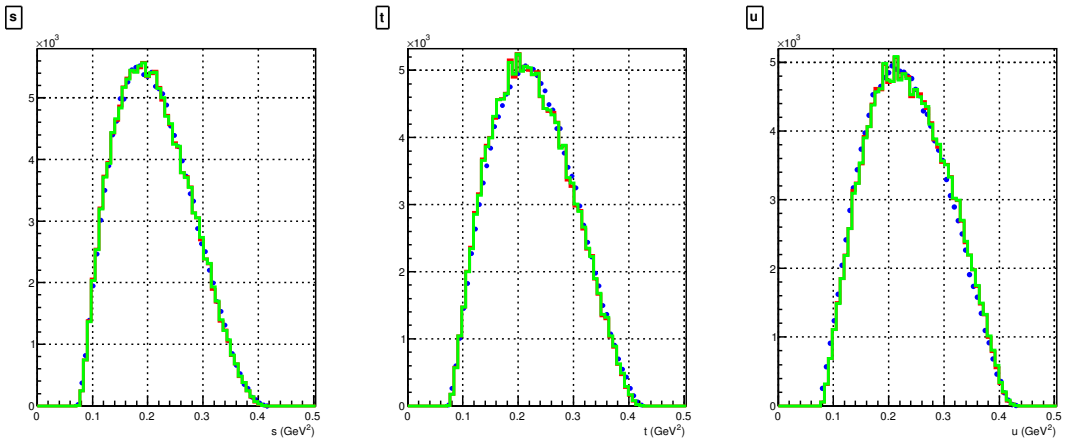

Bin 0 : $W = 2.00$ - 2.01 GeV

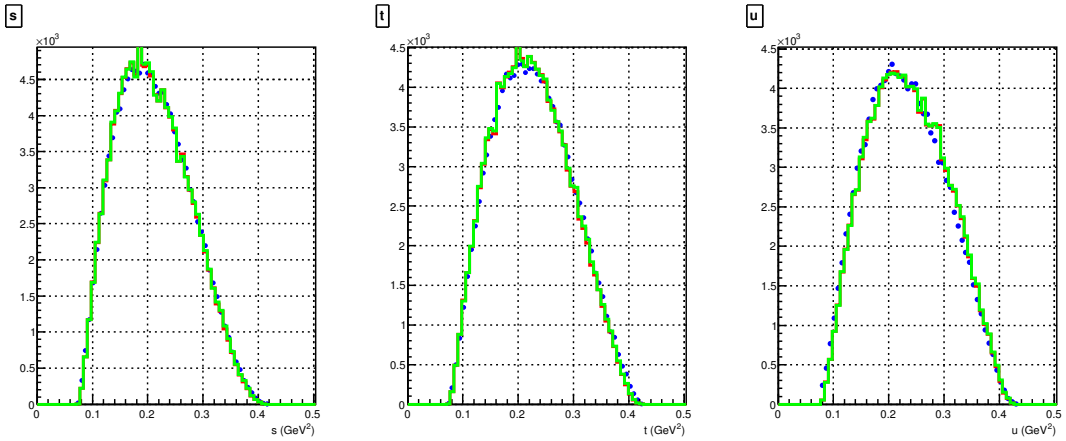

Bin 1 : $W = 2.01$ - 2.02 GeV

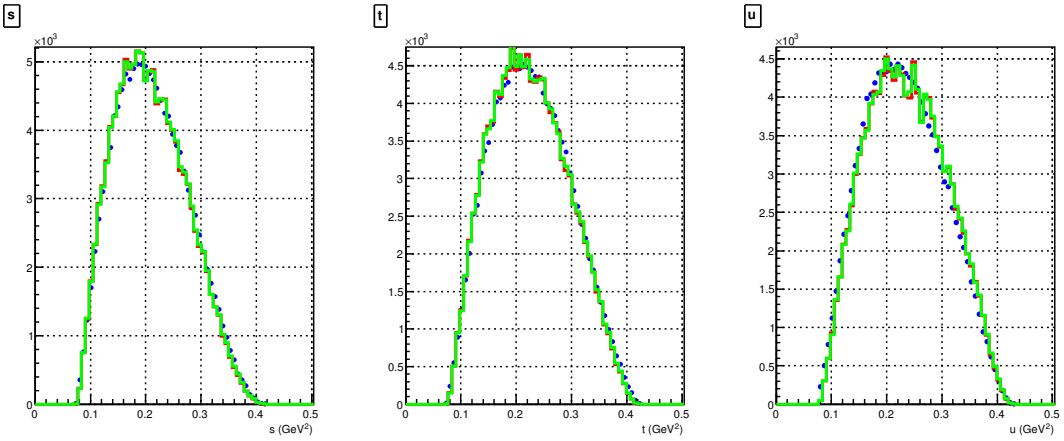

Bin 2 : $W = 2.02$ - 2.03 GeV

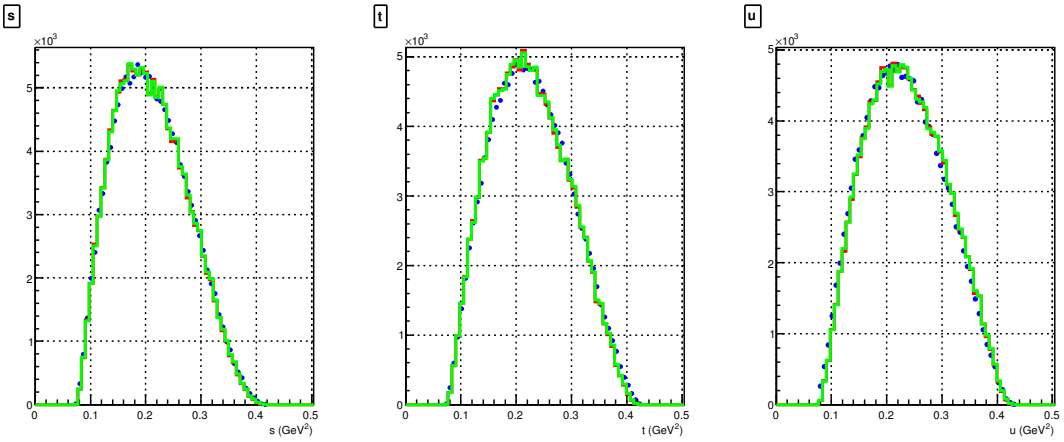

Bin 3 : $W = 2.03$ - 2.04 GeV

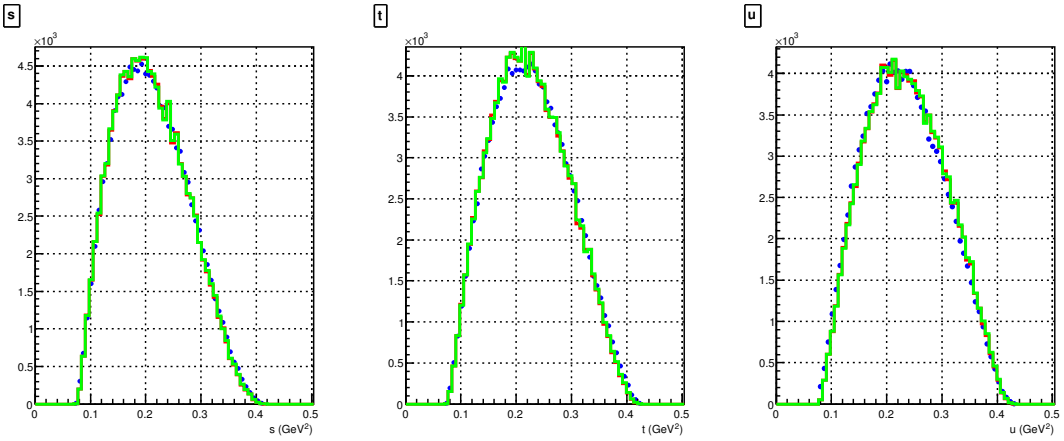

Bin 4 : $W = 2.04$ - 2.05 GeV

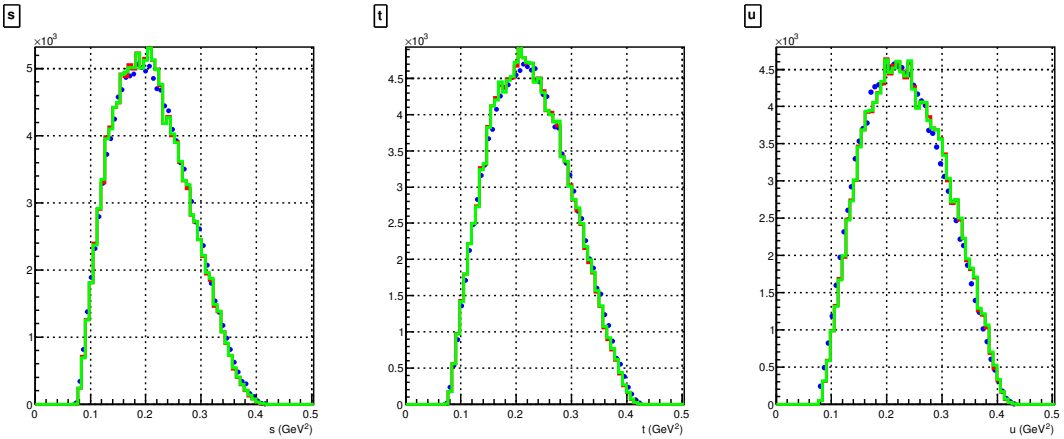

Bin 5 : $W = 2.05$ - 2.06 GeV

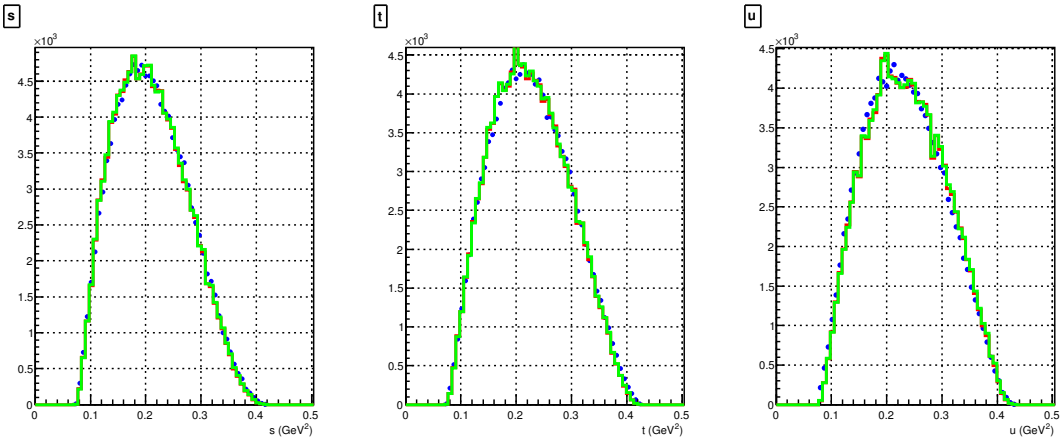

Bin 6 : $W = 2.06$ - 2.07 GeV

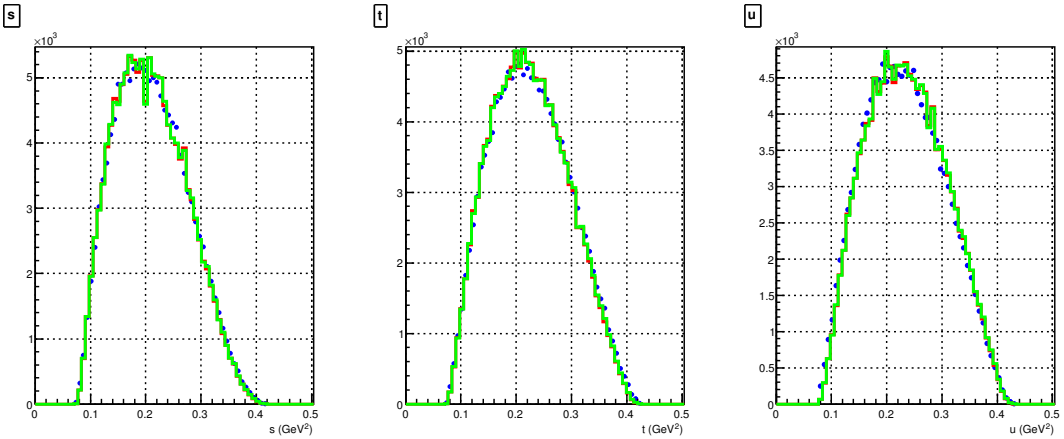

Bin 7 : $W = 2.07$ - 2.08 GeV

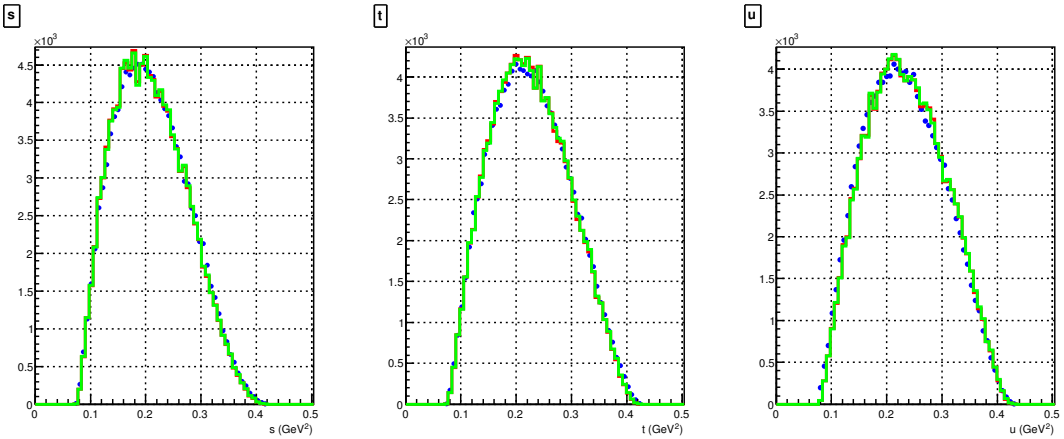

Bin 8 : $W = 2.08$ - 2.09 GeV

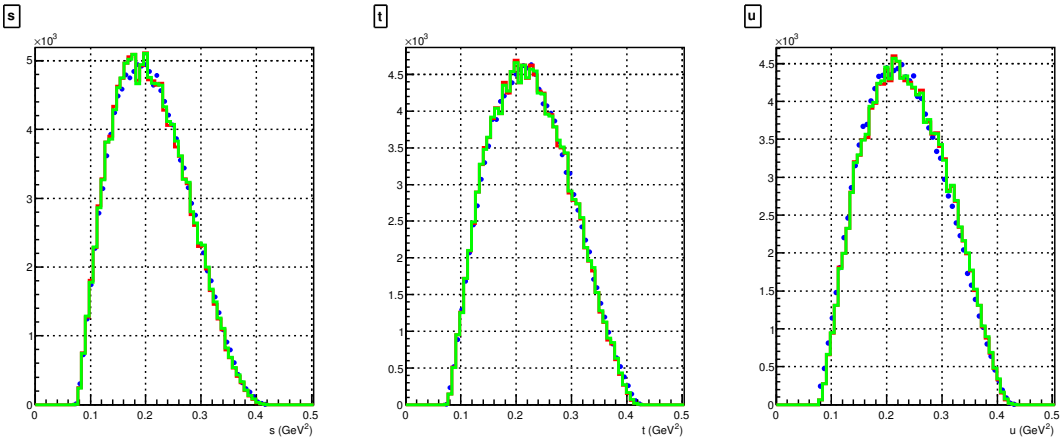

Bin 9 : $W = 2.09$ - 2.10 GeV

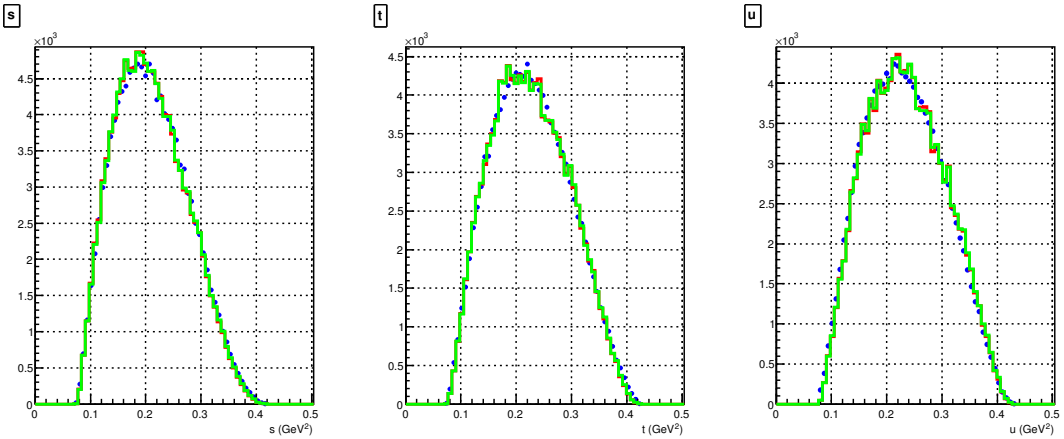

Bin 10 : $W = 2.10$ - 2.11 GeV

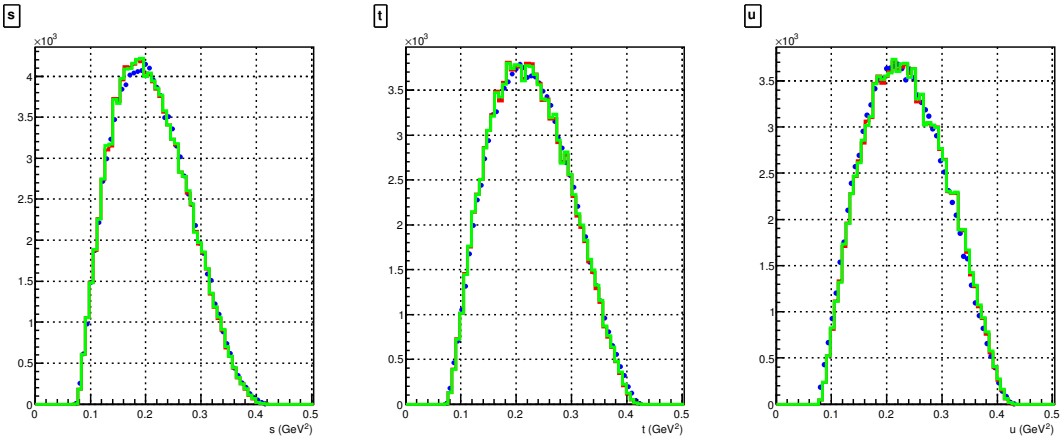

Bin 11 : $W = 2.11$ - 2.12 GeV

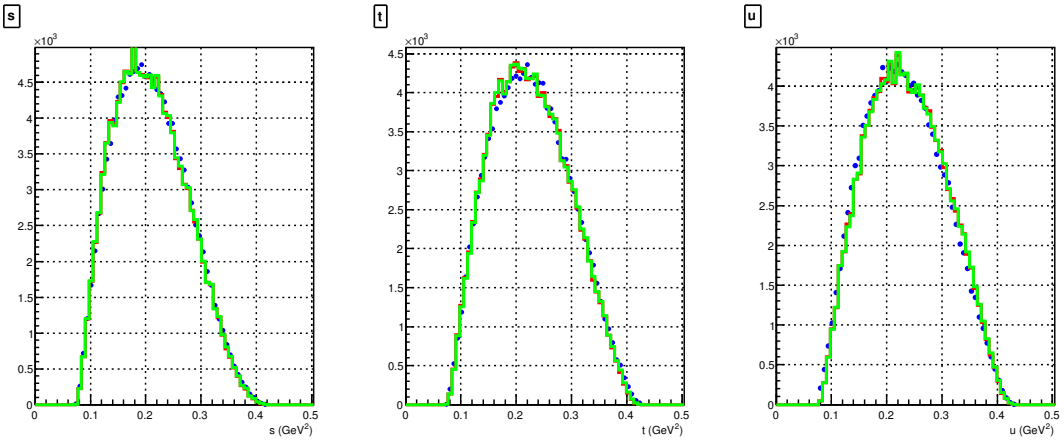

Bin 12 : $W = 2.12$ - 2.13 GeV

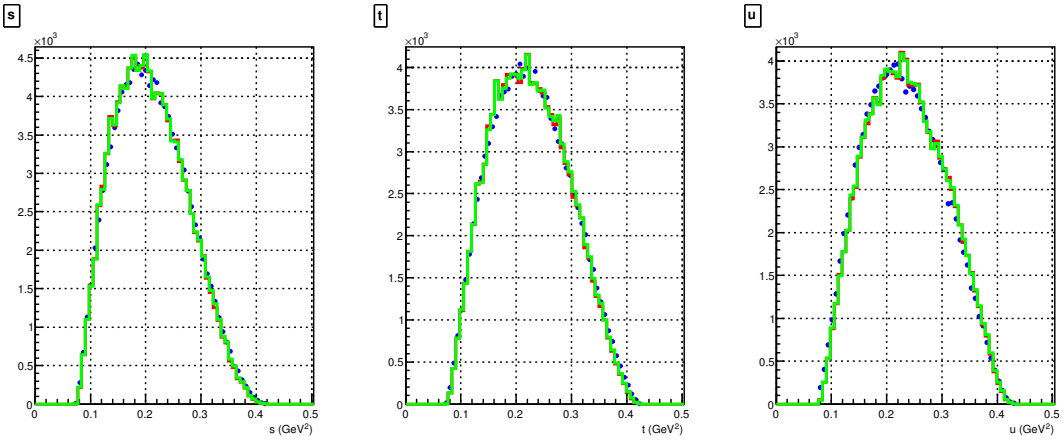

Bin 13 : $W = 2.13$ - 2.14 GeV

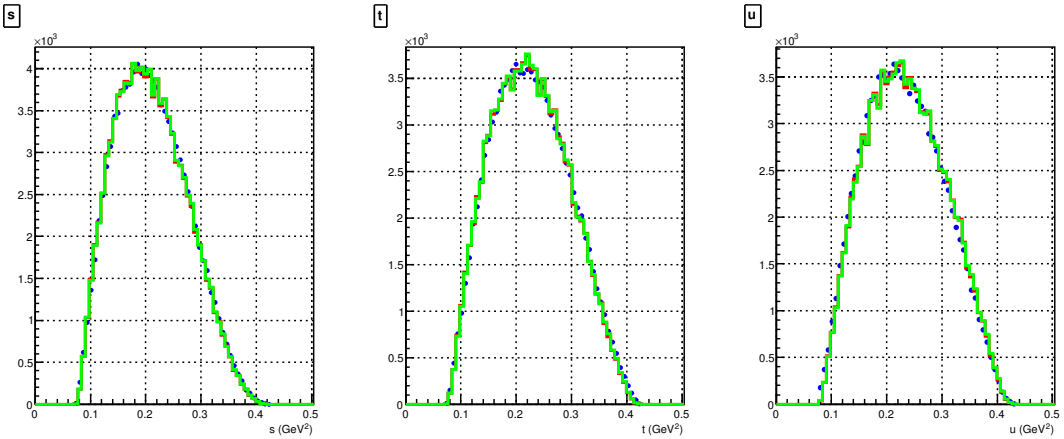

Bin 14 : $W = 2.14$ - 2.15 GeV

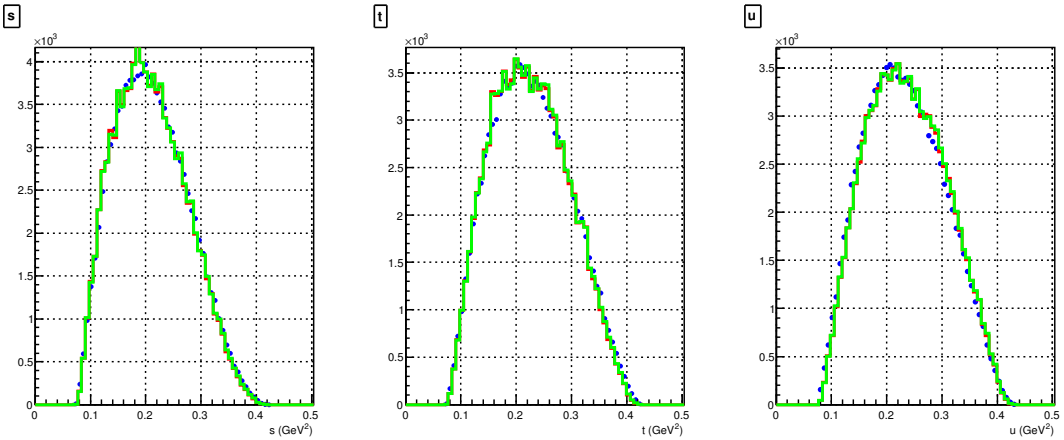

Bin 15 : $W = 2.15$ - 2.16 GeV

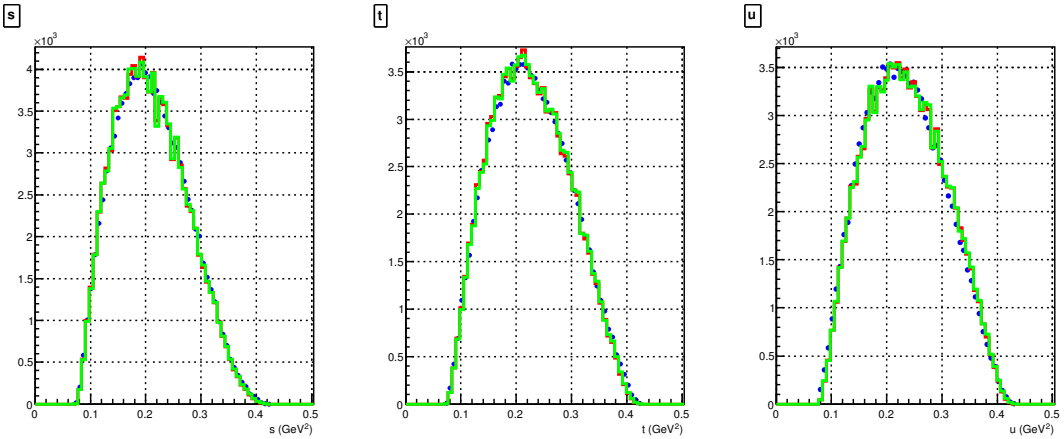

Bin 16 : $W = 2.16$ - 2.17 GeV

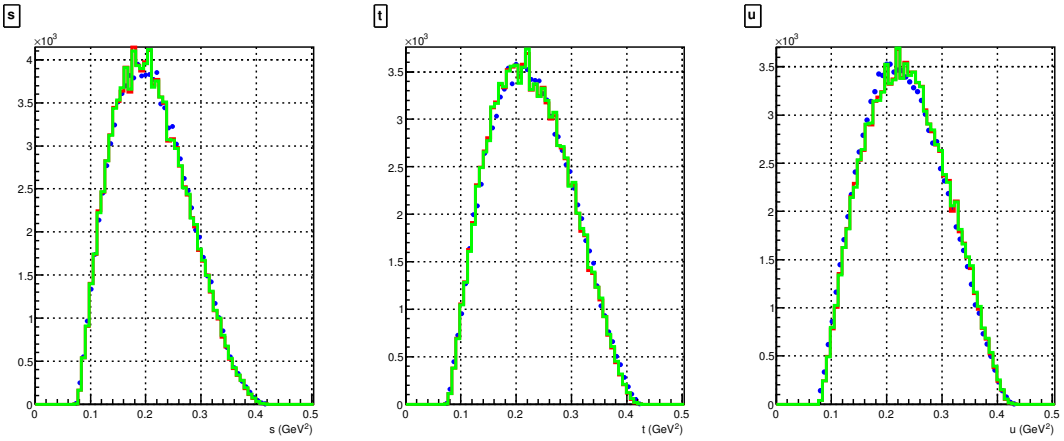

Bin 17 : $W = 2.17$ - 2.18 GeV

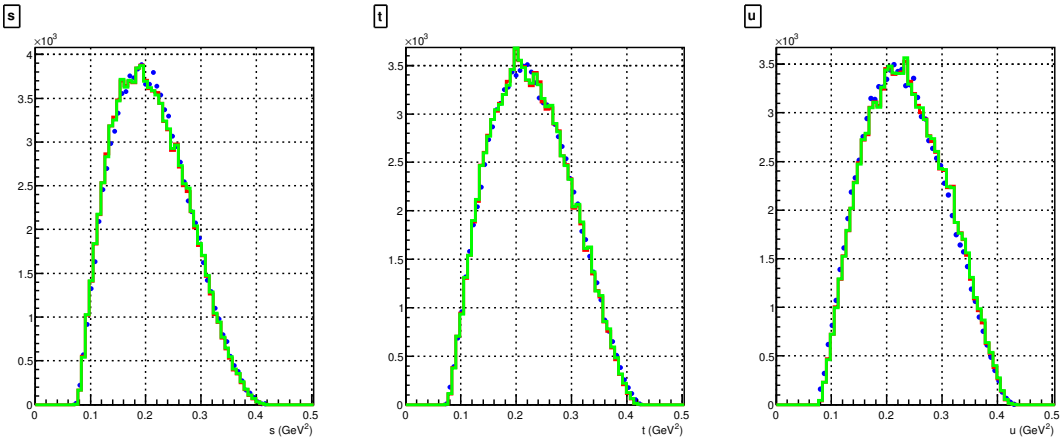

Bin 18 : $W = 2.18$ - 2.19 GeV

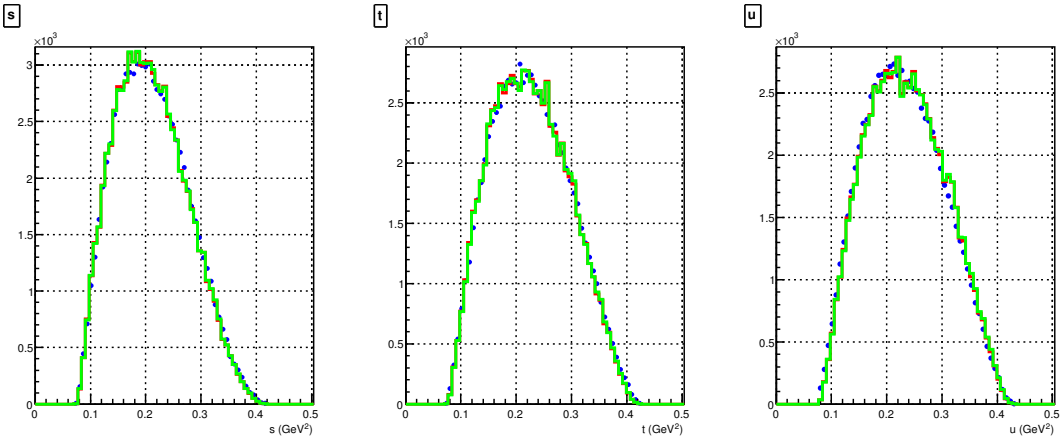

Bin 19 : $W = 2.19$ - 2.20 GeV

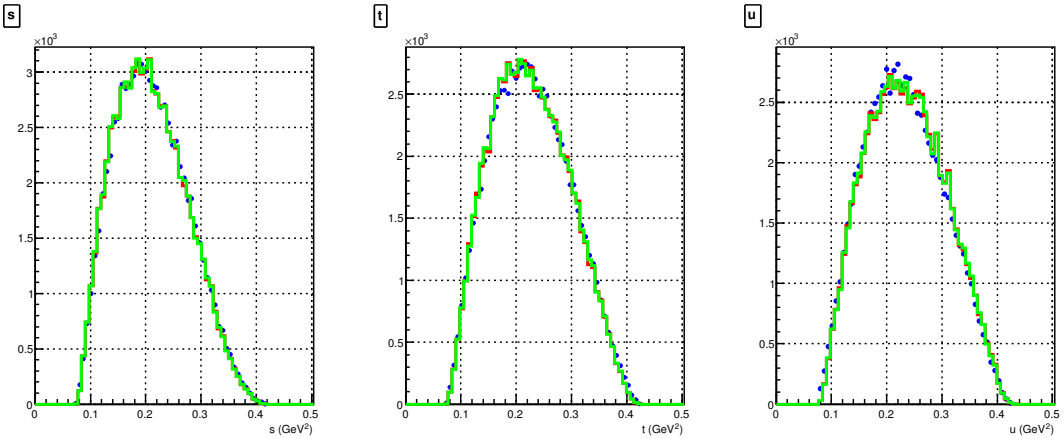

Bin 20 : $W = 2.20$ - 2.21 GeV

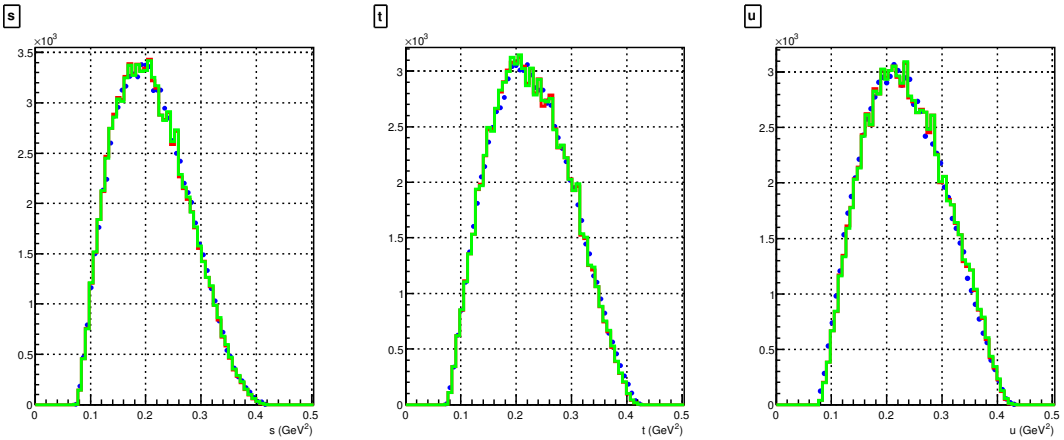

Bin 21 : $W = 2.21$ - 2.22 GeV

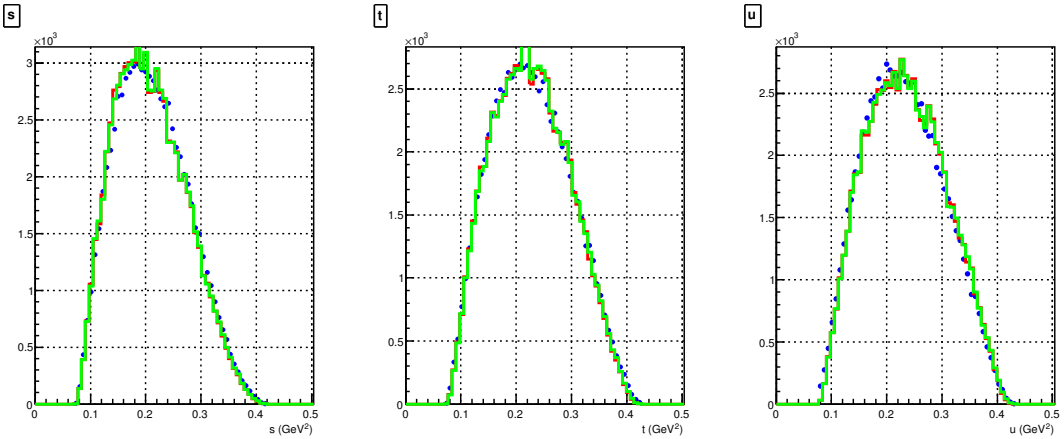

Bin 22 : $W = 2.22$ - 2.23 GeV

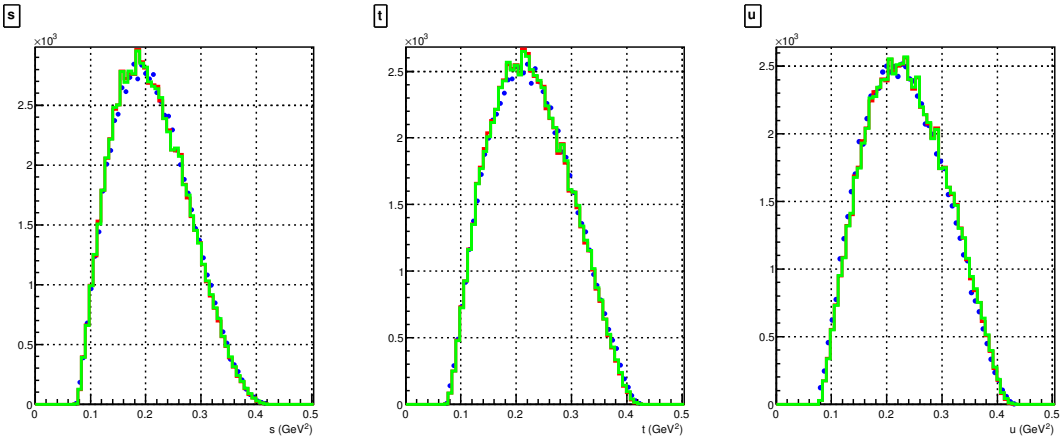

Bin 23 : $W = 2.23$ - 2.24 GeV

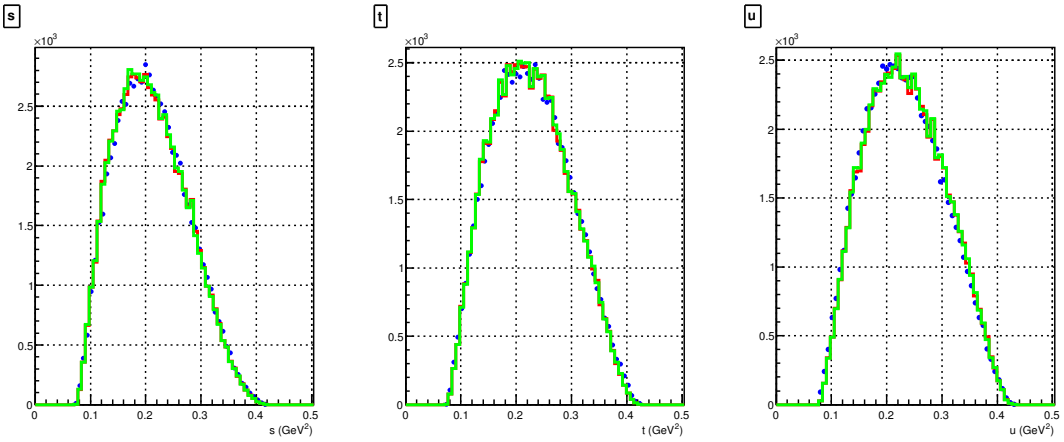

Bin 24 : $W = 2.24$ - 2.25 GeV

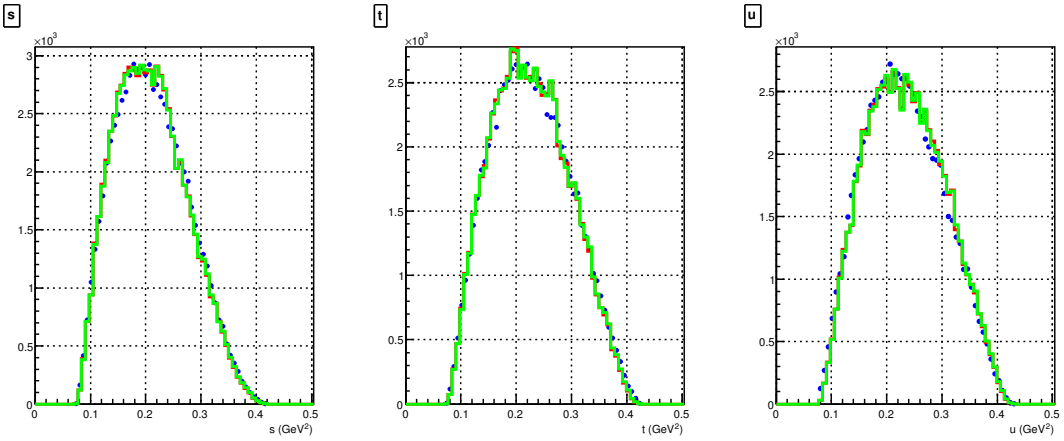

Bin 25 : $W = 2.25$ - 2.26 GeV

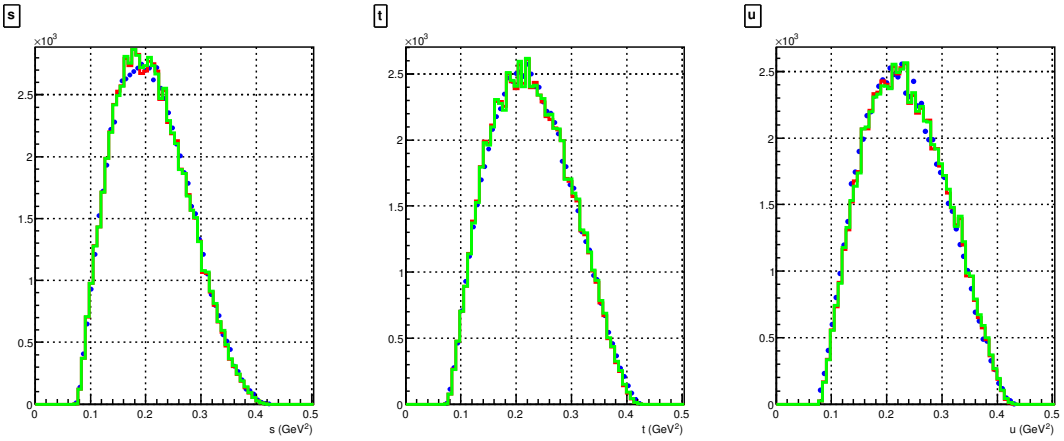

Bin 26 : $W = 2.26$ - 2.27 GeV

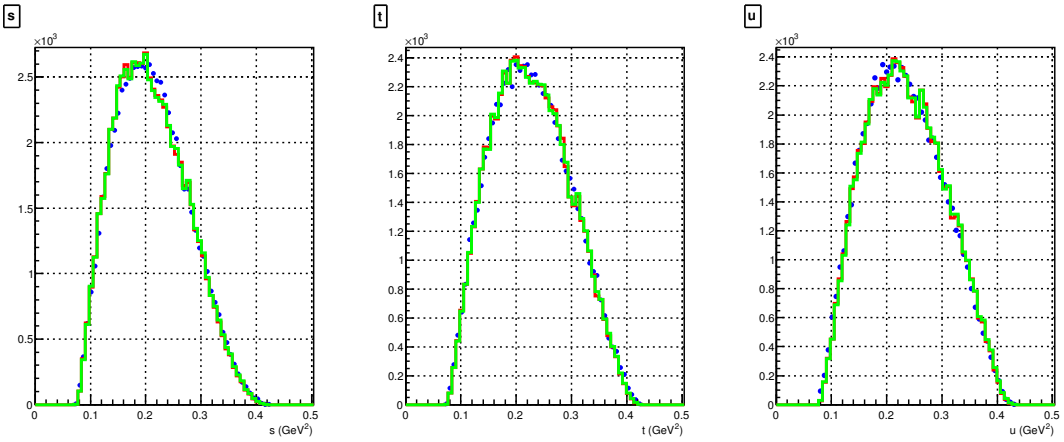

Bin 27 : $W = 2.27$ - 2.28 GeV

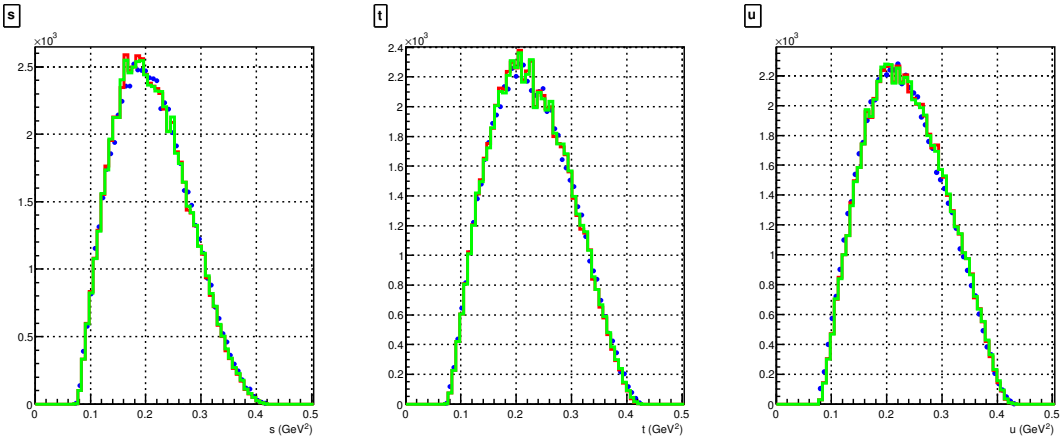

Bin 28 : $W = 2.28$ - 2.29 GeV

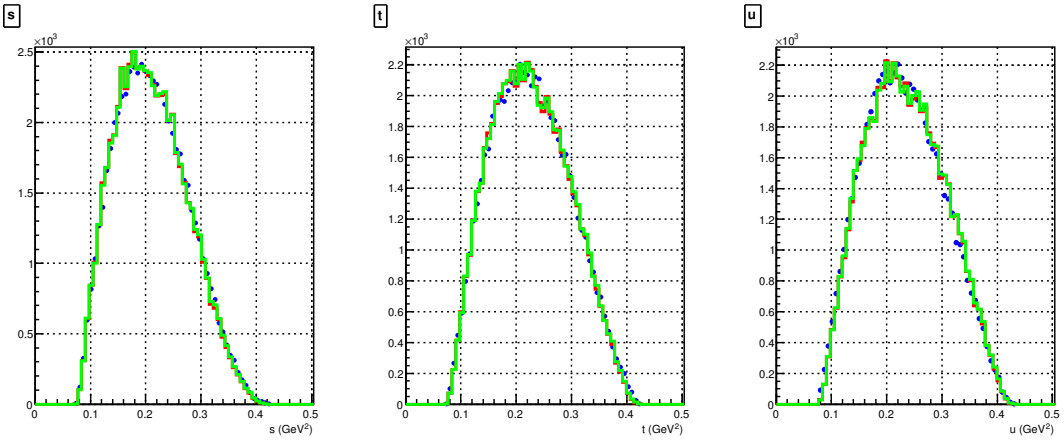

Bin 29 : $W = 2.29$ - 2.30 GeV

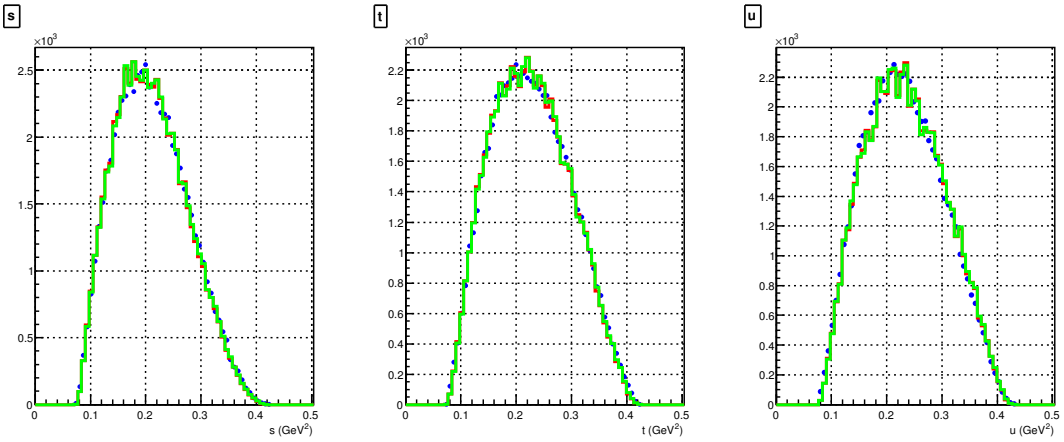

Bin 30 : $W = 2.30$ - 2.31 GeV

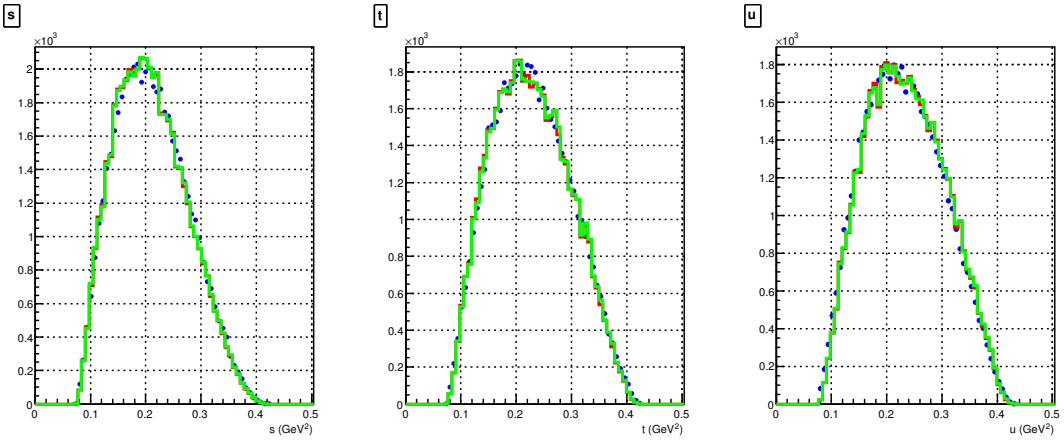

Bin 31 : $W = 2.31$ - 2.32 GeV

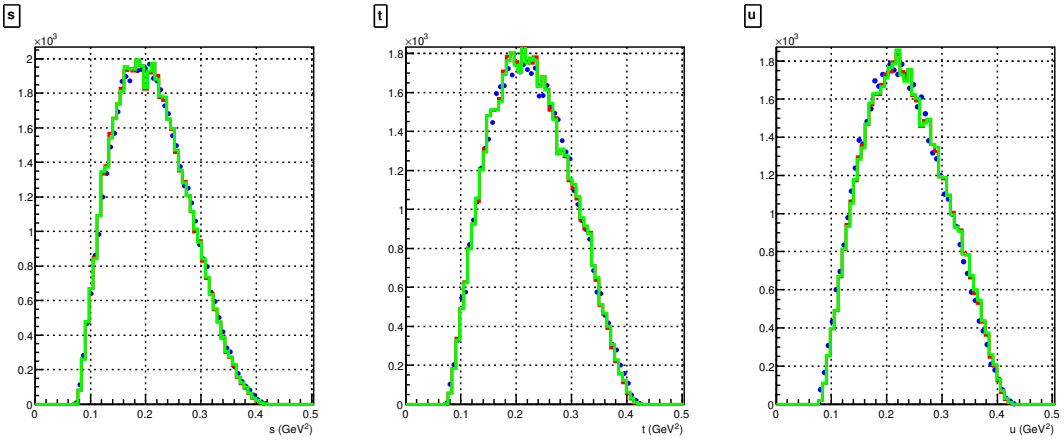

Bin 32 : $W = 2.32$ - 2.33 GeV

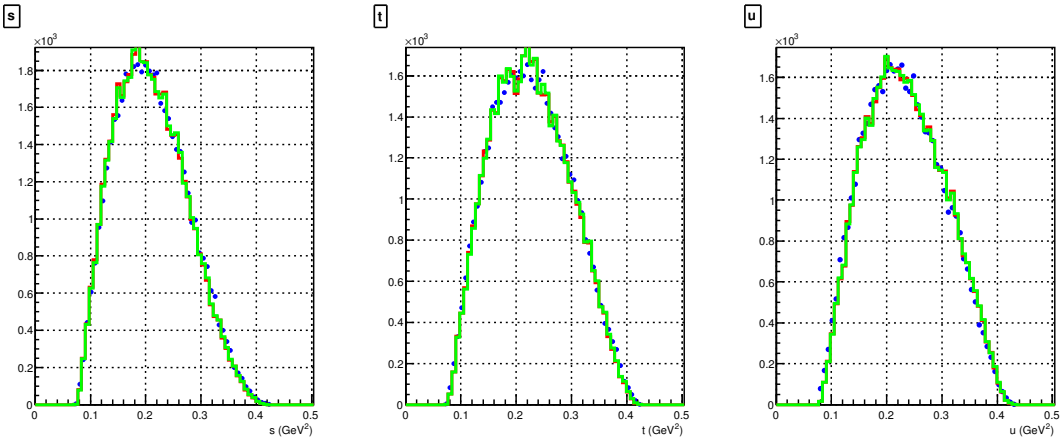

Bin 33 : $W = 2.33$ - 2.34 GeV

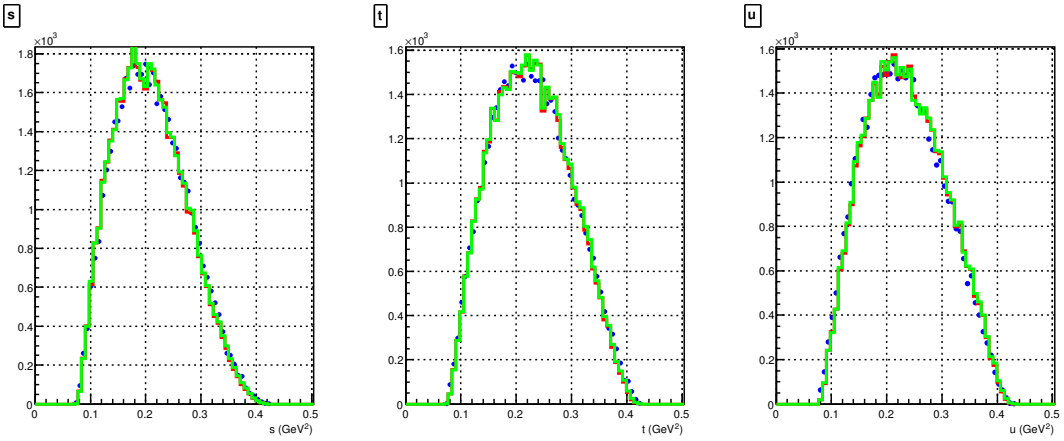

Bin 34 : $W = 2.34$ - 2.35 GeV

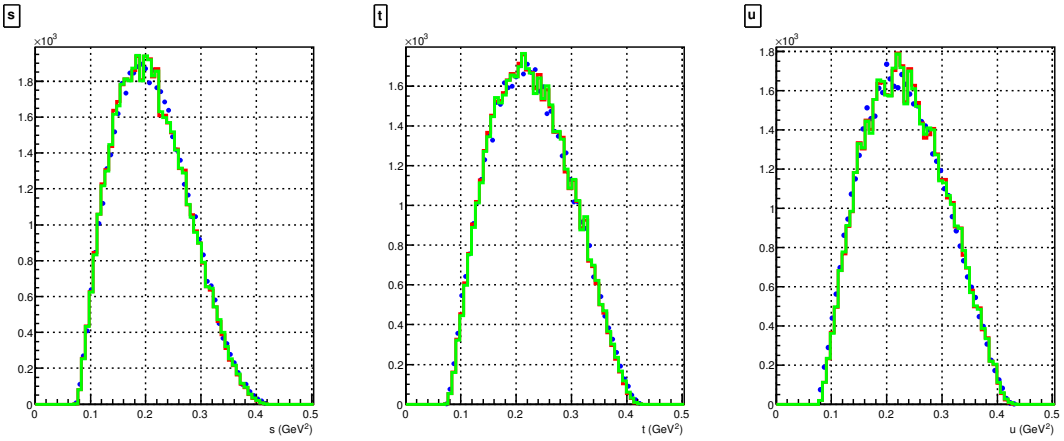

Bin 35 : $W = 2.35$ - 2.36 GeV

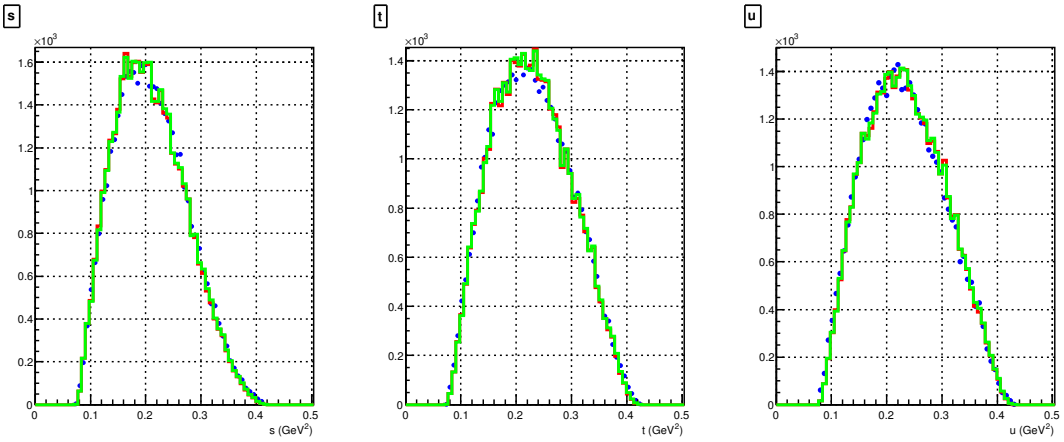

Bin 36 : $W = 2.36$ - 2.37 GeV

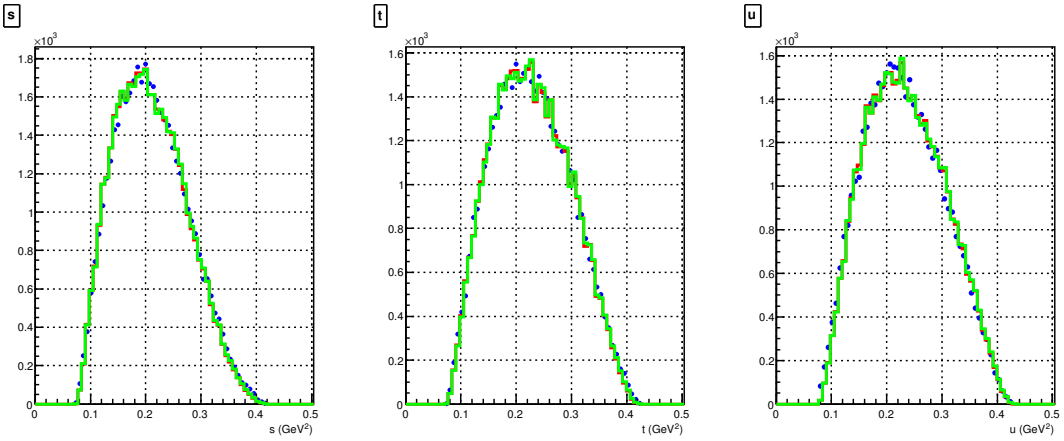

Bin 37 : $W = 2.37$ - 2.38 GeV

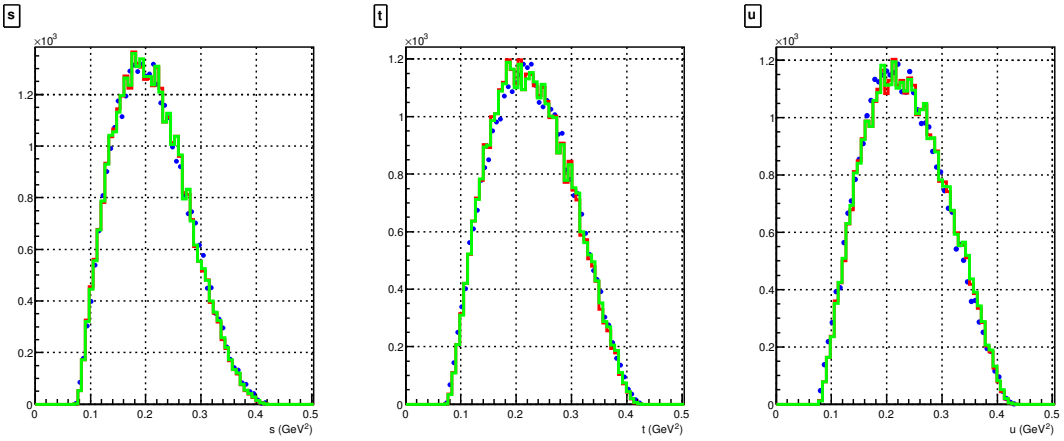

Bin 38 : $W = 2.38$ - 2.39 GeV

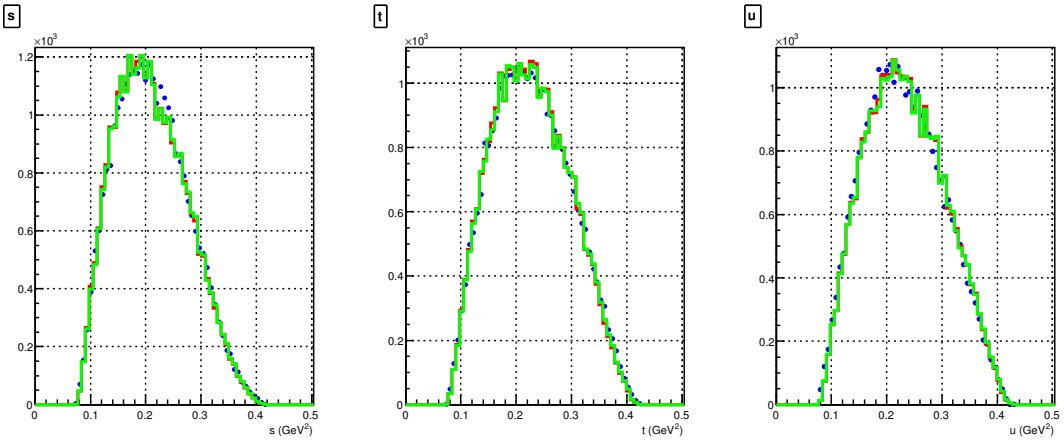

Bin 39 : $W = 2.39$ - 2.40 GeV

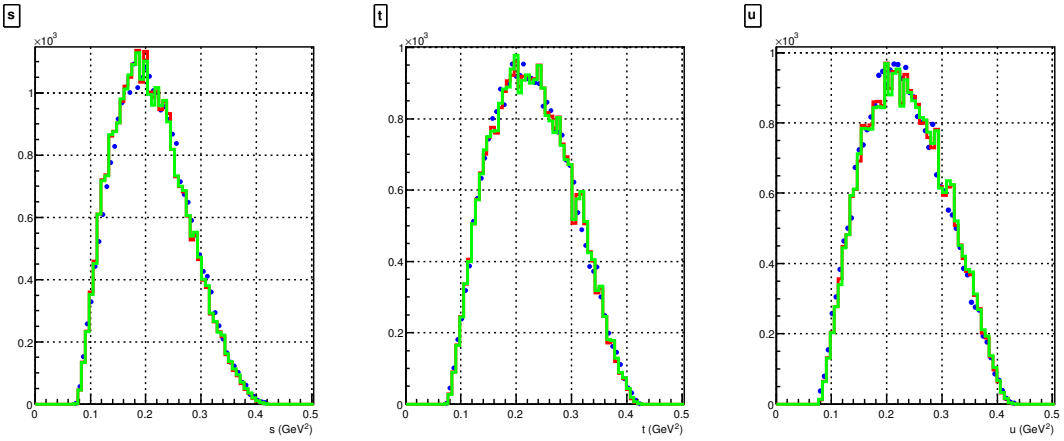

Bin 40 : $W = 2.40$ - 2.41 GeV

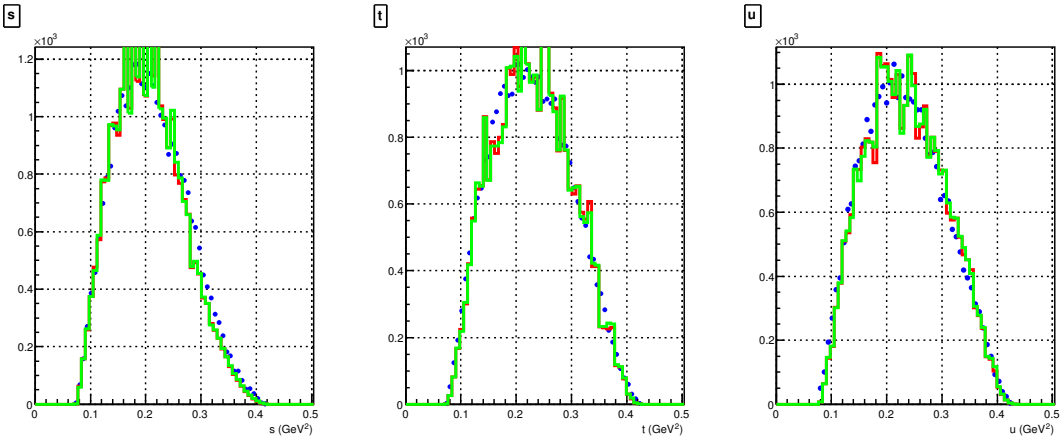

Bin 41 : $W = 2.41$ - 2.42 GeV

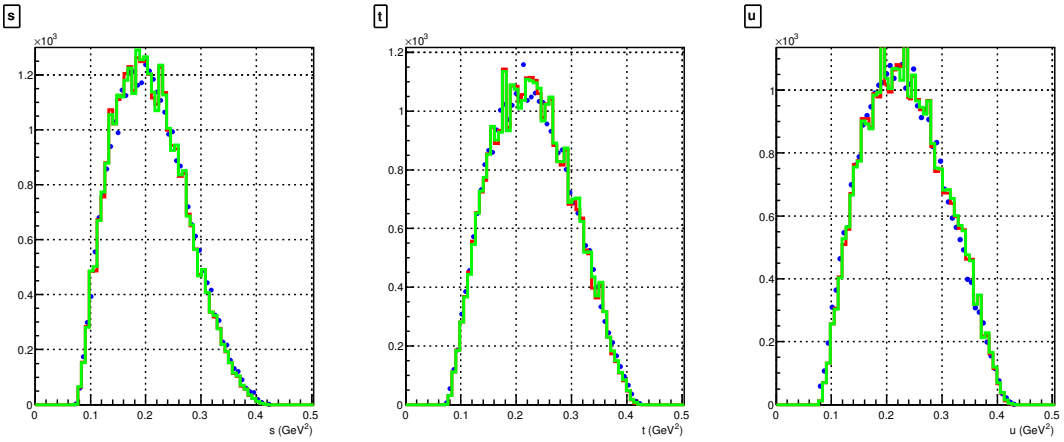

Bin 42 : $W = 2.42$ - 2.43 GeV

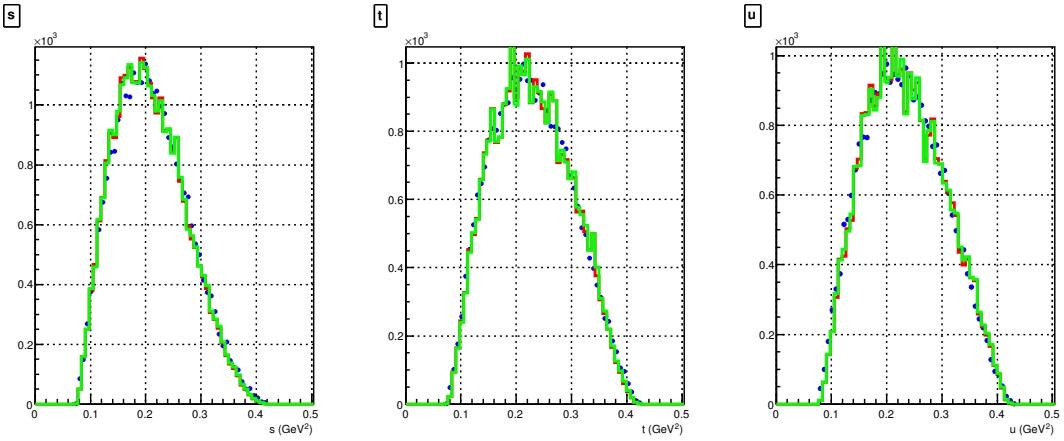

Bin 43 : $W = 2.43$ - 2.44 GeV

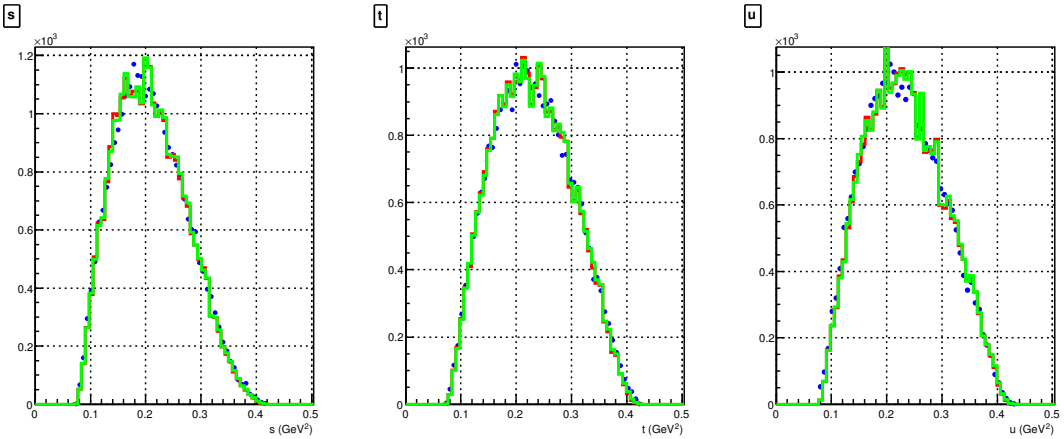

Bin 44 : $W = 2.44$ - 2.45 GeV